# Universidad de Málaga
## Facultad de ciencias
**Departamento de Química Inorgánica, Cristalografía y Mineralogía**


**Tesis doctoral**
**por compendio de artículos**

**2025, Málaga**

# EARLY AGE ACTIVATION OF LOW $CO_2$ FOOTPRINT CEMENT


**Alejandro Morales Cantero**

**Directores:**
**Prof. Miguel Ángel García Aranda**
**Prof. María de los Ángeles Gómez de la Torre**


**Programa de doctorado:**
**Química y Tecnologías Químicas Materiales y Nanotecnologías**

AUTOR: Alejandro Morales Cantero

https://orcid.org/0000-0002-4688-7589

EDITA: Publicaciones y Divulgación Científica. Universidad de Málaga

## DECLARACIÓN DE AUTORÍA Y ORIGINALIDAD DE LA TESIS PRESENTADA PARA OBTENER EL TÍTULO DE DOCTOR

D. ALEJANDRO MORALES CANTERO, estudiante del programa de doctorado en QUÍMICA Y TECNOLOGÍAS QUÍMICAS, MATERIALES Y NANOTECNOLOGÍA de la Universidad de Málaga, autor de la tesis presentada para la obtención del título de doctor por la Universidad de Málaga, titulada: **EARLY AGE ACTIVATION OF LOW $CO_2$ FOOTPRINT CEMENT.**

Realizado bajo la tutorización de MARÍA DE LOS ÁNGELES GÓMEZ DE LA TORRE y dirección de MARÍA DE LOS ÁNGELES GÓMEZ DE LA TORRE y MIGUEL ÁNGEL GARCÍA ARANDA.

DECLARO QUE:

La tesis doctoral presentada es una obra original que no infringe los derechos de propiedad intelectual ni los derechos de propiedad industrial u otros, conforme el ordenamiento jurídico vigente (Real Decreto Legislativo 1/1996, de 12 de abril, por el que se aprueba el texto refundido de la Ley de Propiedad Intelectual, regularizando, aclarando y armonizando las disposiciones legales vigentes sobre la materia), modificado por la Ley 2/2019, de 1 de marzo.

Igualmente asumo, ante a la Universidad de Málaga y ante cualquier otra instancia, la responsabilidad que pudiera derivarse en caso de plagio de contenidos en la tesis doctoral presentada, conforme al ordenamiento jurídico vigente.

En Málaga, a 13 de enero de 2025

| | |
|---|---|
| Fdo.: ALEJANDRO MORALES CANTERO<br><br>Doctorando | Fdo.: Mª DE LOS ÁNGELES GÓMEZ DE LA TORRE<br><br>Tutor |
| Fdo.: MARÍA DE LOS ÁNGELES GÓMEZ DE LA TORRE y MIGUEL ÁNGEL GARCÍA ARANDA<br><br>Directores de tesis | |

La Prof. MARÍA DE LOS ÁNGELES GÓMEZ DE LA TORRE, Catedrática de Universidad, y el Prof. MIGUEL ÁNGEL GARCÍA ARANDA, Catedrático de Universidad.

HACEN CONSTAR:

Que la tesis doctoral presentada por compendio de publicaciones, titulada: **EARLY AGE ACTIVATION OF LOW $CO_2$ FOOTPRINT CEMENT**, ha sido realizada por D. ALEJANDRO MORALES CANTERO bajo la tutorización y dirección de la Prof. MARÍA DE LOS ÁNGELES GÓMEZ DE LA TORRE, y la dirección del Prof. MIGUEL ÁNGEL GARCÍA ARANDA.

AUTORIZAMOS:

En cumplimiento de la legislación vigente, a su trámite y presentación para la obtención del grado de Doctor en el Programa de Doctorado de la Universidad de Málaga de QUÍMICA Y TECNOLOGÍAS QUÍMICAS. MATERIALES Y NANOTECNOLOGÍA por parte del interesado. Además, informamos que las publicaciones en coautoría que la avalan no han sido utilizadas en tesis anteriores.

En Málaga, a 13 de enero de 2025

Tutora:

Fdo. María de los Ángeles Gómez de la Torre

Directores:

Fdo. María de los Ángeles Gómez de la Torre

Fdo. Miguel Ángel García Aranda

UNIVERSIDAD DE MÁLAGA

# EARLY AGE ACTIVATION OF LOW $CO_2$ FOOTPRINT CEMENT

Memoria presentada para optar al título de:

**Doctor en Química y Tecnologías Químicas. Materiales y Nanotecnología**

En Málaga, a 13 de enero de 2025


Doctorando:

Fdo: Alejandro Morales Cantero

Directores:

Fdo: María de los Ángeles Gómez de la Torre
Catedrática Química Inorgánica

Fdo: Miguel Ángel García Aranda
Catedrático Química Inorgánica

Facultad de Ciencias
Departamento de Química Inorgánica, Cristalografía y Mineralogía

TESIS DOCTORAL

por compendio de publicaciones

Universidad de Málaga

Facultad de Ciencias, Departamento de Química Inorgánica, Cristalografía y Mineralogía

Programa de doctorado: Química y Tecnologías Químicas, Materiales y Nanotecnología

Alejandro Morales Cantero

# Early age activation of low-$CO_2$ footprint cement

Directores

María de los Ángeles Gómez de la Torre

Miguel Ángel García Aranda

DOCTORAL THESIS

by compendium of publications

University of Malaga

Faculty of Science, Department of Inorganic Chemistry, Crystallography and Mineralogy

Doctoral program: Chemistry and Chemical Technologies, Materials and Nanotechnology

Alejandro Morales Cantero

# Early age activation of low-$CO_2$ footprint cement

Supervisors

María de los Ángeles Gómez de la Torre

Miguel Ángel García Aranda

# Agradecimientos

A la Universidad de Málaga, por brindarme la oportunidad y las herramientas necesarias para llevar a cabo este doctorado. Gracias por proporcionar un entorno académico de excelencia, donde he podido desarrollar mis capacidades investigadoras y donde he encontrado los recursos y el apoyo imprescindible para alcanzar mis metas. La Universidad de Málaga no solo ha sido un lugar de aprendizaje, sino también un espacio donde he podido crecer personal y profesionalmente.

A mis directores, Mª de los Ángeles Gómez de la Torre y Miguel Ángel García Aranda, por su inestimable ayuda, conocimiento, consejos y apoyo constante a lo largo de todo el proceso. Sus orientaciones han sido fundamentales para guiar mis pasos y su confianza en mi trabajo ha sido una fuente constante de motivación. Su experiencia y dedicación han sido un pilar en la consecución de este proyecto, y no puedo estar más agradecido por todo lo que me han enseñado.

Al resto de los miembros del grupo de cemento (presentes y pasados), por su colaboración y apoyo en cada etapa de esta investigación. En especial:

A María Isabel Santacruz, por estar siempre dispuesta a ayudarme cuando lo he necesitado, brindándome su tiempo y experiencia de manera desinteresada.

A Ana Cuesta, por su apoyo incondicional, su entusiasmo y su disposición a colaborar en cualquier circunstancia, lo que ha hecho de este proceso una experiencia mucho más llevadera y enriquecedora.

A Jesús David Zea, antiguo miembro del grupo y actual técnico de laboratorio del departamento, por acogerme desde el primer día, por ser un excelente compañero y por compartir conmigo su amplio conocimiento sobre cementos. Su paciencia y disposición para enseñar han sido clave en mi formación.

A Shiva, por su ayuda en este tramo final, espero que sigas así y llegues lejos.

A Isa, por explicarme y aclararme las dudas siempre que lo he necesitado y por su ayuda durante los experimentos realizados en ALBA.

A Imane, por su agradable compañía, por enseñarme tanto de su cultura, por compartir sus habilidades culinarias con todos los compañeros y por su disposición a escuchar siempre que lo necesitaba.

A Diego, por su generosidad, por enseñarme la riqueza de la gastronomía asturiana y por toda su ayuda mientras me encontraba fuera durante mi estancia.

A Jaime, por su buena compañía tanto dentro como fuera del entorno laboral, por las tardes juntos entrenando y por enseñarme que se puede vivir la vida a todo color.

Al resto de mis compañeros con los que comparto sala a diario y que forman parte de mi vida tanto dentro como fuera del entorno laboral. Vuestra amistad y apoyo han sido fundamentales

para superar los desafíos que se presentaron a lo largo de este camino. Gracias por las conversaciones, las risas y por estar siempre ahí, tanto en los momentos de trabajo como en los de descanso. Habéis hecho que este proceso sea mucho más llevadero.

A Abraham, por apoyar a la gente cuando están al borde de la grieta, invocador de alegrías, si estás junto a él en el abismo, no será un lamento.

A Álvaro, "el capi", por mantener el orden en la sala, por su habilidad para motivar al equipo y mantenernos siempre centrados en el objetivo.

A Antonio, por crear un ambiente de trabajo agradable y colaborativo, y por su buen humor, que hace que los días complicados sean más llevaderos.

A Benjamín por su compañía durante todos estos años. Hemos recorrido este camino juntos desde el máster hasta esta recta final de la tesis. Estoy seguro que nuestros caminos seguirán juntos. Nos seguiremos viendo en el campo de batalla, ya sea frente a un tablero o en el mundo virtual.

A Fernando, por su compañía y por su *intenso* apoyo durante todo este tiempo de tesis, sin duda, ha sido una *fuerte* conocerlo.

A todos los profesores del Departamento de Química Inorgánica, Cristalografía y Mineralogía, por su constante apoyo y colaboración. En especial a, mi compañero y amigo, José Manuel por su inestimable ayuda desde el primer día, tanto en la instalación de los programas necesarios para el análisis y tratamiento de datos, como en mi integración con el resto de compañeros.

A mis padres, por criarme, educarme y estar a mi lado en cada momento, ofreciéndome su apoyo incondicional en todo lo que he necesitado. Gracias por inculcarme valores de esfuerzo y perseverancia, y por estar siempre ahí, celebrando mis éxitos y brindándome consuelo en los momentos difíciles. Vuestro amor y sacrificio han sido el motor que me ha impulsado a seguir adelante.

A mi hermano, por su apoyo constante, por ser siempre una fuente de motivación e inspiración, y por estar ahí en todo momento, dispuesto a ayudarme y a ofrecerme su perspectiva cuando más la necesitaba. Gracias por ser un ejemplo a seguir y por el aliento que me has brindado durante todo este proceso.

Al resto de mi familia, por su cariño, comprensión y por estar siempre a mi lado, en las buenas y en las malas. Vuestra confianza en mí me ha dado la fuerza necesaria para enfrentar cada reto, y vuestras palabras de aliento han sido un bálsamo en los momentos de duda.

A Sandra, por compartir su vida conmigo, por estar presente tanto en los buenos momentos como por aguantarme en los tiempos de agobio y estrés, y por ser mi apoyo incondicional en cada paso del camino. Gracias por tu paciencia infinita, por motivarme cuando más lo necesitaba, por celebrar cada uno de mis logros como si fueran tuyos y por brindarme tu amor y comprensión en los momentos más difíciles. Sin ti, este viaje habría sido mucho más complicado y menos gratificante.

A mis suegros, por tratarme y cuidarme como a un hijo desde que estoy con ellos, por su cariño incondicional, su hospitalidad y por hacerme sentir siempre bienvenido en su hogar. Gracias por su apoyo constante y por confiar en mí tanto como lo hacen. Su amor y generosidad han sido una parte fundamental en mi vida y en este camino que hemos recorrido juntos.

A mi cuñada Mari, por llevar tantísimos años al lado de mi hermano, tanto de amistad como de noviazgo, por ser una persona tan cercana y entrañable, por compartir tantos momentos en familia y por su dedicación y cariño hacia todos nosotros. Eres una hermana más para mí, y agradezco profundamente todo lo que haces por la familia.

A mi cuñada Desi, por tu alegría contagiosa, por estar siempre dispuesta a ayudar y por tu generosidad. Gracias por tu apoyo, por formar parte de momentos importantes de mi vida y por tu presencia siempre positiva en cada reunión familiar. Valoro muchísimo la relación que hemos construido con el tiempo, y espero que siga creciendo.

A mis amigos, que son mi otra familia.

A mi gran amigo Ángel, por llevar tantísimos años a mi lado, apoyándome en las buenas y en las malas. Gracias por estar siempre dispuesto a escucharme, por tus consejos y por compartir conmigo tantas experiencias a lo largo de estos años. Tu amistad ha sido un pilar fundamental en mi vida.

A Inés, que no solo ha sido una buena compañera de carrera y trabajo, sino también una de mis grandes amigas y una excelente compañera de baile. Gracias por tu alegría, por los momentos compartidos y por estar siempre dispuesta a apoyarme.

A Cinthya, mi compañerita cementera, a la cual conocí en el grupo y que, aunque siguió por otro camino, seguimos manteniendo el contacto. Gracias por los momentos compartidos, por las risas y por ser una amiga en quien puedo confiar. Aunque nuestros caminos se hayan separado, nuestra amistad ha perdurado.

De los meses que estuve de estancia en Italia, me gustaría expresar mi más profundo agradecimiento a la Università del Piemonte Orientale y Buzzi S.p.A. - Built por acogerme y brindarme la oportunidad de realizar una estancia tan enriquecedora en sus instalaciones. Durante este período, tuve la fortuna de aprender y crecer en un entorno académico excepcional que me permitió ampliar mis horizontes y profundizar en mi campo de estudio.

A los profesores Enrico Boccaleri y Geo Paul por su generosidad al compartir conmigo su vasto conocimiento en sus respectivos campos. Su dedicación a la docencia y la investigación es verdaderamente inspiradora. Gracias a ellos, pude adquirir nuevas habilidades y conocimientos que han sido fundamentales para el desarrollo de mi tesis.

A Fulvio Canonico y Daniela Gastaldi, les agradezco profundamente por acogerme en su laboratorio y darme la oportunidad de utilizar sus instalaciones. Su hospitalidad y generosidad me hicieron sentir como en casa desde el primer momento, y su confianza en mi trabajo me permitió llevar a cabo experimentos clave para mi investigación. La posibilidad de trabajar en sus instalaciones fue un privilegio.

A todos los trabajadores de Built, quiero expresar mi sincero agradecimiento por tomarse el tiempo de explicarme y enseñarme todo lo relacionado con la durabilidad de los cementos, un tema que es crucial para mi investigación. En especial, a Valentino y Fabrizio, por su paciencia y por compartir su experiencia de manera tan clara y detallada. Su apoyo y disposición para ayudarme a entender conceptos complejos han sido fundamentales para mi desarrollo profesional durante esta estancia.

A mi compañero de sala, Sarwar, quiero agradecerle por su amabilidad y disposición durante mis primeros días en Italia. Su ayuda fue invaluable para adaptarme rápidamente al nuevo entorno, y su compañía hizo que la experiencia fuera mucho más agradable. Gracias por estar ahí para guiarme, responder a mis preguntas y por ser un gran apoyo durante mi estancia.

A los amigos que hice en Italia, quiero agradecerles por hacer que mi estancia fuera no solo productiva, sino también inolvidable. Vuestra compañía, amistad y el tiempo que compartimos hicieron que esta experiencia fuera mucho más llevadera y entretenida. Gracias por enseñarme los lugares más emblemáticos y los platos típicos de la región, por mostrarme la cultura local y por hacerme sentir bienvenido en todo momento. En especial, a Alessia y Gabriele, gracias por vuestra amabilidad, por estar siempre dispuestos a compartir una comida, una conversación o una salida, y por hacer que me sintiera parte de vuestra comunidad.

Quiero también agradecer a los técnicos de laboratorio del SCAI por su labor incansable en la realización de los análisis necesarios para mi investigación. Sin su profesionalismo, precisión y dedicación, no habría sido posible avanzar en la investigación de manera tan efectiva. En especial me gustaría agradecer a Laura, Estefanía, María Dolores, Carmen y Lourdes. Vuestro trabajo ha sido esencial para alcanzar los resultados obtenidos en esta tesis, y estoy profundamente agradecido por vuestro apoyo y colaboración.

Por último, me gustaría expresar mi agradecimiento por la aportación económica recibida a través de los contratos “18-FEDERJA-095”, “8.07/5.41.5260”, “P-18-RT-720” y “8.06/5.41.5700-1”, sin los cuales no habría sido posible realizar mi tesis. Estos fondos no solo han permitido que esta investigación se lleve a cabo, sino que también han facilitado la creación de un entorno de investigación robusto y sostenible. Gracias a estos recursos, he podido concentrarme plenamente en mi trabajo, desarrollar mis ideas y alcanzar los objetivos que me propuse al inicio de este camino.

# Contents

# Figure index

# Table index

# Equations index

# Cement nomenclature

Below are the nomenclatures used for cement, including both its oxides and phases.

*Table 0.1. Cement notation of oxide compounds*

| Cement Notation | Oxide compounds |
|---|---|
| **C** | $CaO$ |
| **S** | $SiO_2$ |
| **A** | $Al_2O_3$ |
| **F** | $Fe_2O_3$ |
| **$\bar{S}$** | $SO_3$ |
| **N** | $Na_2O$ |
| **K** | $K_2O$ |
| **M** | $MgO$ |
| **B** | $B_2O_3$ |
| **H** | $H_2O$ |
| **$\bar{C}$** | $CO_2$ |
| **P** | $P_2O_5$ |
| **T** | $TiO_2$ |

*Table 0.2. Cement notation of phases compounds used in this thesis*

| Cement nomenclature | Chemical formula | Oxide compounds | Name |
|---|---|---|---|
| **$C_3S$** | $Ca_3SiO_5$ | $3CaO{\cdot}SiO_2$ | Alite |
| **$C_2S$** | $Ca_2SiO_4$ | $2CaO{\cdot}SiO_2$ | Belite |
| **$C_4AF$** | $Ca_4Al_2Fe_2O_{10}$ | $4CaO{\cdot}Al_2O_3{\cdot}Fe_2O_3$ | Brownmillerite |
| **$C_3A$** | $Ca_3Al_2O_3$ | $3CaO{\cdot}Al_2O_3$ | Tricalcium aluminate |
| **$C\bar{S}H_2$** | $CaSO_4(H_2O)_2$ | $CaO{\cdot}SO_3{\cdot}2H_2O$ | Gypsum / Gyp |
| **$C\bar{S}H_{0.5}$** | $CaSO_4(H_2O)_{0.5}$ | $CaO{\cdot}SO_3{\cdot}0.5H_2O$ | Bassanite |
| **$C\bar{S}$** | $CaSO_4$ | $CaO{\cdot}SO_3$ | Anhydrite |
| **$C\bar{C}$** | $CaCO_3$ | $CaO{\cdot}CO_2$ | Calcite |
| **CaO** | $CaO$ | C | Free lime |
| **MgO** | $MgO$ | M | Periclase |
| **CH** | $Ca(OH)_2$ | $CaO{\cdot}H_2O$ | Portlandite |
| **$C_6A\bar{S}_3H_{32}$** | $Ca_6Al_2S_3O_{18}(H_2O)_{32}$ | $6CaO{\cdot}Al_2O_3{\cdot}3SO_3{\cdot}32H_2O$ | Ettringite / AFt |
| **$C_{1.8}SH_4$** | $Ca_{1.8}SiO_{3.8}(H_2O)_{4.0}$ | $1.8CaO{\cdot}SiO_2{\cdot}4H_2O$ | C-S-H gel |
| **$C_{1.2}Al_{0.1}SH_4$** | $Ca_{1.2}Al_{0.2}SiO_{3.5}(H_2O)_{4.0}$ | $1.2CaO{\cdot}0.1Al_2O_3{\cdot}SiO_2{\cdot}4H_2O$ | C-(A-)S-H gel |
| **$C_4A\bar{C}_{0.5}H_{12}$** | $Ca_4Al_2(OH)_{13}(CO_3)_{0.5}(H_2O)_{5.5}$ | $4CaO{\cdot}Al_2O_3{\cdot}0.5CO_2{\cdot}12H_2O$ | AFm-Hc / HC |
| **$C_4A\bar{C}H_{11}$** | $Ca_4Al_2(OH)_{12}CO_3(H_2O)_5$ | $4CaO{\cdot}Al_2O_3{\cdot}CO_2{\cdot}11H_2O$ | AFm-Mc / Mc |
| **$AS_2$** | $Al_2Si_2O_7$ | $Al_2O_3{\cdot}2SiO_2$ | Metakaolin |

# Special terms

BC: Belite cement

BET: Brunauer-Emmett-Teller

BW: Bound Water

bwc: by weight of cement

bwb: by weight of binder

bw(c,b): by weight of cement/binder

CC: Calcined clay

Comp. Str.: Compressive Strength

C-S-H: Calcium Silicate Hydrate

DTA-TG: Differential Thermal Analysis and Thermogravimetry

DEIPA: Diethanol Isopropanol Amine

DLS: Dynamic Light Scattering

EDIPA: Ethylene Diamine Isopropanol Amine

EPD: Environmental Product Declarations

FA: Fly Ash

FW: Free Water

GGBS: Ground Granulated Blast-furnace Slag

ICS: Intelligent Cluster System

$LC^3$: Limestone Calcined Clay Cement

LoI: Loss on Ignition

LXRPD: Laboratory X-ray Powder Diffraction

MIP: Mercury Intrusion Porosimetry

Mk: Metakaolin

NP: Natural pozzolans

PC: Portland Cement

PCE: Polycarboxylate Ether

PSD: Particle Size Distribution

SF: Silica Fume

SP: Superplasticizer

SSA: Specific Surface Area

Str. Enh.: Strength enhancing admixtures

SXRPD: Synchrotron X-ray Powder Diffraction

TEA: Triethanolamine

TIPA: Triisopropanolamine

TEM: Transmission Electron Microscopy

UPV: Ultrasonic Pulse Velocity

w/b: Water-to-Binder Ratio

w/c: Water-to-Cement Ratio

w/(c,b): Water-to-Cement Ratio or Water-to-Binder Ratio

WDXRF: Wavelength Dispersive X-Ray Fluorescence

XRD: X-ray Diffraction

# Summary

Portland cement (PC) remains the most widely used construction material worldwide due to its robust mechanical properties, versatility, and availability. However, the environmental cost of its production is considerable. The manufacturing process of PC is responsible for the emission of approximately 0.9 tons of $CO_2$ for every ton of cement produced, contributing to about 8% of total global anthropogenic $CO_2$ emissions. These emissions primarily originate from three key stages in the production process.

First, during the calcination stage, limestone (calcium carbonate, $CaCO_3$), the principal raw material, is heated to high temperatures, leading to its decomposition into lime (calcium oxide, CaO) and carbon dioxide ($CO_2$). This chemical reaction is responsible for a significant portion of the $CO_2$ emissions. Secondly, the process of clinkering, where the raw materials are heated to temperatures ranging between 1400-1450°C, is highly energy-intensive. The heat required for this process is typically generated by burning fossil fuels, further contributing to the overall carbon footprint. Lastly, the grinding process, which converts the clinker into the fine powder known as cement, consumes substantial amounts of electricity, leading to indirect greenhouse gas emissions through energy consumption.

Given the substantial environmental impact of PC, there is a pressing need for alternative solutions that maintain the material's desirable properties while reducing its carbon footprint.

Belite Cements as an Alternative

One promising alternative to PC is the use of Belite Cements (BCs). These cements share similar chemical components with PC but differ in their mineral composition, which results in lower $CO_2$ emissions during production. BCs are characterized by a higher proportion of belite ($C_2S$) and a lower proportion of alite ($C_3S$) compared to traditional PC. This alteration in composition offers several environmental and technical benefits.

Firstly, BCs produce about 8% lower $CO_2$ emissions due to the reduced amount of limestone required in their production. This reduction is significant in the context of global efforts to decrease greenhouse gas emissions. Secondly, the hydration process of BCs generates a lower temperature rise and less chemical shrinkage, which reduces the risk of thermal cracking in concrete structures. Thirdly, BCs tend to have a longer lifespan, partly due to the higher relative content of C-S-H (calcium silicate hydrate) gel, which is the principal binding phase in cement. Moreover, the lower operating temperatures required in the kiln (approximately 1250–1300°C) not only reduce energy consumption but also result in fewer harmful gas emissions and simplify the maintenance of the kiln's lining. Lastly, the energy requirements for producing BCs are slightly lower due to the difference in the formation enthalpies of belite and alite, with belite requiring less energy to form.

However, despite these advantages, the widespread adoption of BCs faces several challenges. The primary issue is the slower reactivity of the non-activated belite phase at ambient temperatures, which leads to lower early-age strength development in concrete. Additionally, the production of BCs requires approximately 15% more energy for grinding, as the materials are harder to process. The need for faster clinker cooling rates also increases energy consumption and capital investment. Furthermore, the lower kiln temperatures required for BC

production limit the use of alternative fuels, which could otherwise help reduce the overall carbon footprint of the process.

Reducing the Clinker Factor: The Role of Supplementary Cementitious Materials (SCMs)

Reducing the clinker factor in cement production is considered one of the most effective strategies for lowering $CO_2$ emissions. This approach involves the use of SCMs to replace a portion of the clinker in cement. SCMs are materials that, when combined with lime or PC, exhibit cementitious properties. The most commonly used SCMs include ground granulated blast-furnace slag (GGBS), fly ash (FA), calcined clays (CC), natural pozzolans (NP), and silica fume (SF). These materials can significantly reduce the carbon footprint of cement production.

The use of SCMs is driven by both environmental and economic factors. While FA and GGBFS have traditionally been the most widely used SCMs, supply constraints and increasing demand have led to the exploration of alternative materials. Among these, limestone calcined clay cements ($LC^3$) have emerged as a particularly promising option. $LC^3$ is a ternary blend of PC, limestone, and calcined clay, specifically kaolinitic clays, which are abundant and widely available.

SCMs contribute to the durability and long-term performance of concrete through their pozzolanic activity. Pozzolanic activity refers to the ability of a material to react with portlandite (calcium hydroxide) released during cement hydration, forming additional C–(A)-S–H gel, which enhances the strength and durability of concrete. Moreover, SCMs can improve the hydration kinetics of cement by acting as nucleation sites for C–S–H precipitation during the acceleratory period. This “filler effect” can enhance early-age strength and reduce the permeability of the concrete, leading to better long-term durability.

However, the use of SCMs also presents challenges. The dilution of cement by SCMs generally results in lower early-age strength, which can be a significant drawback in applications where rapid strength development is critical. Additionally, the increased water demand associated with SCMs, due to their finer particle size, can lead to a loss of workability in fresh concrete. In the case of $LC^3$ binders, the reduced portlandite content can accelerate the carbonation of concrete, which is the process by which $CO_2$ from the atmosphere reacts with calcium hydroxide in the cement paste, leading to a loss of alkalinity and potential reinforcement corrosion.

Addressing the Challenges with Admixtures

To make less polluting cements like $LC^3$ and BCs more competitive with traditional PC, the use of chemical admixtures has become essential. These admixtures are designed to address the specific challenges associated with alternative cements, such as reduced fluidity and lower early-age strength.

Superplasticizers, particularly those based on polycarboxylate ether (PCE), have been developed to improve the workability of cementitious mixes. The new generation PCE-based superplasticizers with Intelligent Cluster System (ICS) are especially effective in $LC^3$ binders, where they help maintaining fluidity over time, preventing the rapid slump loss that is typical with conventional superplasticizers. These admixtures work by releasing clusters of PCE

molecules gradually, ensuring that the concrete remains workable for a longer period, which is crucial for practical applications.

In addition to superplasticizers, strength-enhancing admixtures are used to improve the early-age strength of alternative cements. One effective approach is the use of C-S-H seeding, where nanostructured particles of C-S-H are added to the cement mix to accelerate the hydration process. When combined with alkanolamines, which are chemical compounds that accelerate the hydration of aluminate phases, these admixtures can significantly improve the early-age strength of both BC and $LC^3$ cements without compromising their long-term performance. The mechanism behind this improvement involves the creation of additional nucleation sites for C-S-H growth, reducing the microporosity of the cement paste and leading to a denser, stronger material.

Chapter Summaries

Chapter 1: Introduction and Methodology

The first chapter of this thesis is divided into two main sections. The first section introduces the nature of cements, focusing on PC and its environmental impact. It discusses the various challenges faced by the cement industry, particularly in relation to carbon emissions, and presents alternative types of cement that aim to reduce the carbon footprint. The section also delves into the role of admixtures in enhancing the properties of these alternative cements, making them more viable for widespread use.

The second section of the chapter outlines the experimental methodology used in the thesis. It describes the sample preparation procedures and provides a detailed overview of the techniques employed in the research, including calorimetry, X-ray powder diffraction, thermal analysis, and mercury intrusion porosimetry. Detailed descriptions of these techniques and methodologies are crucial for understanding the results obtained regarding the hydration processes and mechanical properties of the studied cements.

Chapter 2: Objectives of the thesis

Chapter two details the primary objectives of the thesis, which focus on reducing $CO_2$ emissions in cement production through the use of sustainable materials. The research examines two types of cement: belite cements, which offer a 10-12% reduction in $CO_2$ emissions, and $LC^3$, which can achieve a $CO_2$ reduction of up to 40% by substituting a portion of the clinker with calcined clay and limestone.

While both materials face early-age strength challenges, $LC^3$ is emphasized for its greater environmental benefits. The objectives of the research are to evaluate the impact of ICS-based superplasticizers on $LC^3$ workability, enhance early and long-term strength using C-S-H seeding admixtures, study the influence of admixtures on hydration kinetics, and improve microstructure while reducing porosity through admixture use. These efforts aim to advance $LC^3$ as a key solution for low-$CO_2$ cement production.

Chapter 3: Consolidation of Research Papers

Chapter three consolidates the research findings presented in a series of papers derived from the thesis. Each paper addresses a specific aspect of the research, contributing to a comprehensive understanding of the effects of various admixtures on the properties of Belite and $LC^3$ cements.

Article 1 (A#1)

The first article investigates the effects of C-S-H gel seeding on the hydration and mechanical properties of one PC and two BCs at w/c of 0.50 and 0.40. The study focuses on two C-S-H nano-seed-based admixtures, Master X-Seed 130 and Master X-Seed STE 53. The investigation employs a range of techniques, including calorimetry, thermal analysis, X-ray powder diffraction (XRPD), mercury intrusion porosimetry (MIP), and mechanical strength testing.

Key findings from this study reveal that the compressive strength at 1 day for the PC sample with a w/c of 0.50 increased significantly from 15 MPa for the unseeded mortar to 24 MPa and 22 MPa for mortars seeded with Master X-Seed 130 and Master X-Seed STE-53, respectively. Despite the lack of significant acceleration in the hydration of alite and belite phases within the first 1 and 28 days, C-S-H seeding notably enhanced the hydration rates of $C_4AF$ and $C_3A$. For the PC paste with a w/c of 0.40, the degree of $C_4AF$ reaction increased from 10%, 30%, and 40% at 1, 7, and 28 days to 20%, 45%, and 60% with seeding, respectively. This increase led to a higher early ettringite content, although the increase in this phase did not persist at 28 days, at which point an increase in carbonate-containing AFm-type phases was observed. Additionally, the admixtures contributed to the formation of more amorphous components in the pastes at later hydration stages, partly due to increased amorphous iron siliceous hydrogarnet formation from enhanced $C_4AF$ reactivity.

Article 2 (A#2)

The second article aims to elucidate the mechanisms underlying the effects of C-S-H gel seeding by examining one commercial PC and two industrial trial BCs. Three different admixtures were tested: two commercial C-S-H seeding products (Master X-Seed 100 and Master X-Seed 130) and triisopropanolamine (TIPA), a commonly used alkanolamine. The study utilized a variety of analytical techniques, including calorimetry, ultrasonic pulse velocity, thermal analysis, and Rietveld refinement of XRPD data. Notably, an in situ X-ray synchrotron powder diffraction study allowed for detailed monitoring of the evolution of each crystalline phase over time. The internal standard method was employed to measure changes in the overall amorphous content.

The findings indicate that C-S-H seeding did not significantly accelerate the hydration of alite and belite phases in the three cements studied. However, the seeding did enhance the dissolution of sulfate and aluminate phases, which led to faster ettringite crystallization and improved early-age mechanical properties. The study also demonstrated a synergistic effect between C-S-H seeding and alkanolamine, resulting in enhanced performance.

Article 3 (A#3)

In the third article, the acceleration of hydration in three different $LC^3$-50 binders (comprising 50 wt% clinker, 30 wt% calcined clay, 15 wt% limestone, and 5 wt% gypsum) was studied using a commercial C-S-H-based admixture. The binders were prepared from clays with varying

kaolinite contents. Both mortars and pastes were prepared using a new polycarboxylate ether (PCE)-based superplasticizer, specifically designed to address the common problem of early-age fluidity loss in $LC^3$ binders. The superplasticizer works by gradually releasing clusters of PCE molecules over time. The chosen strength enhancing admixture was Master X-Seed STE 53.

The results demonstrate that the initial fluidity loss in $LC^3$ mortars can be effectively managed with the new PCE-based superplasticizer. Moreover, the use of the C-S-H seeding admixture significantly enhanced the compressive strengths of $LC^3$ mortars at 1 day, with this improvement sustained up to 28 days.

Article 4 (A#4)

The fourth article, similar in scope to A#3, investigates the acceleration of hydration in three different $LC^3$-50 binders, each with different kaolinite contents. However, in this study, Master X-Seed 130 was used as the strength enhancing admixture. Both A#3 and A#4 utilized the new PCE-based superplasticizer, Master$CO_2$re 3240, specifically developed to address the early-age fluidity loss in $LC^3$ binders. The results from both studies confirm that this superplasticizer effectively counteracts the initial fluidity loss in $LC^3$ mortars. Additionally, the respective C-S-H seeding admixtures in each study significantly improved the compressive strengths of $LC^3$ mortars at 1 day, with these improvements maintained for up to 28 days.

Article 5 (A#5)

In the fifth article, the researchers employed in situ synchrotron X-ray powder diffraction to analyse the hydration reactions during the first day in $LC^3$ binders. The effects of two different superplasticizers and three strength enhancing admixtures were examined. The diffraction data were analysed using the Rietveld method and were compared with mass balance calculations to provide a comprehensive understanding of the hydration process.

The study found that for $LC^3$ binders without strength enhancing admixtures, the hydration rates of clinker phases ($C_3S$, $C_3A$, and $C_4AF$) were accelerated due to the filler effect of the calcined clay and limestone components. When C-S-H-based admixtures were added, the hydration of tricalcium aluminate and ferrite was further accelerated. The study also conclusively demonstrated that the pozzolanic reaction begins approximately 7 hours after mixing under the studied conditions. The degree of metakaolin hydration at 22 hours was estimated to be around 10%.

Article 6 (A#6)

The sixth article analyses an $LC^3$-35 binder (containing 35 wt% Portland clinker) and compares its performance to both traditional PC and a standard $LC^3$-50 binder. This research investigates the effects of two superplasticizers and a strength enhancing admixture in both mortars and pastes. The study found that higher calcined clay content exacerbates the slump retention problem, which was effectively resolved by using the new superplasticizer. Furthermore, the low early-age mechanical strengths of the $LC^3$-35 binder were partially improved through the addition of a C-S-H nucleation seeding admixture. With the appropriate combination of admixtures, $LC^3$-35 binders were able to achieve strength values comparable to those of pure PC and $LC^3$-50 at 7 and 28 days.

X-ray powder diffraction results for the $LC^3$-35 pastes, when treated with the strength enhancing admixture, indicated an accelerated reaction rate of $C_4AF$, leading to the greater formation of AFt and AFm phases. Approximate mass balance calculations were used to estimate the degree of metakaolin reaction. The study also introduced an environmental performance indicator to evaluate the environmental impact of the binders within the $LC^3$ framework, emphasizing the potential for sustainable construction practices using $LC^3$ technology.

Together, these publications contribute to a deeper understanding of how to optimize alternative cements for sustainability, offering practical solutions to reduce the carbon footprint of the construction industry.

Chapter 4: General results and discussion

The fourth chapter is the general discussion section, in which the results of these papers are not repeated but an integrative approach is developed by inspecting the effect of different admixtures on samples with a low $CO_2$ footprint. First, the discussion focuses on the impact of superplasticizers on the slump retention of $LC^3$ systems. The analysis emphasizes how PCEs based on ICS technology contribute to improved workability and hydration behaviour, facilitating the effective use of SCMs.

Second, the chapter examines the effect of strength enhancing admixtures, particularly the incorporation of C-S-H seeding admixtures, on the mechanical performance and durability of $LC^3$ binders. The discussion highlights the significant improvements in compressive strength, both in the early stages and over time, due to the refined microstructure and enhanced distribution of hydration products. Furthermore, it explores how the accelerated hydration of specific phases, such as aluminates and sulfates, not only expedites strength development but also contributes to a more cohesive cement matrix, thereby enhancing resistance to environmental degradation.

Overall, this chapter aims to integrate the findings from the various studies to illustrate a comprehensive understanding of how these innovative admixtures can optimize the performance of $LC^3$ binders while maintaining a sustainable approach in construction applications.

Chapter 5 and 6: Conclusion (English and Spanish version)

The fifth chapter of the thesis contains a brief overview and conclusion. It summarizes the main findings regarding the enhancement of the hydration process and microstructural development of $LC^3$ binders through the use of PCEs based on ICS technology and strength enhancing admixtures based on C-S-H seeding.

The chapter highlights the significant improvements in both early and long-term compressive strength achieved by incorporating C-S-H seeding admixtures, which refine the microstructure, enhance packing density, and optimize the distribution of hydration products, particularly C-S-H gel. The chapter also discusses the role of strength enhancing admixtures in accelerating the hydration of specific phases, such as aluminates and sulfates, which further improve mechanical properties. Although the reactivity of $C_3S$ remains largely unchanged, the expedited hydration of $C_3A$ and $C_4AF$ contributes to a more cohesive cement matrix. This rapid formation of solid hydration products leads to early strength development and increased microstructural density,

improving resistance to environmental degradation. Overall, the chapter emphasizes the synergistic effects of alkanolamines and C-S-H seeding admixtures in optimizing the performance of $LC^3$ binders through enhanced hydration kinetics and microstructural quality. The sixth chapter is the Spanish translation of the previous one.

# Resumen (Summary in Spanish)

El PC sigue siendo el material de construcción más utilizado en todo el mundo debido a sus sólidas propiedades mecánicas, versatilidad y disponibilidad. Sin embargo, el costo ambiental de su producción es considerable. El proceso de fabricación del PC es responsable de la emisión de aproximadamente 0,9 toneladas de $CO_2$ por cada tonelada de cemento producida, lo que contribuye a aproximadamente el 8% de las emisiones antropogénicas globales de $CO_2$. Estas emisiones se originan principalmente en tres etapas clave en el proceso de producción.

En primer lugar, durante la etapa de calcinación, la piedra caliza (carbonato de calcio, $CaCO_3$), la principal materia prima, se calienta a altas temperaturas, lo que lleva a su descomposición en cal (óxido de calcio, CaO) y dióxido de carbono ($CO_2$). Esta reacción química es responsable de una parte significativa de las emisiones de $CO_2$. En segundo lugar, el proceso de clinkerización, donde las materias primas se calientan a temperaturas que oscilan entre 1400 y 1450 °C, es muy demandante de energía. El calor necesario para este proceso generalmente se produce quemando combustibles fósiles, lo que contribuye aún más a la huella de carbono general. Por último, el proceso de molienda, que convierte el clínker en el polvo fino conocido como cemento, consume cantidades significantes de electricidad, lo que genera emisiones indirectas de gases de efecto invernadero a través del consumo de energía.

Dado el importante impacto ambiental del PC, existe una necesidad de soluciones alternativas que mantengan las propiedades deseables del material y al mismo tiempo reduzcan su huella de carbono.

Cementos ricos en belita como alternativa

Una alternativa prometedora al PC es el uso de cementos belíticos (BC). Estos cementos tienen similares componentes químicos al PC, pero difieren en su composición mineral, lo que da como resultado menores emisiones de $CO_2$ durante la producción. Los BC se caracterizan por una mayor proporción de belita ($C_2S$) y una menor proporción de alita ($C_3S$) en comparación con el PC tradicional. Esta alteración en la composición ofrece varios beneficios ambientales y técnicos.

En primer lugar, los cementos belíticos producen alrededor de un 8% menos de emisiones de $CO_2$ debido a la menor cantidad de caliza requerida en su producción. Esta reducción es significativa en el contexto de los esfuerzos globales para disminuir las emisiones de gases de efecto invernadero. En segundo lugar, el proceso de hidratación de los BC genera un menor aumento de temperatura y una menor contracción química, lo que reduce el riesgo de agrietamiento térmico en las estructuras de hormigón. En tercer lugar, los BC tienden a tener una vida útil más larga, en parte debido al mayor contenido relativo de gel C-S-H (hidrato de silicato de calcio), que es la principal fase aglutinante del cemento. Además, las temperaturas de funcionamiento más bajas requeridas en el horno (aproximadamente 1250–1300 °C) no solo reducen el consumo de energía, sino que también dan como resultado menos emisiones de gases nocivos y simplifican el mantenimiento del revestimiento del horno. Por último, los requisitos de energía para producir BC son ligeramente inferiores debido a la diferencia en las entalpías de formación de la belita y la alita, ya que la belita requiere menos energía para formarse.

Sin embargo, a pesar de estas ventajas, la adopción generalizada de los cementos belíticos enfrenta varios desafíos. El problema principal es la reactividad más lenta de la fase belítica no activada a temperatura ambiente, lo que conduce a un menor desarrollo de la resistencia inicial del hormigón. Además, la producción de cementos belíticos requiere aproximadamente un 15 % más de energía para la molienda, ya que los materiales son más difíciles de procesar. La necesidad de velocidades de enfriamiento más rápidas del clínker también aumenta el consumo de energía y la inversión de capital. Además, las temperaturas más bajas del horno necesarias para la producción de cemento belítico limitan el uso de combustibles alternativos, que de otro modo podrían ayudar a reducir la huella de carbono general del proceso.

Reducción del factor clínker: el papel de los materiales cementantes suplementarios (SCM)

Reducir el factor clínker en la producción de cemento se considera una de las estrategias más eficaces para reducir las emisiones de $CO_2$. Este enfoque implica el uso de SCM para reemplazar una parte del clínker en el cemento. Los SCM son materiales que, cuando se combinan con cal o PC, exhiben propiedades cementantes. Los SCM más comúnmente utilizados incluyen escoria de alto horno granulada molida (GGBS), cenizas volantes (FA), arcillas calcinadas (CC), puzolanas naturales (NP) y humo de sílice (SF). Estos materiales pueden reducir significativamente la huella de carbono de la producción de cemento.

El uso de SCM está impulsado tanto por factores ambientales como económicos. Si bien las cenizas volantes y los GGBFS han sido tradicionalmente los SCM más utilizados, las limitaciones de la oferta y la creciente demanda han llevado a la exploración de materiales alternativos. Entre estos, los cementos de arcilla calcinada de piedra caliza ($LC^3$) han surgido como una opción particularmente prometedora. $LC^3$ es una mezcla ternaria de PC, piedra caliza y arcilla calcinada, específicamente arcillas caoliníticas, que son abundantes y están ampliamente disponibles.

Los SCM contribuyen a la durabilidad y el rendimiento a largo plazo del hormigón a través de su actividad puzolánica. La actividad puzolánica se refiere a la capacidad de un material de reaccionar con la portlandita (hidróxido de calcio) liberada durante la hidratación del cemento, formando un gel C–(A)-S–H adicional, que mejora la resistencia y la durabilidad del hormigón. Además, los SCM pueden mejorar la cinética de hidratación del cemento al actuar como sitios de nucleación para la precipitación de C–S–H durante el período de aceleración. Este “efecto de relleno” puede mejorar la resistencia en edad temprana y reducir la permeabilidad del hormigón, lo que conduce a una mejor durabilidad a largo plazo.

Sin embargo, el uso de SCM también presenta desafíos. La dilución del cemento por SCM generalmente da como resultado una menor resistencia en edad temprana, lo que puede ser un inconveniente significativo en aplicaciones donde el desarrollo rápido de la resistencia es crítico. Además, la mayor demanda de agua asociada con los SCM, debido a su tamaño de partícula más fino, puede provocar una pérdida de trabajabilidad en el hormigón fresco. En el caso de los aglutinantes $LC^3$, el contenido reducido de portlandita puede acelerar la carbonatación del hormigón, que es el proceso por el cual el $CO_2$ de la atmósfera reacciona con el hidróxido de calcio en la pasta de cemento, lo que lleva a una pérdida de alcalinidad y una posible corrosión de las armaduras.

Abordar los desafíos con aditivos

Para hacer que los cementos menos contaminantes, como los cementos $LC^3$ y Belite, sean más competitivos con el PC tradicional, el uso de aditivos químicos se ha vuelto esencial. Estos aditivos están diseñados para abordar los desafíos específicos asociados con los cementos alternativos, como la fluidez reducida y la resistencia en edad temprana.

Se han desarrollado superplastificantes, en particular los basados en PCE, para mejorar la trabajabilidad de las mezclas cementosas. La nueva generación de superplastificantes basados en PCE con Sistema Inteligente de Clúster (ICS) son especialmente eficaces en los aglutinantes $LC^3$, donde ayudan a mantener la fluidez a lo largo del tiempo, evitando la rápida pérdida de asentamiento que es típica de los superplastificantes convencionales. Estos aditivos funcionan liberando grupos de moléculas de PCE de forma gradual, lo que garantiza que el hormigón siga siendo trabajable durante un período más largo, lo que es crucial para aplicaciones prácticas.

Además de los superplastificantes, se utilizan aditivos que mejoran la resistencia para mejorar la resistencia inicial de los cementos alternativos. Un enfoque eficaz es el uso de la siembra de C-S-H, donde se añaden partículas nanoestructuradas de C-S-H a la mezcla de cemento para acelerar el proceso de hidratación. Cuando se combinan con alcanolaminas, que son compuestos químicos que aceleran la hidratación de las fases de aluminato, estos aditivos pueden mejorar significativamente la resistencia inicial de los BC y $LC^3$ sin comprometer su rendimiento a largo plazo. El mecanismo detrás de esta mejora implica la creación de sitios de nucleación adicionales para el crecimiento de C-S-H, reduciendo la microporosidad de la pasta de cemento y dando lugar a un material más denso y resistente.

Resúmenes de los capítulos

Capítulo 1: Introducción y metodología

El primer capítulo de esta tesis se divide en dos secciones principales. La primera sección introduce a la naturaleza de los cementos, centrándose en el PC y su impacto ambiental. Analiza los diversos desafíos que enfrenta la industria del cemento, en particular en relación con las emisiones de carbono, y presenta tipos alternativos de cemento que tienen como objetivo reducir la huella de carbono. La sección también profundiza en el papel de los aditivos para la mejora de las propiedades de estos cementos alternativos, haciéndolos más viables para un uso generalizado.

La segunda sección del capítulo describe la metodología experimental utilizada en la tesis. Describe los procedimientos de preparación de muestras y proporciona una descripción detallada de las técnicas empleadas en la investigación, incluida la calorimetría, la difracción de polvo de rayos X, el análisis térmico y la porosimetría por intrusión de mercurio. Estas técnicas son cruciales para comprender los procesos de hidratación y las propiedades mecánicas de los cementos estudiados.

Capítulo 2: Objetivos de la tesis

El capítulo dos detalla los principales objetivos de la tesis, que se centran en reducir las emisiones de $CO_2$ en la producción de cemento mediante el uso de materiales sostenibles. La investigación examina dos tipos de cemento: los cementos belíticos, que ofrecen una reducción

del 10-12% en las emisiones de $CO_2$, y los cementos de arcilla calcinada y caliza ($LC^3$), que pueden lograr una reducción de hasta el 40% al sustituir parte del clínker con arcilla calcinada y caliza.

Aunque ambos materiales presentan desafíos en cuanto a la resistencia en las primeras edades, se da mayor énfasis al $LC^3$ debido a sus mayores beneficios ambientales. Los objetivos de la investigación son evaluar el impacto de los superplastificantes basados en Sistema de Clúster Inteligente (ICS) sobre la trabajabilidad del $LC^3$, mejorar la resistencia a corto y largo plazo mediante el uso de aditivos de siembra de C-S-H, estudiar la influencia de los aditivos en la cinética de hidratación y mejorar la microestructura al reducir la porosidad mediante el uso de aditivos. Estos esfuerzos tienen como objetivo promover el $LC^3$ como una solución clave para la producción de cemento con bajas emisiones de $CO_2$.

Capítulo 3: Consolidación de los trabajos de investigación

El capítulo tres consolida los resultados de la investigación presentados en una serie de trabajos derivados de la tesis. Cada trabajo aborda un aspecto específico de la investigación, contribuyendo a una comprensión integral de los efectos de diversos aditivos en las propiedades de los cementos belíticos y $LC^3$.

Artículo 1 (A#1)

El primer artículo investiga los efectos de la siembra de gel de hidrato de silicato de calcio (C-S-H) en la hidratación y las propiedades mecánicas de un PC y dos cementos belíticos con relaciones agua-cemento (w/c) de 0,50 y 0,40. El estudio se centra en dos aditivos basados en nanosemillas de C-S-H, Master X-Seed 130 y Master X-Seed STE-53. La investigación emplea una variedad de técnicas, que incluyen calorimetría, análisis térmico, difracción de rayos X en polvo (XRPD), porosimetría por intrusión de mercurio (MIP) y pruebas de resistencia mecánica.

Los hallazgos clave de este estudio revelan que la resistencia a la compresión a 1 día para la muestra de PC con una relación agua/cemento de 0,50 aumentó significativamente de 15 MPa para el mortero sin sembrar a 24 MPa y 22 MPa para los morteros sembrados con Master X-Seed 130 y Master X-Seed STE-53, respectivamente. A pesar de una significativa falta de aceleración en la hidratación de las fases de alita y belita dentro de los primeros 1 y 28 días, la siembra de C-S-H mejoró notablemente las tasas de hidratación del $C_4AF$ y $C_3A$. Para la pasta de PC con una relación agua/cemento de 0,40, el grado de reacción de $C_4AF$ aumentó de 10 %, 30 % y 40 % a los 1, 7 y 28 días a 20 %, 45 % y 60 % con siembra, respectivamente. Este aumento condujo a un mayor contenido de etringita temprana, aunque el aumento de esta fase persistió a los 28 días, momento en el que se observó un aumento de las fases tipo AFm que contenían carbonato. Además, las mezclas contribuyeron a la formación de más componentes amorfos en las pastas en etapas de hidratación posteriores, en parte debido a una mayor formación de hidrogranate silíceo de hierro amorfo a partir de una reactividad mejorada de $C_4AF$.

Artículo 2 (A#2)

El segundo artículo tiene como objetivo dilucidar los mecanismos subyacentes a los efectos de la siembra de gel C-S-H mediante el examen de un PC comercial y dos cementos belíticos industriales. Se probaron tres mezclas diferentes: dos productos de siembra C-S-H comerciales (Master X-Seed 100 y Master X-Seed 130) y triisopropanolamina (TIPA), una alcanolamina de

uso común. El estudio utilizó una variedad de técnicas analíticas, incluida la calorimetría, la velocidad del pulso ultrasónico, el análisis térmico y el refinamiento de Rietveld de los datos de XRPD. Cabe destacar que un estudio de difracción de polvo de rayos X *in situ* permitió un seguimiento detallado de la evolución de cada fase cristalina a lo largo del tiempo. Se empleó la metodología de estándar interno para medir los cambios en el contenido amorfo general.

Los hallazgos indican que la siembra de C-S-H no aceleró significativamente la hidratación de las fases de alita y belita en los tres cementos estudiados. Sin embargo, la siembra sí mejoró la disolución de las fases de sulfato y aluminato, lo que condujo a una cristalización más rápida de la etringita y mejoró las propiedades mecánicas en edad temprana. El estudio también demostró un efecto sinérgico entre la siembra de C-S-H y la alcanolamina, lo que resultó en un mejor rendimiento.

Artículo 3 (A#3)

En el tercer artículo, se estudió la aceleración de la hidratación en tres aglutinantes $LC^3$-50 diferentes (que comprenden 50% de clínker, 30% de arcilla calcinada, 15% de piedra caliza y 5% de yeso) utilizando un aditivo comercial basado en C-S-H. Los aglutinantes se prepararon a partir de arcillas con distintos contenidos de caolinita. Tanto los morteros como las pastas se prepararon utilizando un nuevo superplastificante basado en éter de policarboxilato (PCE), diseñado específicamente para abordar el problema común de la pérdida de fluidez en etapas tempranas en los aglutinantes $LC^3$. El superplastificante funciona liberando gradualmente grupos de moléculas de PCE con el tiempo. El aditivo para mejorar la resistencia elegido fue Master X-Seed STE 53.

Los resultados del estudio demuestran que la pérdida de fluidez inicial en los morteros $LC^3$ se puede gestionar de forma eficaz con el nuevo superplastificante basado en PCE. Además, el uso del aditivo de siembra C-S-H mejoró significativamente las resistencias a la compresión de los morteros $LC^3$ al día, y esta mejora se mantuvo hasta los 28 días.

Artículo 4 (A#4)

El cuarto artículo, de alcance similar al A#3, investiga la aceleración de la hidratación en tres ligantes $LC^3$-50 diferentes, cada uno con diferentes contenidos de caolinita. Sin embargo, en este estudio, se utilizó Master X-Seed 130 como aditivo potenciador de la resistencia. Tanto el A#3 como el A#4 utilizaron el nuevo superplastificante basado en PCE, Master$CO_2$re 3240, desarrollado específicamente para abordar la pérdida de fluidez en edad temprana en los ligantes $LC^3$. Los resultados de ambos estudios confirman que este superplastificante contrarresta eficazmente la pérdida de fluidez inicial en los morteros $LC^3$. Además, los respectivos aditivos de siembra C-S-H en cada estudio mejoraron significativamente las resistencias a la compresión de los morteros $LC^3$ al día, y estas mejoras se mantuvieron hasta 28 días.

Artículo 5 (A#5)

En el quinto artículo, se empleó difracción de polvos de rayos X de sincrotrón *in situ* para analizar las reacciones de hidratación durante el primer día en aglutinantes $LC^3$. Se examinaron los efectos de dos superplastificantes diferentes y tres aditivos mejoradores de la resistencia. Los

datos de difracción se analizaron utilizando el método de Rietveld y se compararon con cálculos de balance de masa para proporcionar una comprensión integral del proceso de hidratación.

El estudio encontró que para los aglutinantes $LC^3$ sin aditivos mejoradores de la resistencia, las tasas de hidratación de las fases de clínker ($C_3S$, $C_3A$ y $C_4AF$) se aceleraron debido al efecto de relleno de los componentes de arcilla calcinada y piedra caliza. Cuando se agregaron aditivos basados en C-S-H, la hidratación del aluminato tricálcico y la ferrita se aceleró aún más. El estudio también demostró de manera concluyente que la reacción puzolánica comienza aproximadamente 7 horas después de la mezcla en las condiciones estudiadas. El grado de hidratación del metacaolín a las 22 horas se estimó en alrededor del 10%.

Artículo 6 (A#6)

El sexto artículo analiza un aglutinante $LC^3$-35 (que contiene un 35% de clínker Portland) y compara su rendimiento con el del PC tradicional y con un aglutinante $LC^3$-50 estándar. Esta investigación investiga los efectos de dos superplastificantes y un aditivo potenciador de la resistencia tanto en morteros como en pastas. El estudio descubrió que un mayor contenido de arcilla calcinada aumenta el problema de retención del asentamiento, que se resolvió de manera efectiva mediante el uso de un nuevo superplastificante. Además, las bajas resistencias mecánicas iniciales del aglutinante $LC^3$-35 se mejoraron parcialmente mediante la adición de un aditivo de siembra de nucleación C-S-H. Con la combinación adecuada de aditivos, los aglutinantes $LC^3$-35 pudieron lograr valores de resistencia comparables a los del PC puro y el $LC^3$-50 a los 7 y 28 días.

Los resultados de difracción de rayos X de polvos para las pastas $LC^3$-35, cuando se trataron con el aditivo para mejorar la resistencia, indicaron una velocidad de reacción acelerada de $C_4AF$, lo que llevó a una mayor formación de fases AFt y AFm. Se utilizaron cálculos aproximados de balance de masa para estimar el grado de reacción del metacaolín. El estudio también introdujo un indicador de desempeño ambiental para evaluar el impacto ambiental de los aglutinantes dentro del marco $LC^3$, enfatizando el potencial de prácticas de construcción sustentables utilizando la tecnología $LC^3$.

En conjunto, estas publicaciones contribuyen a una comprensión más profunda de cómo optimizar los cementos alternativos para la sustentabilidad, ofreciendo soluciones prácticas para reducir la huella de carbono de la industria de la construcción.

Capítulo 4: Resultados generales y discusión

El cuarto capítulo es la sección de discusión general, en la cual no se repiten los resultados de estos artículos, sino que se desarrolla un enfoque integrador al inspeccionar el efecto de diferentes aditivos en muestras con una baja huella de $CO_2$. Primero, la discusión se centra en el impacto de los superplastificantes en la retención de asentamiento de los sistemas $LC^3$. El análisis enfatiza cómo los PCE basados en la tecnología ICS contribuyen a mejorar la trabajabilidad y el comportamiento de hidratación, facilitando el uso efectivo de SCM.

En segundo lugar, el capítulo examina el efecto de los aditivos potenciadores de resistencia, en particular la incorporación de aditivos de siembra de C-S-H, en el rendimiento mecánico y la durabilidad de los aglomerantes $LC^3$. La discusión destaca las mejoras significativas en la

resistencia a la compresión, tanto en las etapas tempranas como a lo largo del tiempo, debido a la microestructura refinada y la mejor distribución de los productos de hidratación. Además, explora cómo la hidratación acelerada de fases específicas, como los aluminatos y sulfatos, no solo acelera el desarrollo de la resistencia, sino que también contribuye a una matriz de cemento más cohesiva, mejorando así la resistencia a la degradación ambiental.

En general, este capítulo tiene como objetivo sintetizar los hallazgos de los diversos estudios para ilustrar una comprensión completa de cómo estos aditivos innovadores pueden optimizar el rendimiento de los aglomerantes $LC^3$ mientras se mantiene un enfoque sostenible en las aplicaciones de construcción.

Capítulo 5 y 6: Conclusiones (Versiones en inglés y español)

El quinto capítulo de la tesis contiene un breve resumen y conclusión (en inglés). Resume los hallazgos principales sobre la mejora del proceso de hidratación y el desarrollo microestructural de los aglomerantes $LC^3$ mediante el uso de PCE basados en la tecnología del ICS y aditivos de mejora de fuerza basados en siembra de C-S-H.

El capítulo destaca las mejoras significativas en la resistencia a la compresión, tanto a corto como a largo plazo, logradas al incorporar aditivos de siembra de C-S-H, que refinan la microestructura, mejoran la densidad de empaquetamiento y optimizan la distribución de los productos de hidratación, particularmente el gel de C-S-H. El capítulo también discute el papel de los aditivos potenciadores de resistencia en la aceleración de la hidratación de fases específicas, como los aluminatos y sulfatos, que mejoran aún más las propiedades mecánicas. Aunque la reactividad de $C_3S$ permanece en gran medida sin cambios, la hidratación acelerada de $C_3A$ y $C_4AF$ contribuye a una matriz de cemento más cohesiva. Esta rápida formación de productos de hidratación sólidos conduce a un desarrollo temprano de la resistencia y a una mayor densidad microestructural, mejorando la resistencia a la degradación ambiental. En general, el capítulo enfatiza los efectos sinérgicos de alcanolaminas y los aditivos de siembra de C-S-H en la optimización del rendimiento de los aglomerantes $LC^3$ a través de una mejor cinética de hidratación y calidad microestructural. El sexto capítulo es la traducción al español del anterior.

# 1. Introduction

## 1.1. Introduction to cements

In the field of construction, cements play a fundamental role as essential materials for the creation of durable and functional structures. Since ancient times, cement has been used to bond various construction materials, providing stability and strength to buildings. In the context of growing concern over climate change and the need to reduce greenhouse gas emissions, the cement industry faces a crucial challenge: mitigating its carbon footprint. With global production accounting for a significant portion of $CO_2$ emissions, it becomes imperative to explore and develop innovative strategies to reduce the environmental impact of cement production. In this study, we will delve into the various techniques and technologies employed to decrease $CO_2$ emissions in cement manufacturing, evaluating their effectiveness, feasibility, and potential to promote a more sustainable and environmentally friendly industry.

### 1.1.1. Environmental problem in the cement industry

Despite being the most widely used material in current construction, cement remains highly controversial due to its significant environmental impact in the 21st century. With every ton of cement produced, a substantial amount of fuel and electricity—ranging between 60 and 130 kg and 110 kWh, respectively—is consumed, leading to the emission of approximately 0.83 tons of $CO_2$ into the atmosphere. Aware of this impact, chemists and engineers have dedicated considerable efforts over the past three decades to mitigate the environmental consequences of cement production and enhance the durability of structures, both old and new.

The cement industry's extensive use results in the emission of a staggering 2.3 billion tonnes of $CO_2$ annually [1]. Recognizing the urgency of addressing its environmental footprint, the industry is actively pursuing approaches to achieve carbon neutrality by 2050 through various initiatives [2–4]. Despite significant progress in reducing $CO_2$ emissions per ton of cement clinker through the use of alternative fuels and advanced production methods, limestone decomposition remains an unavoidable stage in the process.

While the environmental impact of cement production extends beyond $CO_2$ emissions [4–6], efforts to mitigate the $CO_2$ footprint are prioritized [7,8]. However, decarbonizing cement production presents significant challenges, particularly due to the essential role of limestone.

Global concerns about climate change have prompted action from governments, industries, and society at large. The Paris Agreement, endorsed by 175 parties, underscores the need to limit the global temperature rise to below 2°C above preindustrial levels, with further efforts to keep it below 1.5°C [9].

Cement is the most massive manufactured product on Earth, forming the backbone of concrete production—a material second only to water in human consumption [10]. Approximately 8% of total anthropogenic $CO_2$ emissions are attributed to cement production, with the industry also representing 7% of global industrial energy use. While 90% of cement is produced in non-OECD countries to meet high concrete demand, this trend is expected to continue, emphasizing the need for sustainable solutions [11,12].

Reducing the clinker factor is identified as the most effective strategy for reducing the $CO_2$ footprint of PC. This has led to the increasing adoption of blended cements, which incorporate SCMs to replace part of the clinker. GGBS and FA are among the commonly used SCMs, accounting for approximately 15% of total cement production [11]. However, the availability of FA is expected to decline due to the shift towards cleaner energy production, necessitating the exploration of new sources for SCMs to significantly alter the current landscape.

### 1.1.2. Portland cement, PC

PC is the most common type of cement used in construction and civil engineering. It consists of clinker and a source of sulfates, with or without additions. The chemical composition of typical Portland clinker is 67% CaO, 22% $SiO_2$, 5% $Al_2O_3$, 3% $Fe_2O_3$, and 3% other minor components. Portland clinker is composed of four major phases, two calcium silicates called alite and belite, and two aluminate bearing phases, tricalcium aluminate and calcium ferrite. There may also be other minor phases such as alkaline sulfates or Ca and Mg oxides [13]. A typical mineralogical composition may be 60% alite, 20% belite, 6% tricalcium aluminate, 12% calcium ferrite, and 2% minor components.

### 1.1.3. Belite cement, BC

Belite clinkers typically contain minimal amounts of alite (10–30 wt%) and a substantial proportion of belite (40–60 wt%). The anticipated reduction in direct $CO_2$ footprint from belite clinker (BC) is moderate, approximately 10–12%.

Additional incentives to favour belite over alite include a lower maximum kiln operating temperature, around 1200–1350 °C, compared to 1450-1500 °C in PC [14]. This results in further reductions in $CO_2$ and $NO_x$ emissions during combustion. Moreover, the slower temperature rise during belite cement early hydration and their lower chemical shrinkage minimize cracking, while its longer service life is attributed to a greater proportion of C–S–H gel per unit volume when compared to PC.

However, the main issue is that the lower reactivity of ordinary belite with water leads to slow early-age strength development, which does not meet current standards [15].

### 1.1.4. Supplementary cementitious materials, SCMs

SCMs are finely ground powders composed of soluble siliceous, aluminosiliceous, or calcium aluminosiliceous substances. They serve as partial replacements for clinker in cement production or as substitutes for PC in concrete mixtures. Many SCMs are derived from industrial by-products, such as FA generated by coal-fired power plants, while others are naturally occurring minerals requiring significantly less energy for processing compared to PC. SCMs play a crucial role in reducing carbon dioxide emissions associated with concrete production and are considered a key strategy for mitigating environmental impact [16].

The utilization of SCMs to replace a portion of clinker in cement represents the most successful approach for reducing $CO_2$ emissions in the global cement industry [10,16,17]. However, while employing SCMs to lower the clinker factor has proven effective in reducing carbon emissions linked with PC and the broader concrete industry, the current availability of typical SCMs like fly

ash and slag falls short of meeting future demand, accounting for only about 10% of all cement produced. In this scenario, calcined clays emerge as key SCMs because they are sufficiently available [18].

### 1.1.5. Limestone calcined clay cement, $LC^3$

Calcined clays present an ecologically and economically appealing alternative as SCMs. These clays, sourced globally, entail reduced $CO_2$ emissions during calcination owing to their diminished lime content and the lower temperature requirements for treatment compared to cement clinker.

Clay particles consist of numerous layers, usually ranging from tens to hundreds, structured as a mix of alternating silica tetrahedral and alumina octahedral sheets [19,20]. The three most common types of clay are kaolinite, illite, and montmorillonite (smectite). Kaolinite, a 1:1 clay, has a layer structure comprising one silica layer and one alumina layer. In contrast, illite and montmorillonite are 2:1 clays, with layers made up of two silica layers enclosing an alumina layer. In the case of kaolinite, both aluminate and silicate groups are present on separate interlayer surfaces, allowing aluminium and silica to be available for reaction after calcination. Kaolinitic clays are known for their high pozzolanic reactivity following calcination [21].

The way metakaolin reacts is influenced by the composition of the blend undergoing hydration. When metakaolin reacts with portlandite, the primary products formed are C-S-H or C-(A-)S-H gels. Moreover, the formation of other phases in the system can vary depending on their presence or absence. In sulfate or carbonate-rich environments, AFt and/or AFm-Hc/Mc phases are produced, while in their absence, stratlingite and hydroxide-AFm type phases are more likely to form [22,23]. In pozzolanic reactions, both the Ca/Si ratio and the water content in the C-S-H/C-(A-)S-H gel are variable, influenced by factors such as the chemical composition of the pozzolan, hydration conditions, and reactant proportions. The Ca/Si ratio typically ranges from 0.8 to 1.5, while the water content depends on the porosity and curing environment. The main metakaolin reactions are summarized in Equation 1-3 [22–26].

$$AS_2 + CH + H \rightarrow C_4AH_{13}/C_3AH_6/C_2ASH_8 + \text{C-S-H/C-(A-)S-H}$$

*Equation 1. Pozzolanic reaction in absence of sulfates / carbonates*

$$AS_2 + CH + C\bar{S}H + H \rightarrow \text{C-S-H/C-(A-)S-H} + C_6A\bar{S}_3H_{32}$$

*Equation 2. Pozzolanic reaction in presence of sulfates*

$$AS_2 + CH + C\bar{C} + H \rightarrow C_4A\bar{C}H_{11}/C_4A\bar{C}_{0.5}H_{12} + \text{C-S-H/C-(A-)S-H}$$

*Equation 3. Pozzolanic reaction in presence of carbonate*

$LC^3$ is a group of cements incorporating a blend of calcined clay and limestone as a partial substitute for clinker. In the $LC^3$-X designation, X represents the clinker content in percentage by mass. For instance, $LC^3$-50, the most extensively studied composition, comprises 50% clinker, typically, 30% calcined clay, and 15% limestone. However, the proportion of calcined clay to limestone can be adjusted, as elaborated further below. The remaining 5% consists of gypsum.

$LC^3$-50, which substitutes 50% of clinker with a mixture of limestone and calcined clay, stands as the prime formulation for achieving significant $CO_2$, up to 40% $CO_2$ reductions while maintaining strength comparable to PC [27,28]. Numerous studies have corroborated the mechanical [29,30] and durability [31,32] performance of $LC^3$-50. However, the compressive strength of $LC^3$-50 systems, varies with different grades of clay. While early strength is primarily influenced by clinker reaction, a clear correlation between metakaolin content and strength emerges from 2 to 3 days due to synergistic reactions between metakaolin and limestone [30,33].

Reducing clinker content to below 50 wt% presents an opportunity for further $CO_2$ emission reductions. For this reason, studies on PC-SCM mixtures with clinker proportions under 50 wt% are highly pertinent, as highlighted in recent reviews [34–37]. In February 2021, the European Committee for Standardization approved a new standard for CEM II/C-M composite Portland cement, allowing clinker content to be reduced to as low as 50 wt% while maintaining performance. This standard was officially adopted in Spain in July 2021 by the “Comité técnico CTN Cementos y Cales” [38].

## 1.2. Introduction to admixtures

Chemical admixtures commonly found in concrete production may include substances that either delay or accelerate the setting process, thereby directly affecting kinetics [39,40]. Furthermore, in most concrete formulations used in developed countries, a cement dispersing agent is typically incorporated, often referred to as a water-reducing or plasticizing admixture. These water-reducing admixtures, capable of achieving enhanced dispersion, are known as high-range water-reducing admixtures or superplasticizers. Due to their enhanced dispersion properties, these materials improve workability and reduce the formation of cement particle agglomerates [40].

Admixture accelerators, utilized in both standard concrete and shotcrete applications, are extensively employed in contemporary construction due to their capacity to expedite setting time and/or enhance early strength [41,42]. Depending on their precise effects, accelerators can be categorized into two types: setting accelerators, which reduce the transition time of cement-based materials from a plastic to a rigid state, and hardening accelerators, which enhance the early strength of cement-based materials [43].

### 1.2.1. Superplasticiser, SP

Superplasticizers, also referred to as High Water Reducing (HWR) agents, are chemical compounds incorporated into cement to improve the ease of working with and the characteristics of freshly mixed concrete. Various types of superplasticizers exist, primarily categorized based on their chemical composition and how they function. In this thesis, our focus will be on PCE superplasticizers.

All polycarboxylates share two essential components: firstly, a negatively charged (anionic) carboxylate group that facilitates bonding with cement by attaching to the surface of the binder, thereby dispersing it; secondly, a side chain made up of either polyethylene oxide (EO) or a combination of polyethylene and polypropylene oxide (EO/PO) units, which enhances dispersal by creating a barrier effect. The resulting structure, known as a "comb polymer," can be achieved through different chemical processes, leading to a diverse range of PCE products available on the market [44].

In general, superplasticizers achieve dispersion through two primary mechanisms: electrostatic repulsion and steric hindrance [44]. Polycarboxylate superplasticizers interact with cement by physically attaching to positively charged areas on the surface of hydrating cement, primarily targeting compounds such as ettringite, and to a lesser extent, monosulfo-aluminate, and C-S-H gel. It is worth noting that the dissolution of clinker releases calcium ions into the solution, which can adsorb onto the surface of SCMs, providing them with a more positively charged surface and facilitating the adsorption of superplasticizers. The specific surface area (SSA) of the calcined clay and the quantity of calcined clay in the cement composition were found to be the main factors affecting the demand for superplasticizers, irrespective of the type of calcined clay and admixture used [37].

### 1.2.2. Strength enhancing admixtures

There are various strength enhancing admixtures or accelerators available [40–42,45–51]; however, this thesis will focus on three main categories: alkanolamines, C-S-H gel seeds, and mixed admixtures combining C-S-H gel seeds with alkanolamines.

#### 1.2.2.1. Alkanolamines

Alkanolamines have been examined as grinding aids for cement for almost a century, aiming to boost grinding efficiency and decrease $CO_2$ emissions during cement production [51–57]. Due to their organic polar characteristics, alkanolamines act as highly effective dispersants during the cement grinding process, helping to reduce powder clumping and leading to enhanced grinding performance [58].

In recent years, alkanolamines have become increasingly popular as chemical admixtures in cement-based materials, primarily because of their remarkable efficiency even at very low concentrations. Typically, using less than 0.1% (bwc) alkanolamines in cement is suggested to achieve the desired improvements in cement properties [46,53,59,60]. Nevertheless, with the growing use of SCMs, the recommended alkanolamine dosage in cement-based materials needs reassessment due to the considerable chemical differences compared to ordinary PC [61].

The role that alkanolamines play in the hydration process and the microstructural evolution of cement can vary depending on the specific type of alkanolamine employed [62]. Although TEA, TIPA, DEIPA, and EDIPA are the most commonly studied, the most comprehensive research has primarily focused on TEA and TIPA.

##### Alkanolamines in PC

TEA is frequently utilized as accelerator in cement mixtures, significantly shortening setting times and boosting early strength, even in minimal amounts [63]. Earlier findings showed that TEA speeds up the hydration of $C_3A$ but extends the induction period of $C_3S$ [64–66]. This results in reduced formation of portlandite and alters its morphology from large, parallel-stacked lamellar shapes to smaller, distorted actinomorphic forms [63].

Recent research has linked this delay to the adsorption of TEA on the unhydrated components and the chelation between TEA and metal ions present in the pore solution. Around 0.03 wt% TEA led to the formation of the TEA-$Ca^{2+}$ complex, which impeded the precipitation of portlandite (CH) and slowed the hydration process of $C_3S$ [67]. The retardation effect stemmed from the growth of the TEA-AFt complex on the surface of $C_3A$ and partially on $C_3S$, further delaying the formation of C-S-H gel [68,69].

In contrast, TIPA significantly influences the compressive strength of PC after 28 days, enhancing its performance in later hydration stages. TIPA forms complexes with $Fe^{3+}$, which aids in the dissolution and hydration of $C_4AF$ under high-pH conditions [57].

Moreover, TIPA remains in the pore solution longer than TEA, primarily due to the considerable steric hindrance created by its bulky hydroxypropyl groups [59,70,71]. This indicates that TIPA can act as a catalyst for $C_4AF$ hydration once all the gypsum has reacted to form the AFm type phases [72].

### Alkanolamines in $LC^3$ system

The incorporation of alkanolamines plays a key role in the strength development of $LC^3$ [56]. Adjusting sulfate levels appropriately enhances the performance of both TEA and TIPA, with their ability to strengthen $LC^3$ closely tied to changes in hydration kinetics and microstructural evolution. Increasing the sulfate content in $LC^3$ is vital for regulating the accelerated aluminate reaction induced by alkanolamines, leading to more ettringite formation. This higher sulfate content also aids in improving metakaolin hydration, further refining the porosity of the hardened paste and enhancing the material overall performance [62].

Studies have shown that TEA and TIPA both accelerate the aluminate reaction within $LC^3$, although TIPA stands out for its higher efficiency. TIPA significantly increases the hydration degree of $C_4AF$, which results in a greater production of hydrocarboaluminates as $C_4AF$ dissolves, further promoting its interaction with limestone [56,62].

Furthermore, these alkanolamines influence the microstructure of $LC^3$ by altering the morphology of C-A-S-H gel and aluminate hydrates in the hardened paste. They result in thinner inner layers of C-A-S-H, with aluminate hydrates tending to precipitate near unreacted clinker, either blending with or replacing the inner C-A-S-H. TEA is especially useful in reducing porosity at early ages, while TIPA promotes a higher overall hydration degree. However, TIPA also causes the formation of larger capillary pores in the early stages, which limits its effectiveness in enhancing early strength [62].

#### 1.2.2.2. Calcium silicate hydrates seeds, C-S-H seeds

The primary hydration product of the calcium silicates, $C_3S$ and $C_2S$, is C-S-H gel, which largely contributes to the material properties of concrete. C-S-H particles stand out from other seeding agents because they should serve as ideal nucleation substrates for C-S-H formation [73].

C-S-H seeding nanoparticles impact cement hydration in two main ways: i) by affecting secondary nucleation and ii) modifying the composition of the pore solution. Initially, the additional surfaces created by C-S-H seeding speed up alite hydration in its early stages, while also increasing the dissolution rates of aluminates and sulphates. However, the higher concentration of aluminates in the pore solution may eventually slow down alite hydration.

This behaviour makes it challenging to distinguish the effects of C-S-H seeding between alite (pure phase) and PC hydration. In seeded alite pastes, hydration occurs with minimal sulphate and aluminium ions, while in PC hydration, these ions are present in greater quantities, influencing the nucleation and growth of C-(A)-S-H.

Additionally, C-S-H seeding appears to shift the balance between inner and outer C-S-H gels at comparable hydration levels. The outer C-S-H gel, being less dense, occupies more space, improving mechanical properties and lowering porosity. Consequently, even with the same amount of alite hydration, C-S-H seeding enhances cement performance by more effectively connecting anhydrous particles, resulting in increased compressive strength and reduced porosity [49,74,75].

C-S-H seeds not only promote the crystallization of C-S-H from clinker silicates but also speed up the pozzolanic activity in calcined clay, as evidenced by the faster consumption of Portlandite.

They further enhance aluminate hydration, resulting in increased hemicarboaluminate formation, which supports the development of early strength [76–78].

#### 1.2.2.3. Synergy effect of C-S-H seeds with alkanolamines

A synergistic effect has been clearly noted when using C-S-H seeds in combination with alkanolamines, significantly influencing sulfate dissolution as well as the hydration of $C_4AF$ and $C_3A$ [79–82]. The presence of C-S-H seeds, alongside alkanolamines, seems to alter the equilibrium by adsorbing $SO_4^{2-}$. Alkanolamines increase the concentration of $Al^{3+}$ in the pore solution, which promotes ettringite formation, leading to further calcium sulfate dissolution. This is significant because it suggests that using these accelerating admixtures may necessitate a higher sulfate content. Additionally, a study reported that the combined use of TIPA and C-S-H nucleation seeding improved chloride binding capacity [83], which could potentially enhance chloride resistance.

Since SCMs are typically rich in aluminates and exhibit pozzolanic properties that can be accelerated [84], this characteristic could be crucial for activating low-$CO_2$ cements with high levels of Portland clinker replacement.

## 1.3. Methodologies

This section presents the various methodologies employed in the preparation of pastes and mortars. It also outlines the key techniques utilized throughout the development of this thesis. For each technique, any necessary sample pre-adaptations are described in detail, ensuring that the methodology aligns with the specific requirements of the study.

### 1.3.1. Mixing methodologies for paste preparation

Throughout this thesis, the paste preparation methodologies have been adjusted based on scientific reproducibility criteria, aiming to both improve the methodology and ensure that pastes analysed using different techniques were prepared under identical conditions. Consequently, three different methodologies have been employed. In all cases, the admixtures were dosed by weight percentage relative to the binder (bwb) as received, and the water content of the admixtures was factored into the water dosage to maintain a consistent w/(c,b) ratio. Section 1.4. will specify which methodology was used in each particular case.

#### Methodology #1

In the first method, water was combined with the cement powder and manually mixed for 1 minute, followed by 1 minute of mixing using a vortex mixer (RSLab-6PRO), as shown in Figure 1.1.a. When admixtures were used, they were first dissolved in water and stirred magnetically at 400 rpm for 1 minute before adding to the cement.

#### Methodology #2

Water and cement were mixed using a mechanical stirrer (IKA, model RW20-D), as shown in Figure 1.1.b., at 800 rpm for 90 seconds, followed by a 30-second pause, and then stirred again at 800 rpm for another 90 seconds. This methodology is related to mortar Methodology #4 and it could be named as *cement field* methodology.

#### Methodology #3

The mixing procedure with a mechanical stirrer was as follows:

Step 1: Mix for 60 seconds at 800 rpm with the binder and 80% of the water

Step 2: Stop for 30 seconds to add the superplasticizer (SP) and the remaining 20% of water for samples without C-S-H seeding, or 10% for samples with seeding

Step 3: Mix for 60 seconds at 800 rpm

Step 4: (for samples with C-S-H seeding only) Stop for 30 seconds to add the seeding and the remaining 10% of water

Step 5: Mix for 60 seconds at 800 rpm. This methodology is related to mortar Methodology #5 and it could be named as *concrete field* methodology.

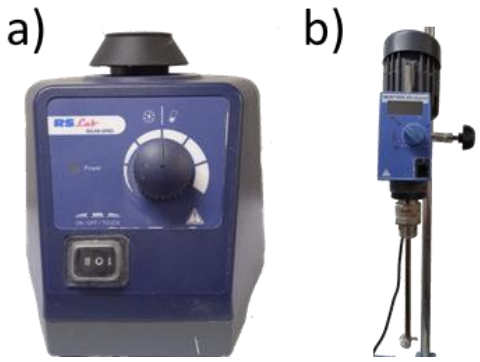


*Figure 1.1. a) Vortex mixer and b) Mechanical stirrer.*

### 1.3.2. Sample preparation for each characterization technique

- In situ measurements, i.e. the samples are place in the sample holder and measured, *mix and measure strategy* [85,86]

- Capillary sample holder. For in situ Synchrotron XRPD the pastes were injected, with the aid of a syringe, in glass capillaries of 0.70 mm of diameter.

- Glass ampoules for calorimetry. The pastes were placed into the glass ampoules for the calorimetries, see Figure 1.17.b.

- Casting pastes as cylinders within Teflon® mould (10 mm of diameter and 35 mm long), Figure 1.2.a. Pastes casted in the cylinders were maintained rolling at 16 rpm in a Wheaton roller for 24 h. Then, demoulded, Figure 1.2.b, and the specimens were kept in saturated portlandite solution until tested.

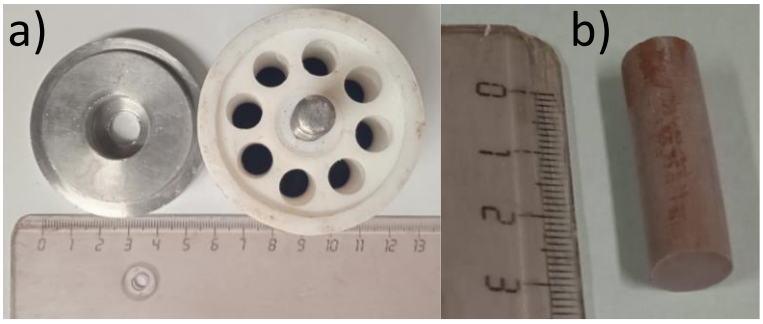


*Figure 1.2. a) Teflon® mould and b) paste cylinder after demolding.*

Figure 1.3. shows a diagram of the different techniques used for mixing, moulding, curing, measuring, and the applied methodology.

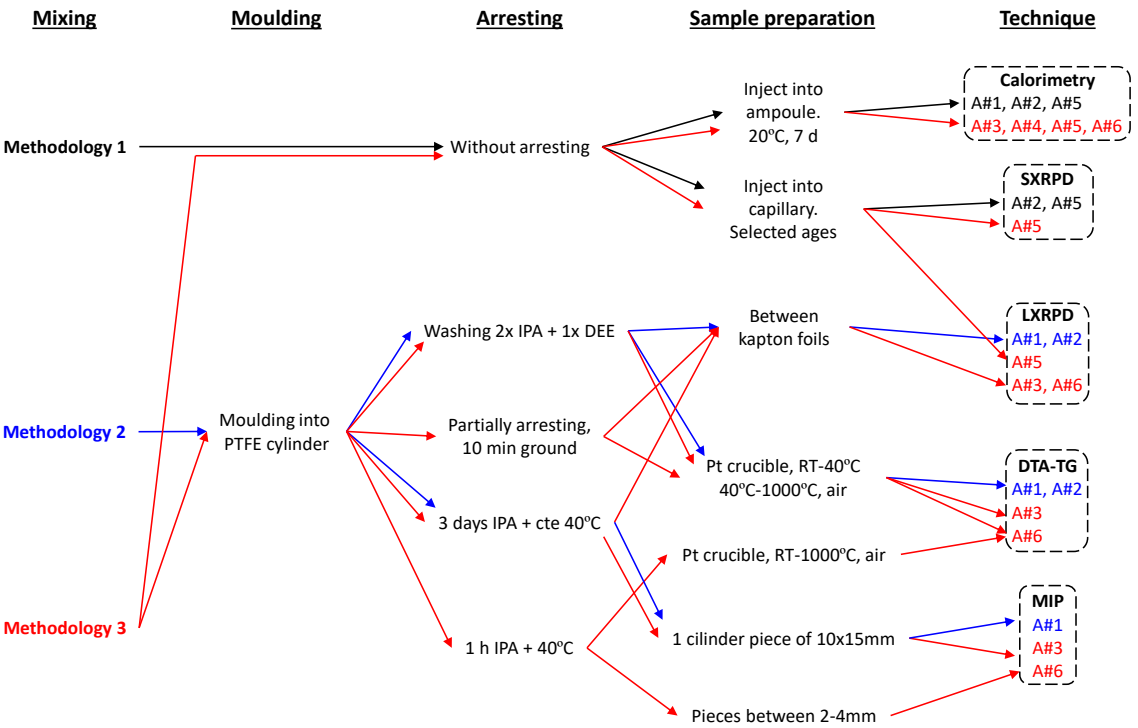


*Figure 1.3. Diagram of the different techniques used with various pastes preparation methodologies.*

### 1.3.3. Mixing methodologies for mortar preparation

Mortars were prepared following two different methodologies. In both cases, the amounts of admixtures added are dosed in weight percent respect to the binder (bwb) as the received products and the amount of water in these admixtures was taken into consideration when carrying out the water dosage, to maintain a fixed w/(c,b) ratio.

#### Methodology #4

The mortars were prepared with a sand-to-cement ratio of 3.00 and a water-to-cement ratio as required by the study (0.40 or 0.50). A mortar mixer (Matest, model E095), Figure 1.4.a., was used in accordance with the UNE-EN 196-1 standard.

#### Methodology #5

Mortars were prepared with a sand/cement ratio of 1.78 and with a water/cement ratio of 0.40 at 20°C. An optimized amount of SP for an initial constant self-flow, i.e. 200±20 mm, was added, see Table 4.3. For the mortar preparation, a mortar mixer was used according to the following procedure:

Step 1: 60 s at 140 rpm (solid, i.e. sand + binder and 80 wt% water)

Step 2: Stop 30 s to add the SP and 20 wt% of water for samples without C-S-H seeding or 10 wt% of water for samples with seeding

Step 3: 60 s at 285 rpm

Step 4: (only for samples incorporating C-S-H seeding) Stop 30 s to add the admixture and the 10 wt% of water left

Step 5: 120 s at 285 rpm.

To cast the mortar into moulds, the mould was initially half-filled, and air bubbles were eliminated by making 60 vertical punctures with a glass rod. The mould was then completely filled, followed by another set of 60 punctures to remove any remaining air pockets.


*Figure 1.4. Mortar mixer (Matest).*

Methodology #6

Mortars were prepared with a sand/cement ratio of 1.78 and with a water/cement ratio of 0.40 at 20°C. An optimized amount of SP for an initial constant self-flow, i.e. 200±20 mm, was added, see Table 4.3. For the mortar preparation, a mechanical stirrer, Figure 1.1.b., was used according to the following procedure:

Step 1: 60 s at 400 rpm (solid, i.e. sand + binder and 80 wt% water)

Step 2: Stop 30 s to add the SP and 20 wt% of water for samples without C-S-H seeding or 10 wt% of water for samples with seeding

Step 3: 60 s at 500 rpm

Step 4: (only for samples incorporating C-S-H seeding) Stop 30 s to add the admixture and the 10 wt% of water left

Step 5: 120 s at 500 rpm.

The mortar were cast into moulds as described in Methodology #5

Figure 1.5. shows a diagram of the different techniques that have been used with various mortar preparation methodologies.

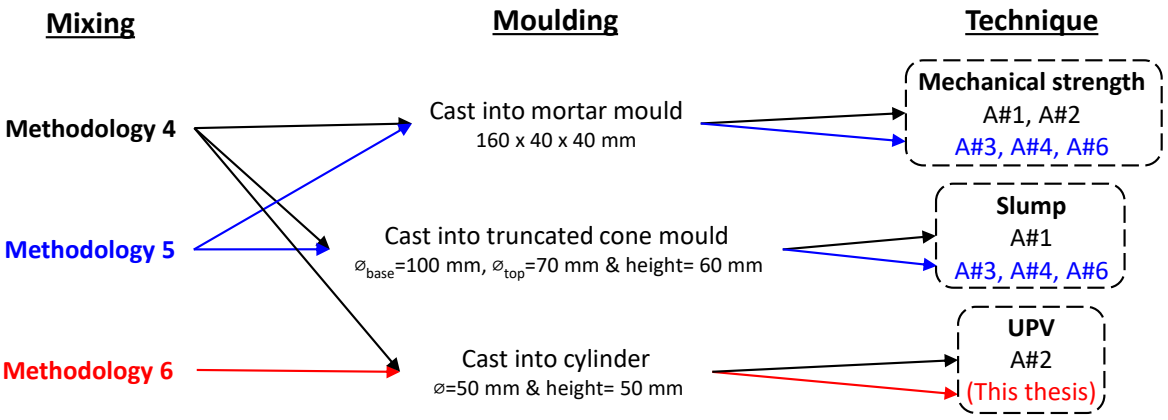


*Figure 1.5. Diagram of the different techniques used with various mortar preparation methodologies.*

### 1.3.4. Slump test

Consistency, which is determined using a flow table, is a measure of the flowability and/or moisture content of the fresh mortar, providing a measure of the deformability of the fresh mortar when subjected to a certain type of stress.

The flow value is determined by measuring the diameter of a sample of fresh mortar placed, with the help of a stainless steel or brass mould (height of 60 mm, an inner diameter of 100 mm at the base, and 70 mm at the top), on the disk of a defined flow table. It is then subjected to a certain number of vertical shakes, lifting the table and allowing it to drop freely from a certain height.

In this thesis, two types of flow measurements of the mortars are performed, according to the purpose and type of sample. In the first procedure, *cement field*, the consistencies were determined using the flow table according to the standard EN 1015–3. The cone was filled with the mortars and lifted following the standard. Then, the initial slump was measured, $t_0$.

In the second procedure, *concrete field*, the mortars were poured into the truncated cone in two steps. Firstly, filling up half of the cone and removing the air bubbles with a glass rod with 60 vertical punctures. In the second step, the cone was completely filled and punctured again 60 times. Then, the slump was measured, after lifting, at $t_0$, 30, and 60 min.

In both methodologies, the reported spread values are the average of two perpendicular measurements, under laboratory temperature conditions of 20 ± 2 °C. A flow table (Matest) was used for the slump measurements, as shown in Figure 1.6.

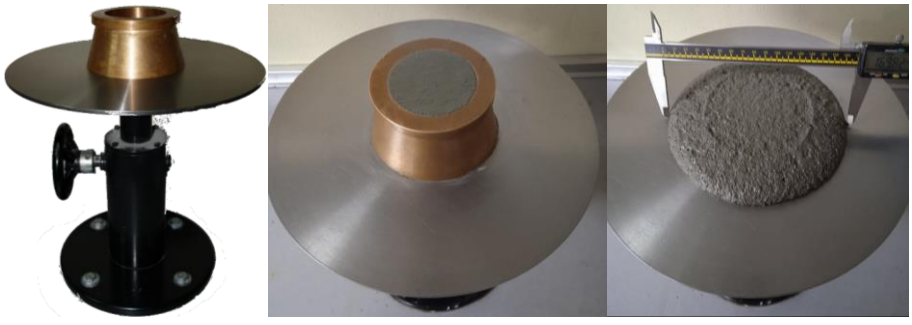

*Figure 1.6. Flow table for the slump measurement.*

### 1.3.5. Mechanical Strength

The mechanical strength of mortar is a crucial factor in determining the structural integrity and durability of buildings and other structures. This test measures the amount of force a mortar can withstand before breaking. By knowing the force and the area of application, pressure is obtained, with values expressed in MPa.

All mechanical strength measurement tests in this thesis were conducted according to the standard EN 196-1. The mortars were tested at 1, 7, and 28 days of hydration. For flexural strength data, three prisms were used, and subsequently, the six resulting specimens were used to obtain the compressive strength data. The reported results represent the average of all measurements. The testing machine used were i) an Autotest 200/10W model (Ibertest, Madrid, Spain), located at Votorantim Cimentos factory, Malaga, Spain and ii) a press Model Autotest 300/20C MD2-ECO, located at Escuela de Ingenierías Industriales, Universidad of Málaga. In Figure 1.7.a, the mould used for the preparation is shown, and in Figure 1.7.b., a mortar prism is displayed after demolding.

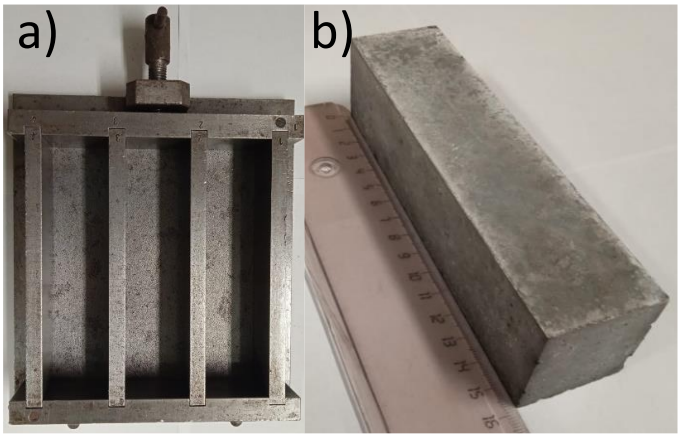


*Figure 1.7. a) Mortar mould and b) prism after demoulding.*

### 1.3.6. Ultra Pulse Velocity, UPV

UPV is a non-destructive technique used to analyse mortars in-situ. It measures the velocity of an ultrasonic pulse passing through a mortar, with variations in velocity reflecting the setting and microstructural development of the mortars, Figure 1.8.a. Low velocities are measured for flowable mortars, while high velocities are acquired for hardened binders, indicating the development of connectivities between solid phases.

The studied mortars were continuously monitored during the first four days of hydration using an IP8 ultrasound system (UltraTest GmbH), as shown in Figure 1.8.b., located at the Universidad de Málaga, Spain. The frequency of the ultrasonic wave was 30 kHz, and the distance between the receiver and the transmitter was 40 mm. The laboratory maintained a constant temperature of 19 ± 1 °C.

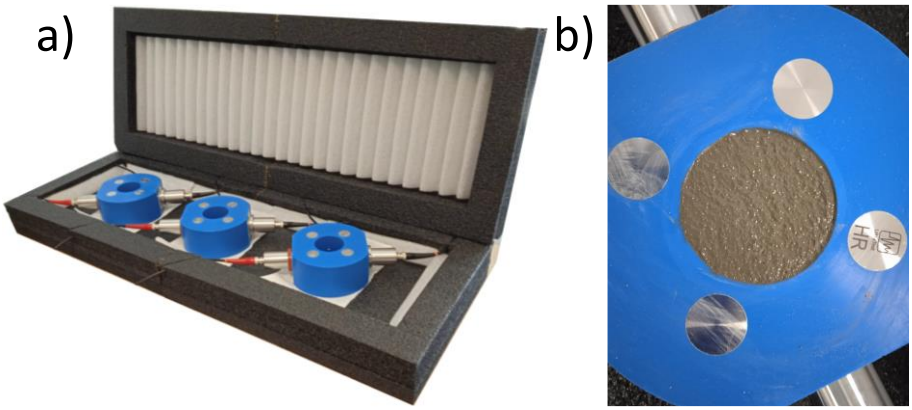


Figure 1.8. a) IP8 ultrasound system sensors and b) sensor filled with a mortar mix.

### 1.3.7. Particle size distribution, PSD

The particle size distribution (PSD) of the anhydrous powders was analyzed using a Mastersizer 3000 from Malvern Panalytical, as shown in Figure 1.9.a, within a dry chamber (Aero S). The device operates with a He-Ne red laser (wavelength: 633 nm) and a blue LED light (wavelength: 470 nm). Particle sizes are determined through laser light diffraction, applying Fraunhofer theory, with adjustments made using the Mie theory as per ISO13320 standards.

For the strength enhancing admixtures, PSD was measured using a Zetasizer Nano-ZS from Malvern Panalytical, depicted in Figure 1.9.b. This instrument is equipped with a red laser at a wavelength of 632.8 nm. The Zetasizer assesses particle size by tracking their Brownian motion via dynamic light scattering (DLS), then calculates the size based on the Stokes-Einstein equation and other relevant theories. To ensure the sample had the right concentration for analysis, it was diluted to 0.005 wt% solids using a NaOH solution at pH 12.0, followed by 2 minutes of ultrasonication for dispersion.

Both equipments are located at SCAI-UMA, Spain.

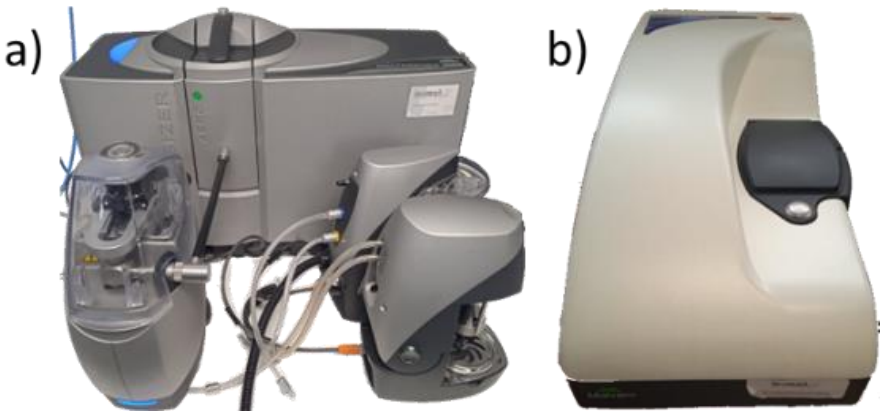


*Figure 1.9. a) Mastersizer 3000 and b) Zetasizer Nano-ZS.*

### 1.3.8. Air permeability test, Blaine

The air permeability method (Blaine) is used to measure the specific surface area (surface area in relation to mass) by comparing it with a reference material sample. Cement fineness is determined by observing the time it takes for a fixed amount of air to pass through a compacted layer of cement with specified dimensions and porosity. Under standardized conditions, the specific surface area of the cement is given by √t, where "t" is the time required for a given amount of air to pass through the compacted layer of cement. The number and distribution of the dimensions of the individual pores are determined by the PSD of the cement, which also influences the time for the passage of the specified air flow.

A Blaine fineness apparatus (Matest, Italy) was employed to get the air permeabilities following UNE-EN 196-6, Figure 1.10.

*Figure 1.10. Blaine fineness apparatus.*

### 1.3.9. Specific surface area, SSA (BET)

Surface area is an important physical property in powders, in general, and in cements, in particular, as it influences reactivity, water consumption, and rheology, among other factors. In general, the greater the surface area of a cement, the higher its reactivity. Likewise, cements with larger surface areas may require more water to maintain a certain consistency and rheology. The specific surface areas were determined by $N_2$ isotherms in a ASAP 2420 (Micromeritics, USA) device, located in SCAI-UMA, Spain, see Figure 1.11.

*Figure 1.11. ASAP 2420 (Micromeritics).*

### 1.3.10. Density

To ensure a comprehensive initial assessment of the materials, the real density of all anhydrous materials was determined. Additionally, the density measurement serves as an essential prerequisite for those materials subjected to the air permeability test, as described in section 1.3.8. The density of the samples was analysed in an Accupyc II 1340 (Micromeritics) with helium Pycnometer, housed in SCAI-UMA, Spain, Figure 1.12.


*Figure 1.12. Accupyc II 1340 (Micromeritics).*

### 1.3.11. Differential Thermal Analysis and Thermogravimetry, DTA-TG

Thermal analysis was used to determine the amount of various phases like gypsum, bassanite, portlandite, or calcium carbonate in dry cements and pastes (after arrested hydration). Additionally, the results obtained from pastes provide information about the bound water content, and thus also the free water (FW) content. These measurements were carried out using a SDT-Q600 analyser (TA instruments, New Castle, DE), Figure 1.13, located in the Universidad de Málaga, Spain. Measurements were carried out in open platinum crucibles under a synthetic air flow and in a range of temperature from 40 to 1000°C at a heating rate of 10 °C/min. The weighed loss from 40 to 550°C was attributed to chemically Bounded Water (BW), Equation 4. The content of portlandite, CH, was calculated using the tangential method in the range above 450°C [87]. The weighed loss from 550 to 1000°C is considered as $CO_2$.

The FW content, Equation 5, expressed as a percentage of weight, was calculated for each cement paste using the subsequent equations:

$$BW(\%) = \frac{W_{RT-550℃} \times (BC - W_{C\bar{s}H_x})}{100 - W_{RT-550℃}}$$

*Equation 4. Bounded water equation*

$$FW(\%) = \left(NW + W_{C\bar{s}H_x}\right) - BW$$

*Equation 5. Free water equation*

Where BW represents the bound water content, NW is the nominal water (33.3% for a w/c= 0.50 and 28.6% for a w/c=0.40), $WL_{Rt\text{-}550℃}$ is the mass loss measured from room temperature to 500 °C, and BC is the binder content in weight percentage (66.7% for w/c= 0.50 and 71.4% for w/c= 0.40).

*Figure 1.13. SDT-Q600 analyser.*

### 1.3.12. Wavelength dispersive X-ray fluorescence, WDXRF

Wavelength Dispersive X-ray Fluorescence, WDXRF, is an analytical technique that utilizes X-ray fluorescence to determine the elemental composition of a material. In X-ray fluorescence spectroscopy, the material is bombarded with high-energy X-rays, causing inner electrons to be excited and jump to higher energy levels. When these electrons return to their original energy levels, they emit characteristic X-ray fluorescence with wavelengths indicative of the elements present in the material. For sample analysis, a sequential ARL PERFORM'X instrument from THERMO was used, see Figure 1.14. The equipment includes an autosampler, a Rh anode X-ray tube, and a goniometer with 4 collimators, 5 crystals, and two detectors. The equipment is located at SCAI-UMA, Spain.

Two different sample processing methods were employed. In the first method, approximately 0.8 g of dry sample and 8 g of flux (a mixture of $LiB_4O_7$ 66.67%, $LiBO_2$ 32.83%, LiBr 0.5%) were weighed using an analytical balance, and a bead was formed by fusion using a bead maker (Katanax X600 model from Spex Sample Prep). For the analysis of strength enhancing admixtures admixture samples, they were first dried at 40°C until constant weight was achieved, and the resulting solid was pressed into a pellet using a hydraulic press (X-PRESS 3635 model from Spex

Sample Prep). In both procedures, the determination of LOI (loss on ignition) was performed by weighing a quantity of dry sample on an analytical balance and calcining it in a muffle furnace at 950°C for 2 hours. Elemental composition is usually expressed as oxides, renormalized considering the percentage of LOI.

*Figure 1.14. ARL PERFORM'X instrument.*

### 1.3.13. Laboratory X-ray powder diffraction, LXRPD

X-ray diffraction (XRD) is one of the most prominent analytical techniques in the characterisation of crystalline, fine-grained materials, such as cements. When X-rays interact with a crystalline substance, they generate an X-ray diffraction pattern. This pattern features peaks of different intensities at specific diffraction angles. The angle or location of these peaks is influenced by the unit cell's symmetry and dimensions, as defined by Bragg's law, while the intensity of each peak depends on the type and arrangement of atoms within the unit cell. In this manner, XRD creates unique patterns of peak locations and intensities that are characteristic of particular crystal structures, allowing for the identification of these structures in unknown samples. In phase mixtures, the total intensity of peaks from a particular phase correlates directly with that phase's weight fraction within the mixture [88].

Anhydrous powders and arrested-hydration pastes were analysed using two different diffractometers.

1. D8 ADVANCE DaVinci (Bruker AXS, Germany), Figure 1.15, employed a Molybdenum X-ray tube and a Johansson Ge(220) primary monochromator to produce monochromatic MoK$\alpha_1$ radiation with a wavelength of 0.7093 Å. The X-ray tube operated at 50 kV and 50 mA, while a linear energy-dispersive detector device, LYNXEYE XE 500 µm, optimized for high energy radiation, was utilized with the maximum opening angle. Measurements were conducted from 3 to 35° (2θ) with a step size of 0.020° over a total measuring time of 2 hours.

2. X'Pert MPD PRO (PANalytical), featuring a Ge(111) primary Johansson monochromator that delivered strictly monochromatic CuK$\alpha_1$ radiation with a wavelength of 1.54059 Å. This setup also utilized an X'Celerator RTMS (Real Time Multiple Strip) detector device in scanning mode with maximum active length. The X-ray tube operated at 45 kV and 40 mA. Data collection spanned from 5 to 70° (2θ) with a step size of 0.016° over approximately 2 hours per pattern.

The samples were placed between two Kapton® foils and measured as flat samples in transmission mode on both diffractometers. To improve particle statistics, a spinning sample holder (rotating at 16 rpm) was used.


*Figure 1.15. D8 ADVANCE diffractometer.*

### 1.3.14. Synchrotron X-ray diffraction, SXRPD

A synchrotron functions by accelerating electron pulses to speeds comparable to that of light, generating a focused beam of polarized and highly energetic white radiation. Utilizing a powerful and monochromatic X-ray source, like synchrotron X-rays, along with a rapid X-ray detection system enables the acquisition of powder diffraction patterns with exceptional counting precision. Furthermore, this setup allows for the swift collection of patterns, facilitating real-time analysis of rapid reaction sequences such as monitoring cement hydration processes [89,90]. The exceptional brilliance of synchrotron radiation significantly enhances the structural analysis and detection sensitivity of mixture components.

The in situ SXRPD studies were performed at the powder diffraction end station of the MSPD-BL04 beamline (see Figure 1.16) within the ALBA synchrotron facility located in Barcelona, Spain [91]. This diffractometer is equipped with a MYTHEN detector, ensuring high signal-to-noise ratios even with short measurement durations. Wavelengths of 0.62005(1) and 0.61907 Å (20 keV) were selected by Si(111) crystal analyzer. Each data collection period lasted 6 minutes per pattern, covering an angular range from 2 to 40 degrees (2θ). A four-capillary sample holder was employed, rotating at 20 rpm during measurements to enhance powder averaging. Measurements were taken at three positions along each capillary and then merged for improved statistical accuracy and powder averaging.

Instrumental parameters were determined using the pattern from a Si SRM 640e standard collected under identical conditions. SXRPD patterns were analysed using the Rietveld methodology with GSAS-II software [92]. The ACn values were determined using the internal standard methodology [93], which accounts for the reduction in FW fraction, the increase in C-S-H gel content, and any other amorphous components (such as any partially crystallized hydrated phases like iron-siliceous hydrogarnet).

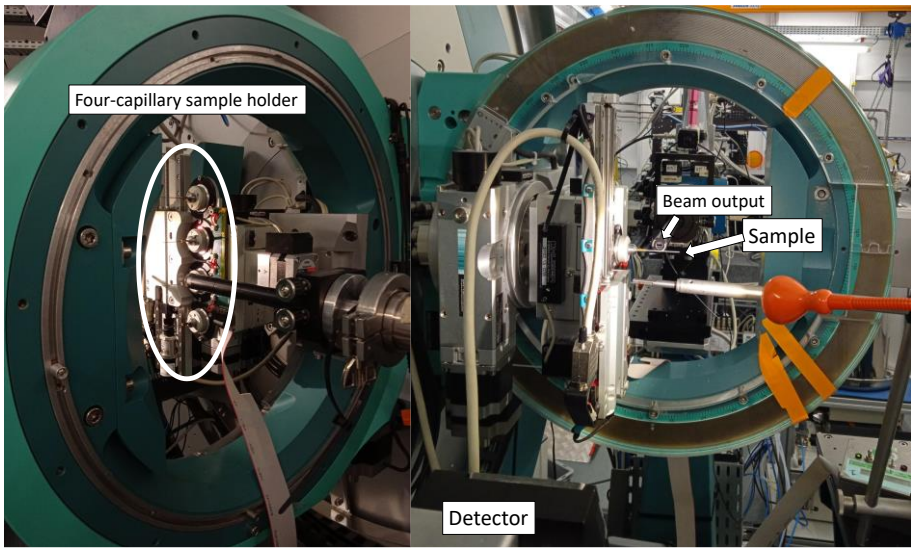


*Figure 1.16. MSPD beamline.*

### 1.3.15. Transmission electron microscopy, TEM

C-S-H particle size and morphology of the strength enhancing admixtures (XS100, XS130 and STE53) were analysed by TEM. The suspensions were diluted (1/1000) with isopropanol and were immersed in an ultrasound bath for 10 seconds. Then, they were applied onto Cu grids, 200 mesh, with formvar®-carbon films. A JEM-1400 microscope (Jeol, Japan), coupled with a Gatan ES1000W camera and operating at 80 kV was utilized. This equipment is housed at SCAI–UMA, Spain.

### 1.3.16. Isothermal calorimetry

Isothermal calorimetry in cements is a technique used to study the hydration reactions of cement over time. This technique involves measuring the amount of heat released during the hydration of cement at a constant temperature. This provides valuable information about the kinetics of hydration reactions, including reaction rate and the amount of heat released at different stages of the hydration process.

The study of isothermal calorimetry was conducted using an eight-channel Thermal Activity Monitor (TAM), Figure 1.17.a., for up to 7 days at 20°C. After the paste preparation, the samples were injected into glass ampoules and then placed within the calorimeter. Heat flow curves were collected starting approximately 50 minutes after hydration began, which allowed time for mixing and filling the ampoule (aprox. 5 minutes), Figure 1.17.b., plus an additional 45 minutes for equipment signals stabilization. Water was used as reference according to [94].

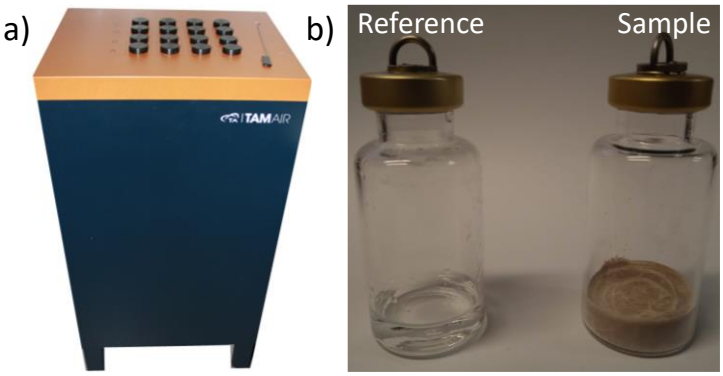


*Figure 1.17. a) Thermal Activity Monitor (TAM) and b) reference and sample ampoules.*

### 1.3.17. Mercury intrusion porosimetry, MIP

MIP, or Mercury Intrusion Porosimetry, offers a means to analyse the intricate pore architecture of hydrated cement-based materials. By employing mercury as a non-wetting fluid and subjecting the material to increasing pressure, MIP selectively infiltrates interconnected pores accessible to the mercury at specific pressure levels. Consequently, MIP findings provide insights into the distribution of pore sizes. The porosity of hydrated cement-based materials is influenced by various factors including cement particle size, water-to-cement ratio, mixing techniques, and curing environments.

For the MIP analysis, an AutoPore IV 9500 porosimeter (Micromeritics) located at SCAI-UMA was used (see Figure 1.18), employing a radius range from 1 mm down to 4 nm. The MIP analysis were conducted on cylindrical pieces approximately 1 cm in diameter and 1.5 cm in height.

The samples were arrested at 1, 7 and 28 days after hydration and then measured. To remove unreacted water, the samples were immersed in isopropanol for 3 days, after which the isopropanol was removed and the sample were dried at 40°C until a constant weight was achieved.

*Figure 1.18. AutoPore IV 9500 porosimeter (Micromeritics).*

Equation 6 shows the Washburn equation, from which the pore diameter size is obtained according to the pressure applied at any given time.

$$D = \frac{-4\gamma cos\theta}{P}$$

*Equation 6. Washburn equation.*

Where “D” is the pore diameter, “γ” is the surface tension, “θ” is the contact angle and “P” is the applied pressure. The applied pressure ranged from 0 to 206 MPa in step mode and a contact angle of 140° was used for the calculations [95].

## 1.4. Sample summary

This section summarizes the samples studied in this thesis, along with the methodology used for their preparation and the techniques employed for each of them, both for pastes and mortars.

In Table 1.1., the primary materials used in this thesis are listed, along with the corresponding nomenclature for each.

*Table 1.1. Summary of the samples, materials, and the nomenclature used.*

| Sample | Nomenclature |
|---|---|
| **CEM-I 52.5R (Votorantin Cimentos, Málaga, Spain)** | **PC-525** |
| **CEM-I 42.5R (Votorantin Cimentos, Málaga, Spain)** | **PC-425** |
| **Belite Cement (Buzzi Unicem SpA, Italy)** | **BC-Buz** |
| **Belite Cement non activated (non-commercial, China)** | **BC-n.a.** |
| **Quartz (Jose Sanchís Penella S.A., Spain)** | **Qz** |
| **Omyacarb® 5F (Omya Clariana S.L.U., Spain)** | **LS** |
| **Gypsum (Maruxiña S.A., Spain)** | **Gyp** |
| **Kaolinitic calcined clay (ref. CVPM3B (71wt% Mk), Arcimu S.A., Spain)** | **CC1** |
| **Kaolinitic calcined clay (ref. F-35 (47wt% Mk), Caolines de Vimianzo S.A.U., Spain)** | **CC2** |
| **Kaolinitic calcined clay (ref. Kaolin-C (28wt% Mk), Caobar S.A., Spain)** | **CC3** |
| **MasterSuna SBS 3890 (Master Builders Solutions, Germany)** | **SP1** |
| **Master$CO_2$re 3240 (Master Builders Solutions, Germany)** | **SP2** |
| **Master$CO_2$re 3400 (Master Builders Solutions, Germany)** | **SP3** |
| **Master X-Seed 100 (Master Builders Solutions, Germany)** | **XS100** |
| **Master X-Seed 130 (Master Builders Solutions, Germany)** | **XS130** |
| **Master X-Seed STE 53 (Master Builders Solutions, Germany)** | **STE53** |
| **Triisopropanolamine (Acros organics, 98%)** | **TIPA** |

From these materials, $LC^3$ binders with varying compositions were developed, specifically $LC^3$-50 and $LC^3$-35. Additionally, a binder named PC-Qz was prepared, which shares a similar composition to $LC^3$-50 but replaces clay with an inert material, quartz. This binder was used as a reference in the study. Table 1.2. outlines the weight percentages of each material used in preparing the different binders for this thesis. The binders were prepared using a Micro-Deval device. For preparation, 1 kg of the total sample was weighed, placed into metal jars with five 32 mm diameter metal balls, which assisted in homogenizing the mixture without altering particle size. The homogenization process lasted for a total of 3 hours, including a 30-minute pause at the halfway point to prevent overheating.

All the initial solid materials underwent a preliminary characterization, which included mineralogical and elemental analysis, as well as particle size and density measurements. Although the full characterization of the solids can be found in the corresponding paper, key parameters will be included in each section for the reader's convenience.

The information about the characterization of the superplasticizers and strength-enhancing admixtures presented in this thesis is provided in accordance with the non-disclosure agreement with Master Builders Solutions. However, a comprehensive description of the C-S-H nucleation admixture is available in the original patent [96,97].

*Table 1.2. Dosage of each component, in weight percentages, to prepare the $LC^3$ binders.*

| Samples | PC-525 (wt%) | CC# (wt%) | Qz (wt%) | LS (wt%) | Gyp (wt%) |
|---|---|---|---|---|---|
| **PC-Qz** | **52** | **-** | **30** | **15** | **3** |
| **$LC^3$-50 (CC#)** | **52** | **30** | **-** | **15** | **3** |
| **$LC^3$-35 (CC#)** | **38** | **40** | **-** | **20** | **2** |
| **$LC^3$-20 (CC#)** | **23** | **50** | **-** | **25** | **2** |

Table 1.3. provides the recording times for the data of different samples using SXRPD at MSPD (ALBA), alongside the methodologies applied. In all cases, a continuous study commenced from $t_0$ (approximately 20 minutes, required for mixture preparation, capillary filling, and equipment alignment). Data collection occurred every 30 minutes from $t_0$ until a pre-determined end point, chosen based on equipment availability and prior calorimetry data (typically between 16-22 hours). For certain samples, additional independent data was recorded at times exceeding 1 day.

*Table 1.3. Timing of data collection with synchrotron radiation (MSPD-ALBA line) for each series and the methodology employed for their preparation.*

| Samples | Str. enh./ SPX | SXRPD | Article |
|---|---|---|---|
| **PC-525** | **-/-** | ($t_0$-19 h)[1(&)] | A#5 |
| | **STE53/-** | ($t_0$-19 h)[1(&)] | A#5 |
| **PC-425** | **-/-** | ($t_0$-18, 53 h)[1(&)] | A#2 |
| | **XS100/-** | ($t_0$-17, 53 h)[1(&)] | A#2 |
| | **XS130/-** | ($t_0$-17, 57 h)[1(&)] | A#2 |
| | **TIPA/-** | ($t_0$-15, 46 h)[1(&)] | A#2 |
| **BC-Buz** | **-/-** | ($t_0$-16, 46 h)[1(&)] | A#2 |
| | **XS100/-** | ($t_0$-16, 46 h)[1(&)] | A#2 |
| | **XS130/-** | ($t_0$-17, 54 h)[1(&)] | A#2 |
| | **TIPA/-** | ($t_0$-16, 46 h)[1(&)] | A#2 |
| **BC-n.a.** | **-/-** | ($t_0$-37 h)[1(&)] | A#2 |
| | **XS130/-** | ($t_0$-37 h)[1(&)] | A#2 |
| **$LC^3$-50 (CC1)** | **-/SP1** | ($t_0$-22, 48, 58 h)[3($)] | A#5 |
| | **-/SP2** | ($t_0$-22, 48, 58 h)[3($)] | A#5 |
| | **XS130/SP1** | ($t_0$-22, 36 h)[3($)] | A#5 |
| | **XS130/SP2** | ($t_0$-19 h)[3($)] | A#5 |
| | **STE53/SP1** | ($t_0$-22, 36 h)[3($)] | A#5 |
| | **STE53/SP2** | ($t_0$-19 h)[3($)] | A#5 |
| | **TIPA/SP1** | ($t_0$-22, 36 h)[3($)] | A#5 |

Paste preparation according to [1]Methodology #1, [2]Methodology #2, [3]Methodology #3. [&]w/b= 0.50. [$]w/b= 0.40.

Table 1.4. provides a detailed overview of the specific ages and experiments carried out on each of the cement and binder pastes studied. It also includes a description of the methodologies applied in preparing the mixtures for each case. This table serves as a key reference, offering insights into the experimental setup and the progression of the studies.

*Table 1.4. Summary of the ages and experiments conducted for each paste analysis.*

| Samples | Str. enh./SP# | Calorimeter | LXRPD | TA | MIP | Article |
|---|---|---|---|---|---|---|
| PC-525 | -/- | ($t_0$-7 d)[3(&)] | | | | A#5 |
| | -/SP1 | ($t_0$-7 d)[3($)] | | | | A#5 |
| | -/SP2 | ($t_0$-7 d)[3(%)] | (1, 7, 28 d)[3(%)] | (1, 7, 28 d)[3(%)] | (1, 7, 28 d)[3(%)] | A#3, A#4 |
| | XS130/SP1 | ($t_0$-7 d)[3($)] | | | | A#5 |
| | XS130/SP2 | ($t_0$-7 d)[3(%)] | - | - | - | A#4 |
| | STE53/- | ($t_0$-7 d)[3(&)] | | | | A#5 |
| | STE53/SP1 | ($t_0$-7 d)[3($)] | | | | A#5 |
| | STE53/SP2 | ($t_0$-7 d)[3(%)] | (1, 7, 28 d)[3(%)] | (1, 7, 28 d)[3(%)] | (1, 7, 28 d)[3(%)] | A#3 |
| | TIPA/SP1 | ($t_0$-7 d)[3($)] | | | | A#5 |
| | TIPA/SP2 | ($t_0$-7 d)[3(%)] | - | - | - | A#5 |
| PC-425 | -/- | ($t_0$-7 d)[1($,&)] | (1, 7, 28 d)[2($,&)] (2 d)[2(&)] | (1, 7, 28 d)[2($,&)] (2 d)[2(&)] | (1, 7, 28 d)[2($,&)] | A#1, A#2 |
| | XS100/- | ($t_0$-7 d)[1($,&)] | - | - | - | A#2 |
| | XS130/- | ($t_0$-7 d)[1($,&)] | (1, 7, 28 d)[2($,&)] (2 d)[2(&)] | (1, 7, 28 d)[2($,&)] (2 d)[2(&)] | (1, 7, 28 d)[2($,&)] | A#1, A#2 |
| | STE53/- | ($t_0$-7 d)[1($,&)] | (1, 7, 28 d)[2($,&)] | (1, 7, 28 d)[2($,&)] | (1, 7, 28 d)[2($,&)] | A#1 |
| | TIPA/- | ($t_0$-7 d)[1(&)] | (1, 2, 7, 28 d)[2(&)] | (1, 2, 7, 28 d)[2(&)] | (1, 7, 28 d)[2(&)] | A#1 |
| BC-Buz | -/- | ($t_0$-7 d)[1($,&)] | (1, 7, 28 d)[2($,&)] (2 d)[2(&)] | (1, 7, 28 d)[2($,&)] (2 d)[2(&)] | (1, 7, 28 d)[2($,&)] | A#1, A#2 |
| | XS100/- | ($t_0$-7 d)[1($,&)] | - | - | - | A#2 |
| | XS130/- | ($t_0$-7 d)[1($,&)] | (1, 7, 28 d)[2($,&)] (2 d)[2(&)] | (1, 7, 28 d)[2($,&)] (2 d)[2(&)] | (1, 7, 28 d)[2($,&)] | A#1, A#2 |
| | STE53/- | ($t_0$-7 d)[1($,&)] | (1, 7, 28 d)[2($,&)] | (1, 7, 28 d)[2($,&)] | (1, 7, 28 d)[2($,&)] | A#1 |
| | TIPA/- | ($t_0$-7 d)[1(&)] | (1, 2, 7, 28 d)[2(&)] | (1, 2, 7, 28 d)[2(&)] | (1, 7, 28 d)[2(&)] | A#2 |
| BC-n.a. | -/- | ($t_0$-7 d)[1($,&)] | (1, 7, 28 d)[2($,&)] (2 d)[2(&)] | (1, 7, 28 d)[2($,&)] (2 d)[2(&)] | (1, 7, 28 d)[2($,&)] | A#1, A#2 |
| | XS100/- | ($t_0$-7 d)[1($,&)] | - | - | - | A#2 |
| | XS130/- | ($t_0$-7 d)[1($,&)] | (1, 7, 28 d)[2($,&)] (2 d)[2(&)] | (1, 7, 28 d)[2($,&)] (2 d)[2(&)] | (1, 7, 28 d)[2($,&)] | A#1, A#2 |
| | STE53/- | ($t_0$-7 d)[1($,&)] | (1, 7, 28 d)[2($,&)] | (1, 7, 28 d)[2($,&)] | (1, 7, 28 d)[2($,&)] | A#1 |
| | TIPA/- | ($t_0$-7 d)[1(&)] | (1, 2, 7, 28 d)[2(&)] | (1, 2, 7, 28 d)[2(&)] | (1, 7, 28 d)[2(&)] | A#2 |
| PC-Qz | -/SP2 | ($t_0$-7 d)[3(%)] | - | - | - | A#3, |

| | | | | | | |
|---|---|---|---|---|---|---|
| | | | | | | A#4 |
| | **XS130/SP2** | ($t_0$-7 d)[3(%)] | - | - | - | A#4 |
| | **STE53/SP2** | ($t_0$-7 d)[3(%)] | - | - | - | A#3 |
| **$LC^3$-50 (CC1)** | **-/SP1** | ($t_0$-7 d)[3($)] | | | | A#5 |
| | **-/SP2** | ($t_0$-7 d)[3(%,$)] | (≈24 h)[3(#)] | (1, 7, 28 d)[3(%)] | (1, 7, 28 d)[3(%)] | A#3, A#4, A#5 |
| | **XS130/SP1** | ($t_0$-7 d)[3($)] | | | | A#5 |
| | **XS130/SP2** | ($t_0$-7 d)[3(%,$)] | - | - | - | A#4, A#5 |
| | **STE53/SP1** | ($t_0$-7 d)[3($)] | | | | A#5 |
| | **STE53/SP2** | ($t_0$-7 d)[3(%,$)] | (1, 7, 28 d)[3(%)] | (1, 7, 28 d)[3(%)] | (1, 7, 28 d)[3(%)] | A#3, A#5 |
| | **TIPA/SP1** | ($t_0$-7 d)[3($)] | | | | A#5 |
| | **TIPA/SP2** | ($t_0$-7 d)[3($)] | - | - | - | A#5 |
| **$LC^3$-50 (CC2)** | **-/SP2** | ($t_0$-7 d)[3(%)] | (1, 7, 28 d)[3(%)] | (1, 7, 28 d)[3(%)] | (1, 7, 28 d)[3(%)] | A#3, A#4 |
| | **XS130/SP2** | ($t_0$-7 d)[3(%)] | - | - | - | A#4 |
| | **STE53/SP2** | ($t_0$-7 d)[3(%)] | (1, 7, 28 d)[3(%)] | (1, 7, 28 d)[3(%)] | (1, 7, 28 d)[3(%)] | A#3 |
| **$LC^3$-50 (CC3)** | **-/SP2** | ($t_0$-7 d)[3(%)] | (1, 7, 28 d)[3(%)] | (1, 7, 28 d)[3(%)] | (1, 7, 28 d)[3(%)] | A#3, A#4 |
| | **XS130/SP2** | ($t_0$-7 d)[3(%)] | - | - | - | A#4 |
| | **STE53/SP2** | ($t_0$-7 d)[3(%)] | (1, 7, 28 d)[3(%)] | (1, 7, 28 d)[3(%)] | (1, 7, 28 d)[3(%)] | A#3 |
| **$LC^3$-35 (CC1)** | **-/SP3** | ($t_0$-7 d)[3($)] | (1, 7, 28 d)[3($)] | (1, 7, 28 d)[3($)] | (1, 7, 28 d)[3($)] | A#6 |
| | **STE53/SP3** | ($t_0$-7 d)[3($)] | (1, 7, 28 d)[3($)] | (1, 7, 28 d)[3($)] | (1, 7, 28 d)[3($)] | A#6 |

Paste preparation according to [1]Methodology #1, [2]Methodology #2, [3]Methodology #3. [&]w/b= 0.50. [$]w/b= 0.40. [%]w/b= 0.35.

Table 1.5. presents a comprehensive summary of the experimental techniques and preparation conditions applied to each of the mortars examined in this study, covering both plain cements and binder-based mixtures. This table highlights the methodological approaches, the parameters used during the preparation process, and the experimental conditions under which the mortars were studied. It is an essential resource for understanding the comparative analysis of the different mortar compositions and their respective performance metrics.

*Table 1.5. Summary of the experimental techniques and preparation conditions for each mortar analysis.*

| Samples | Str. enh. | Slump | Comp. Str. | UPV | Article |
|---|---|---|---|---|---|
| **PC-525** | **-/SP1** | ($t_0$, 30, 60 min)[5($)] | - | - | A#3, A#4 |
| | **-/SP2** | ($t_0$, 30, 60 min)[5($)] | (1, 7, 28 d)[5($)] | (4 d) [6($)]- | A#3, A#4, This thesis |
| **PC-425** | **-/-** | ($t_0$)[4($,&)] | (1, 7, 28 d)[4($,&)] | (4 d)[4(&)] | A#1, A#2 |
| | **-/SP1** | ($t_0$, 30, 60 min)[5($)] | | | This thesis |
| | **-/SP2** | ($t_0$, 30, 60 min)[5($)] | | | This thesis |
| | **XS100/-** | - | - | (4 d)[4(&)] | A#2 |

| | | | | | |
|---|---|---|---|---|---|
| | **XS130/-** | - | (1, 7, 28 d)[4($,&)] | (4 d)[4(&)] | A#1, A#2 |
| | **STE53/-** | - | (1, 7, 28 d)[4($,&)] | - | A#1 |
| | **TIPA/-** | - | - | (4 d)[4(&)] | A#2 |
| **BC-Buz** | **-/-** | ($t_0$)[4($,&)] | (1, 7, 28 d)[4($,&)] | (4 d)[4(&)] | A#1, A#2 |
| | **XS100/-** | - | (1, 7, 28 d)[4(&)] | (4 d)[4(&)] | A#2 |
| | **XS130/-** | - | (1, 7, 28 d)[4($,&)] | (4 d)[4(&)] | A#1, A#2 |
| | **STE53/-** | - | (1, 7, 28 d)[4($,&)] | - | A#1 |
| | **TIPA/-** | - | - | (4 d)[4(&)] | A#2 |
| **BC-n.a.** | **Ref** | ($t_0$)[4($,&)] | (1, 7, 28 d)[4($,&)] | (4 d)[4(&)] | A#1, A#2 |
| | **XS100/-** | - | - | (4 d)[4(&)] | A#2 |
| | **XS130/-** | - | (1, 7, 28 d)[4($,&)] | (4 d)[4(&)] | A#1, A#2 |
| | **STE53/-** | - | (1, 7, 28 d)[4($,&)] | - | A#1 |
| | **TIPA/-** | - | - | (4 d)[4(&)] | A#2 |
| **PC-Qz** | **-/SP2** | ($t_0$, 30, 60 min)[5($)] | - | - | A#3, A#4 |
| **$LC^3$-50 (CC1)** | **-/SP1** | ($t_0$, 30, 60 min)[5($)] | - | - | A#3, A#4 |
| | **-/SP2** | ($t_0$, 30, 60 min)[5($)] | (1, 7, 28 d)[5($)] | (4 d) [6($)]- | A#3, A#4, This thesis |
| | **XS130/SP2** | - | (1, 7, 28 d)[5($)] | (4 d) [6($)]- | A#4, This thesis |
| | **STE53/SP2** | ($t_0$, 30, 60 min)[5($)] | (1, 7, 28 d)[5($)] | (4 d) [6($)]- | A#3, This thesis |
| **$LC^3$-50 (CC2)** | **-/SP1** | ($t_0$, 30, 60 min)[5($)] | - | - | This thesis |
| | **-/SP2** | ($t_0$, 30, 60 min)[5($)] | (1, 7, 28 d)[5($)] | - | A#3, A#4 |
| | **XS130/SP2** | - | (1, 7, 28 d)[5($)] | - | A#4 |
| | **STE53/SP2** | - | (1, 7, 28 d)[5($)] | - | A#3 |
| **$LC^3$-50 (CC3)** | **-/SP1** | ($t_0$, 30, 60 min)[5($)] | - | - | This thesis |
| | **-/SP2** | ($t_0$, 30, 60 min)[5($)] | (1, 7, 28 d)[5($)] | - | A#3, A#4 |
| | **XS130/SP2** | - | (1, 7, 28 d)[5($)] | - | A#4 |
| | **STE53/SP2** | - | (1, 7, 28 d)[5($)] | - | A#3 |
| **$LC^3$-35 (CC1)** | **-/SP2** | ($t_0$, 30, 60 min)[5($)] | - | - | A#6 |
| | **STE53/SP2** | ($t_0$, 30, 60 min)[5($)] | - | - | A#6 |
| **$LC^3$-35 (CC1)** | **-/SP3** | ($t_0$, 30, 60 min)[5($)] | (1, 7, 28 d)[5($)] | - | A#6 |
| | **STE53/SP3** | ($t_0$, 30, 60 min)[5($)] | (1, 7, 28 d)[5($)] | - | A#6 |
| **$LC^3$-20 (CC1)** | **-/SP2** | ($t_0$, 30, 60 min)[5($)] | (1, 7, 28 d)[5($)] | - | This thesis |
| | **STE53/SP2** | ($t_0$, 30, 60 min)[5($)] | (1, 7, 28 d)[5($)] | - | This thesis |

Mortar preparation according to [4]Methodology #4, [5]Methodology #5, [6]Methodology #6. [&]w/b= 0.50. [$]w/b= 0.40

# 2. Objectives

## Global Objective:

The overarching aim of this thesis is to contribute to the reduction of carbon dioxide ($CO_2$) emissions from cement production by developing and optimizing low-carbon cementitious materials with competitive performances. This work will primarily focus on Limestone Calcined Clay Cements ($LC^3$), which offer a significant reduction in $CO_2$ emissions, alongside exploring belite cements (BCs) for a comparative understanding of their environmental impact.

## Specific Objectives:

### 1. Investigate the workability and flowability of $LC^3$ with polycarboxylate-based superplasticizers:

Addressing known issues with the workability of $LC^3$ binders, this objective seeks to optimize the use of polycarboxylate-based superplasticizers to improve flowability. The goal is to ensure consistent performance and extended workability, particularly in large-scale applications requiring prolonged setting times.

### 2. Evaluate the impact of C-S-H seeding on early and long-term strength development in $LC^3$:

This objective involves investigating how C-S-H seeding admixtures influence the early-age compressive strength and long-term mechanical performance of $LC^3$ binders. The study will include microstructural analysis during the hydration process to understand how these admixtures contribute to strength enhancement and the development of a denser cement matrix.

### 3. Analyze the hydration kinetics of $LC^3$ with admixtures:

The research aims to explore the hydration kinetics of key phases (e.g., aluminates and sulfates) in $LC^3$ when combined with C-S-H seeding and other chemical admixtures, such as polycarboxylate-based superplasticizers. Calorimetry and in-situ analytical techniques will be used to study the acceleration of hydration and its impact on the overall strength development of $LC^3$.

### 4. Characterize the influence of admixtures on $LC^3$ microstructure and porosity:

This objective focuses on examining how chemical admixtures, particularly C-S-H seeding and superplasticizers, affect the porosity and microstructural development of $LC^3$. Advanced techniques like mercury intrusion porosimetry and ultrasonic pulse velocity will be employed to correlate porosity reduction and microstructural refinement with mechanical strength and durability.

# 3. Article section

## 3.1. Article 1 (A#1): Portland and Belite Cement Hydration Acceleration by C-S-H Seeds with Variable w/c Ratios

A. Morales-Cantero[1], A. Cuesta[1], A.G. De la Torre[1], O. Mazanec[2], P. Borralleras[3], K.S. Weldert[2], D. Gastaldi[4], F. Canonico[4] and M.A. G. Aranda[1]

[1] Departamento de Química Inorgánica, Cristalografía y Mineralogía, Universidad de Málaga, 29071 Málaga, Spain

[2] Master Builders Solutions Deutschland GmbH, Albert-Frank Str. 32, 83308 Trostberg, Germany;

[3] Master Builders Solutions España S.L.U., Carretera de l'Hospitalet, 147-149, Edificio Viena, 1ª Planta, 08940 Cornellà de Llobregat, Spain;

[4] Research & Development, Buzzi Unicem, Via Luigi Buzzi 6, 15033 Casale Monferrato, Italy;

Journal: Materials, 2022, 15(10), 3553

DOI: 10.3390/ma15103553

**Abstract:** The acceleration of very early age cement hydration by C-S-H seeding is getting attention from scholars and field applications because the enhanced early age features do not compromise later age performances. This acceleration could be beneficial for several low-$CO_2$ cements as a general drawback is usually the low very early age mechanical strengths. However, the mechanistic understanding of this acceleration in commercial cements is not complete. Reported here is a contribution to this understanding from the study of the effects of C-S-H gel seeding in one Portland cement and two belite cements at two widely studied water–cement ratios, 0.50 and 0.40. Two commercially available C-S-H nano-seed-based admixtures, i.e., Master X-Seed 130 and Master XSeed STE-53, were investigated. A multi-technique approach was adopted by employing calorimetry, thermal analysis, powder diffraction (data analysed by the Rietveld method), mercury intrusion porosimetry, and mechanical strength determination. For instance, the compressive strength at 1 day for the PC (w/c = 0.50) sample increased from 15 MPa for the unseeded mortar to 24 and 22 MPs for the mortars seeded with the XS130 and STE53, respectively. The evolution of the amorphous contents was determined by adding an internal standard before recording the powder patterns. In summary, alite and belite phase hydrations, from the crystalline phase content evolutions, are not significantly accelerated by C-S-H seedings at the studied ages of 1 and 28 d for these cements. Conversely, the hydration rates of tetracalcium alumino-ferrate and tricalcium aluminate were significantly enhanced. It is noted that the degrees of reaction of $C_4AF$ for the PC paste (w/c = 0.40) were 10, 30, and 40% at 1, 7, and 28 days. After C-S-H seeding, the values increased to 20, 45, and 60%, respectively. This resulted in larger ettringite contents at very early ages but not at 28 days. At 28 days of hydration, larger amounts of carbonate-containing AFm-type phases were determined. Finally, and importantly, the admixtures yielded larger amounts of amorphous components in the pastes at later hydration ages. This is justified, in part, by the higher content of amorphous iron siliceous hydrogarnet from the enhanced $C_4AF$ reactivity.

## 3.2. Article 2 (A#2): C-S-H seeding activation of Portland and Belite cements: An enlightening *in situ* synchrotron powder diffraction study

A. Morales-Cantero[a], A. Cuesta[a], A.G. De la Torre[a], I. Santacruz[a], O. Mazanec[b], P. Borralleras[c], K.S. Weldert[b], D. Gastaldi[d], F. Canonico[d], M.A.G. Aranda[a]

[a] Departamento de Química Inorg´anica, Cristalografía y Mineralogía, Universidad de M´alaga, M´alaga 29071, Spain

[b] Master Builders Solutions Deutschland GmbH, Albert-Frank Str. 32, 83308 Trostberg, Germany

[c] Master Builders Solutions Espa˜na S.L.U., Carretera de l'Hospitalet, 147-149, Edificio Viena, 1ª planta, 08940 Cornell`a de Llobregat, Spain

[d] Research & Development, Buzzi Unicem, Via Luigi Buzzi 6, 15033 Casale Monferrato, Italy

Journal: Cement and Concrete Research, 161, 2022, 106946

DOI: 10.1016/j.cemconres.2022.106946

**Abstract:** C-S-H seeding in Portland cements is well known from basic scientific works and field applications. Moreover, this activation approach could be beneficial for low-CO2 cements under development where a general drawback is poor mechanical strengths during the first week of hydration. However, a mechanistic understanding of the different processes taking place when seeding is still not developed. Here, we contribute to this knowledge gap by studying one commercial Portland cement and two industrial-trial belite cements. Three different admixtures are employed, viz. two types of commercial C-S-H seeding and triisopropanolamine as a typical alkanolamine. A multitechnique approach is employed including calorimetry, ultrasonic pulse velocity, thermal analysis and Rietveld analysis of laboratory X-ray powder diffraction data. Chiefly, an in situ X-ray synchrotron diffraction study has allowed mapping out the evolution of every crystalline phase. Furthermore, the use of an internal standard permitted to measure the changes in the overall amorphous content. In a nutshell, alite and belite (phases) hydrations are not significantly accelerated by C-S-H seeding for the three studied cements. Conversely, sulphate and aluminate phase dissolutions are enhanced. Faster ettringite crystallisation contributes to the observed improved mechanical properties at early ages. Moreover, a synergistic effect between C-S-H seeding and alkanolamine addition is proved. The importance of these findings for the possible acceleration of low-CO2 cement hydration is discussed.

## 3.3. Article 3 (A#3): Activation of $LC^3$ binders by C-S-H nucleation seeding with a new tailored admixture for low-carbon cements

A. Cuesta[1], A. Morales-Cantero[1], A.G. De la Torre[1], I. Santacruz[1], O. Mazanec[2], A. Dalla-Libera[3], S. Dhers[2], P. Schwesig[2], P.Borralleras[4] and M.A.G. Aranda[1]

[1] Universidad de Málaga, Málaga, Spain

[2] Master Builders Solutions Deutschland GmbH, Trostberg, Germany

[3] Master Builders Solutions Italia Spa, Treviso, Italy

[4] Master Builders Solutions España S.L.U., Cornellà de Llobregat, Spain

Proceedings of the 21st International Conference on Building Materials, Weimar (Germany), 2023

DOI: 10.1002/cepa.2786

**Abstract:** The use of supplementary cementitious materials is currently the most favorable strategy for reducing $CO_2$ emissions in cements. Limestone Calcined Clay Cements, $LC_3$, are a type of cement that allows the reduction of $CO_2$ emissions up to 40%. The proportions of the mixtures can vary, but the most investigated combination, $LC^3$-50, contains about 50 wt% clinker, 30 wt% calcined kaolinitic clay, 15 wt% limestone and an optimised calcium sulphate content. However, the mechanical strengths of $LC_3$ at early ages are not good enough and they should be improved. One way of doing this is by employing commercial strength-enhancing (accelerator) admixtures based on C-S-H nucleation seeding. For this work, $LC^3$-50 cements were prepared with clays with varying kaolinite contents. Mortars and pastes were fabricated using a new PCE-based superplasticizer developed to avoid the loss of fluidity at early ages typical of $LC^3$ binders. The selected accelerator for this study was Master X-Seed STE53. The results show that the loss of fluidity of $LC^3$ mortars during the first hours could be solved by a recently developed PCE-based superplasticizer. The compressive strengths at 1 day for $LC^3$ mortars strikingly improved by using the C-S-H seeding admixture and this behavior was maintained for up to 28 days.

## 3.4. Article 4 (A#4): Activation of $LC^3$ low-carbon cements by C-S-H seeding

A. Morales-Cantero[1], A.G. De la Torre[1], A. Cuesta[1], I. Santacruz[1], O. Mazanec[2], A. Dalla-Libera[2], S. Dhers[2], P. Schwesig[2], P. Borralleras[3] and M.A.G. Aranda[1]

[1] Departamento de Química Inorgánica, Universidad de Málaga, Málaga 29071, Spain

[2] Master Builders Solutions Deutschland GmbH, Albert-Frank Str, 32, 83308 Trostberg, Germany

[3] Master Builders Solutions España S.L.U., Carretera de l´Hospitalet, 147-149, Edificio Viena, 1ª planta, 08940 Cornellà de Llobregat, Spain

Proceedings of the 16th International Congress on the Chemistry of Cement 2023 (ICCC2023), Bangkok, Thailand, 2023

DoI: 10.13140/RG.2.2.26594.09920

**Abstract:** Portland-based Limestone Calcined Clay Cements ($LC^3$) are attracting a lot of the attention from scholars and field applications due to the reduction in $CO_2$ emissions. However, their low mechanical strengths at early ages are a key bottleneck for their widespread use. Calcined clays can also lead to a strong reduction of the fluidity in the first hours after mixing, which is an important second drawback. Here, these two issues have been addressed. Three $LC^3$ binders were prepared based on a PC-52.5R cement and three calcined clays, with variable amounts of kaolinite in the raw materials ranging 29-74 wt%. The particle sizes of the calcined clays were adjusted by milling to $D_{v,50}$=13±2 μm. The results show that the loss of fluidity of $LC^3$ mortars during the first hours can be solved by a recently developed PCE-based superplasticizer, specifically tailored for this application. Moreover, the compressive strengths at 1 day for $LC^3$ mortars have been boosted by a C-S-H nucleation seeding admixture and the gains are maintained at 28 days. It is noted that the compressive strengths at 1 day and room temperature were increased by 45-100 %, when compared to the corresponding unseeded mortars.

## 3.5. Article 5 (A#5): *In situ* synchrotron powder diffraction study of $LC^3$ cement activation at very early ages by C-S-H nucleation seeding

A. Morales-Cantero[a], A.G. De la Torre[a], A. Cuesta[a], I. Santacruz[a], I.M.R. Bernal[a], O. Mazanec[b], A. Dalla-Libera[c], P. Borralleras[d] and M.A.G. Aranda[a]

[a] Departamento de Química Inorgánica, Cristalografía y Mineralogía, Universidad de Málaga, Málaga 29071, Spain

[b] Master Builders Solutions Deutschland GmbH, Albert-Frank Str. 32, 83308 Trostberg, Germany

[c] Master Builders Solutions Italia Spa, Via Vicinale delle Corti, 21, 31100 Treviso, Italy

[d] Master Builders Solutions Espa˜na S.L.U., Carretera de l'Hospitalet, 147-149, Edificio Viena, 1ª planta, 08940 Cornell`a de Llobregat, Spain

Journal: Cement and Concrete Research, 2024, 178, 107463

DOI: 10.1016/j.cemconres.2024.107463

**Abstract:** Limestone Calcined Clay Cements, $LC^3$, are being widely researched as low-carbon binders. However, the hydration reactions during the first day are key for their performances and they were not well known. Here, we employ *in situ* synchrotron X-ray powder diffraction to understand the hydration reactions that take place during the first day. The influence of two superplasticisers and three strength-enhancing admixtures have been investigated. The diffraction data were analysed by the Rietveld method and the results compared to mass balance calculations. For $LC^3$ binders and in the absence of strength-enhancing admixtures, the hydration rates of the clinker phases, *i. e.* $C_3S$, $C_3A$ and $C_4AF$, are accelerated because of the filler effect. The C-S-H based-admixtures further accelerate the hydration of tricalcium aluminate and ferrite. Chiefly, it is firmly proved that the pozzolanic reaction takes place from 7 h onwards in the studied experimental conditions. The estimated degree of hydration of metakaolin at 22 h, in the studied binders, was ~10 %.

## 3.6. Article 6 (A#6): Enhancing fluidity and mechanical properties in $LC^3$ binders with one-third Portland clinker content

A. Morales-Cantero[a], D. Vallina[1], A.G. De la Torre[1], A. Cuesta[1], I. Santacruz[1], A. Dalla-Libera[2], P. Borralleras[3], S. Dhers[4], P. Schwesig[4], O. Mazanec[4] and M.A.G. Aranda[1]

[1] Departamento de Química Inorgánica, Cristalografía y Mineralogía, Universidad de Málaga, Málaga, 29071, Spain

[2] Master Builders Solutions Italia Spa, Via Vicinale delle Corti, 21, 31100 Treviso, Italy

[3] Master Builders Solutions España S.L.U., Carretera de l'Hospitalet, 147-149, Edificio Viena, 1ª planta, 08940 Cornellà de Llobregat, Spain

[4] Master Builders Solutions Deutschland GmbH, Albert-Frank Str. 32, 83308 Trostberg, Germany

Journal: Journal of Building Engineering, 2024, 95, 110334

DOI: https://doi.org/10.1016/j.jobe.2024.110334

**Abstract:** Limestone Calcined Clay Cements ($LC^3$) are attracting considerable attention due to their low $CO_2$ footprints and relatively fast hydration kinetics. $LC^3$-50 formulations (approximately 50 % Portland clinker, 30 % kaolinitic calcined clay, 15 % limestone and 5 % gypsum) are being extensively investigated and the hydration chemistry, rheology, mechanical strength developments and durability performances are starting to be well established. $LC^3$ binders with lower clinker factors are possible, offering an opportunity for further $CO_2$ footprint reduction. However, these blends have been much less studied. This work contributes to fill this gap. Here, a $LC^3$-35 binder (i.e. 35 % Portland clinker content) is investigated and its performances are compared to those of the original Portland cement (PC) and a standard $LC^3$-50 binder. The effects of two superplasticizers and a strength-enhancing admixture are thoroughly investigated in mortars and pastes. Larger calcined clay contents result in an exacerbation of the slump retention problem, but this issue is solved by the use of a new superplasticizer. Moreover, the low mechanical strengths at early ages can be partly mitigated with a C-S-H nucleation seeding admixture. Employing the right admixtures, $LC^3$-35 binders can develop strength values similar to those of neat PC and $LC^3$-50 at 7 and 28 days. The laboratory X-ray powder diffraction results for $LC^3$-35 pastes, when using the strength-enhancing admixture, show that $C_4AF$ exhibits an accelerated reaction rate, leading to the formation of larger amounts of AFt and AFm phases. Approximate mass balance calculations are carried out to estimate the metakaolin reaction degree. Finally, an environmental performance indicator is used to place the footprints of the reported binders within the $LC^3$ landscape.

# 4. General results and discussion

The development of mechanical strengths of a given mortar is a multifactorial dependent process, i.e. depends on mineralogical composition of the binder, fineness of the binder, w/(c,b) ratio, temperature, mixing methodology, flowability in the first hours of hydration, etc. Consequently, in this thesis in order to be able to compare the performances of different binders some parameters have been fixed such as the mixing methodology to prepare either pastes or mortars or the initial flowability, optimized with the used of superplasticizers.

## 4.1. Superplasticizers: type and amount optimization

Although it is not a primary objective of this thesis, it is essential to control the fluidity of the mortars when using superplasticizers, as this behaviour will influence the hydration kinetics, the future microstructure of the mortars, and their evolution over time, having a direct impact on mechanical strengths. For this reason, different commercial superplasticizers have been tested to control not only the initial fluidity but also the fluidity over time.

Superplasticizers are frequently required due to the specific surface area of the binder and the proportion of MK it contains. Blends of PC-SCMs, especially $LC^3$ binders, tend to have a high SSA, which reduces workability, thus making superplasticizers necessary [37]. A notable issue in this context is the significant loss of fluidity, particularly within the first 1-3 hours after mixing when using calcined clays with high MK levels [98], a challenge that must be carefully managed [44,99].

The superplasticizers used in this thesis are commercially available, with their complete brand names listed in Table 1.1. A concise summary of their main features can be found in Table 4.1.

The solid content of the SPs used in this study, as shown in Table 4.1., is consistently around 36 wt% for all samples, ensuring a similar concentration of active material across SP1, SP2, and SP3. This high solid content is important for effectively dispersing cement particles, as it provides a sufficient amount of active polymer to interact with the system.

The pH of the superplasticizer plays a crucial role in its effectiveness. For example, SP2 and SP3, with a higher pH of 10, may interact differently with cement components compared to SP1, which has a neutral pH of 7. However, the key difference between these superplasticizers lies not in the pH or their solid content, but in the form of the polymers. SP1 contains all its polymers in a free, fully dispersed state, while SP2 and SP3 have part of their polymers encapsulated in clusters. This encapsulation alters how the polymers are released with time and interact with the binder, potentially affecting their efficiency in maintaining workability and other performance characteristics. These differences in polymer structure will be explored in greater detail in the next section.

*Table 4.1. pH and solid content of the superplasticizers used.*

| Sample | pH | Solid content (wt%) |
|---|---|---|
| **SP1** | 7 | 36 |
| **SP2** | 10 | 36 |
| **SP3** | 10 | 36 |

The relatively high specific surface area of $LC^3$ binders, tends to reduce workability when maintaining a constant w/b ratio, making the use of superplasticizers necessary [37,100]. This

issue becomes more pronounced during the early hydration stages, particularly for $LC^3$ systems incorporating calcined clays with elevated metakaolin content, where the loss of fluidity in the first hour of hydration can be significant. Addressing this challenge is essential for optimizing performance [44,98,101–103].

### 4.1.1. Technology under SPs used

Figure 4.1. illustrates the mechanism of a conventional PCE. In Figure 4.1, the polycarboxylates from the PCE are freely dispersed in the medium. These free polycarboxylates bind to the cement particles due to their positive charge, while the negatively charged part remains oriented outward. This configuration enables the polycarboxylates to exert their dispersing effect, which leads to an immediate improvement in the flowability of the medium, as shown in Figure 4.1.b. However, as hydration products form over time, the increasing specific surface area and decreasing polymer surface coverage result in particle agglomeration, which leads to a loss of flow in the cement. As a result, they lose their ability to disperse, thereby diminishing their dispersing capacity, as depicted in Figure 4.1.c.

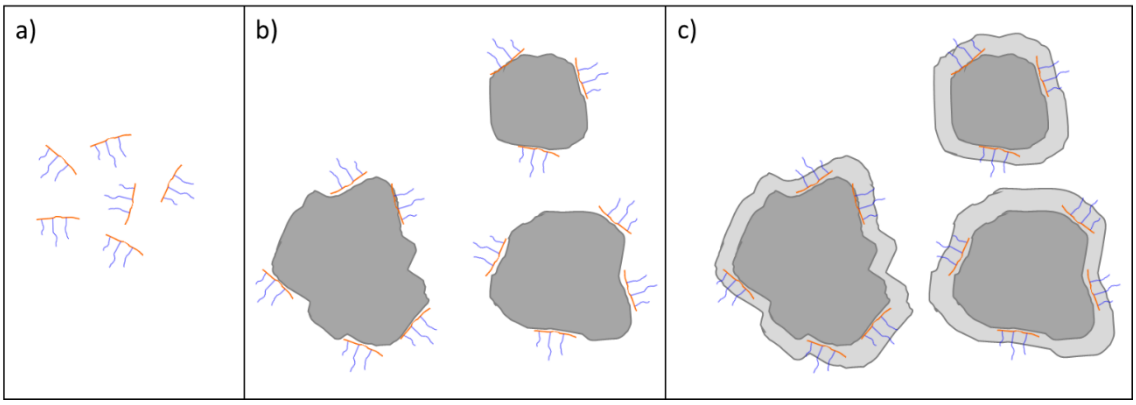


*Figure 4.1. Conventional PCE system (the dimensions and proportions of the grains and PCE are not depicted to scale). a) PCE polycarboxylates freely dispersed). b) Dispersing effect of polycarboxylates. c) Encapsulated polycarboxylates by the growing hydrated layers (light grey).*

Figure 4.2. illustrates the mechanism of a PCE based on the Intelligent Cluster System (ICS), such as Master$CO_2$re. In this system, the superplasticizer contains polycarboxylates in two forms: clusters and an initial portion of freely available polycarboxylate polymers. The freely available polycarboxylates are released first, allowing for the immediate dispersion of cement and calcined clay particles, as shown in Figure 4.2.a. This early release enhances workability at the beginning of the hydration process.

The remaining polycarboxylates, which are still bound within clusters (Figure 4.2.b), are gradually released as hydration progresses, responding to the increasing pH of the medium. This controlled, gradual release ensures sustained dispersion, optimizing slump retention and maintaining the workability of the mixture over an extended period, as depicted in Figure 4.2.c.

The gradual release mechanism allows the PCE to continue performing as the hydration phases evolve, extending fluidity beyond the initial dispersion phase. A key advantage of the ICS mechanism is the larger size of these clusters compared to conventional dispersants. This larger cluster size helps prevent the polycarboxylates from penetrating the micro-pores of SCMs, an issue often encountered with smaller dispersants.

This adaptability makes ICS-based PCEs particularly ideal for modern, sustainable cementitious blends, such as $LC^3$ systems with calcined kaolinite clay, as well as systems containing montmorillonite [104,105]. In both cases, the controlled release of polycarboxylates allows for superior fluidity control even in challenging environments [106].

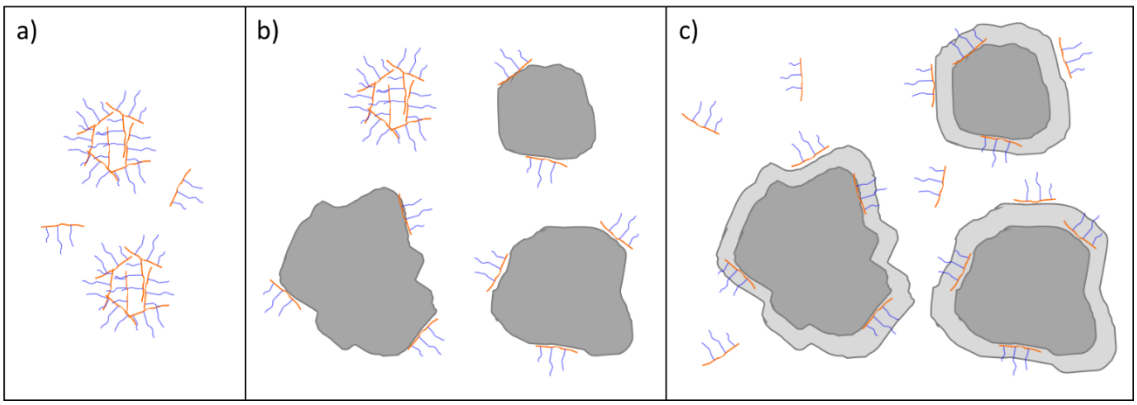


*Figure 4.2. PCE with the Intelligent Cluster System (the dimensions and proportions of the grains, PCE and clusters are not depicted to scale). a) Polycarboxylates in clusters and free polymers. b) Dispersing effect of free polycarboxylates and remaining bound PCE in clusters. c) Release of clusters as hydration progresses.*

Thus, the key difference between these two systems is that the ICS-based PCE uses a controlled release of polycarboxylates over time, ensuring prolonged fluidity and workability. In contrast, the conventional PCE relies on an immediate, but short-lived, dispersing action due to the free polycarboxylates being available only at the starting of hydration. This makes the ICS-based PCE particularly suitable for use in PC-SCM systems, and more specifically in $LC^3$ systems, where extended workability is crucial for performance.

Additionally, by modifying the type or size of the clusters' nuclei, it is possible to fine-tune the rate and amount of PCE released over time. This level of control allows for customization of the dispersing effect to meet the specific needs of different cementitious systems, making it an adaptable solution for optimizing slump retention and workability in various construction applications. The ability to adjust the release profile ensures that the PCE performs efficiently throughout the hydration process, even in systems requiring extended fluidity.

### 4.1.2. SP optimization in $LC^3$ systems: amount and type of SP

This section provides a comprehensive overview of several key findings obtained during this thesis regarding the use of superplasticizers in $LC^3$ systems, which contain varying levels of metakaolinite: high (CC1), medium (CC2), and low (CC3), see Table 8.1. The aim is to investigate how different types of superplasticizers influence the performance and workability of these cementitious systems.

All the mortars were prepared following Methodology #5 with w/(c,b) ratio of 0.40, and the slump test was performed measuring the initial, 30 and 60 minutes flow, Table 1.5.

Table 4.2. shows the specific surface area (SSA) of the blended studied in this section.

*Table 4.2. SSA values of the samples.*

| Sample | SSA of the blend ($m^2/g$) |
|---|---|
| **PC-425** | 1.9 |
| **PC-525** | 2.1 |
| **PC-Qz** | 1.9 |
| **$LC^3$-50 (CC1)** | 10.5 |
| **$LC^3$-50 (CC2)** | 4.2 |
| **$LC^3$-50 (CC3)** | 2.7 |
| **$LC^3$-35 (CC1)** | 13.2 |
| **$LC^3$-20 (CC1)** | 15.9 |

Table 4.3. presents the optimized quantities of each type of superplasticizer required to achieve a consistent initial slump of 200±20 mm. This was accomplished using the mortar preparation method outlined in section 1.3.3., subsection 0, for all plain PC and $LC^3$ samples studied. To streamline the data presentation, only the samples that did not include additional strength enhancing admixtures are included in this table, allowing for a clearer comparison of the effects of the different superplasticizers.

*Table 4.3. SP required to achieve a target initial slump of 200±20 mm.*

| Sample | SP1 | SP2 | SP3 |
|---|---|---|---|
| **PC-425** | 0.29 | 1.00 | - |
| **PC-525** | 0.34 | 1.20 | - |
| **PC-Qz** | - | 0.40 | - |
| **$LC^3$-50 (CC1)** | 1.00 | 1.20 | - |
| **$LC^3$-50 (CC2)** | 0.62 | 1.00 | - |
| **$LC^3$-50 (CC3)** | 0.38 | 0.50 | - |
| **$LC^3$-35 (CC1)** | - | 1.35 | 1.75 |

Figure 4.4. illustrates the slump spread over time for the various samples and superplasticizer quantities indicated in Table 4.3. The device used for the slump test has the bottom diameter of 100 mm, and what is represented in Figure 4.4. is the increase in spread relative to this initial value. For the superplasticizer SP1, the amount required to achieve the target slump increases as the sample's specific surface area rises, see Table 4.2., a relationship that will be further discussed in subsequent sections. As shown in Figure 4.4.a, when utilizing the conventional superplasticizer SP1, the slump spread gradually diminishes over time, ultimately reaching approximately 60 mm at the 60-minute mark for the PC and $LC^3$-50 samples with medium and low metakaolinite content. In stark contrast, the $LC^3$-50 sample with high metakaolinite content experiences a significant slump loss, dropping to nearly 0 mm after the first 30 minutes.

In Figure 4.4.b, the slump spread of selected samples using superplasticizer SP2 as a function of time are presented, specifically PC-525, two $LC^3$-50 samples (one with low (CC3) and high (CC1) kaolinite content), and the $LC^3$-35 series. SP2 has been specifically engineered for use in $LC^3$-50 systems characterized by high kaolinite content. From the data presented in Table 4.3., it is evident that a greater quantity of SP2 is necessary to achieve the target slump when compared to SP1. This increased requirement can be attributed to a higher proportion of PCE in cluster form and a correspondingly lower proportion of free PCE. This situation presents a dual effect: first, the larger amount of SP needed to meet the same target slump, and second, the gradual release of a greater portion of PCE due to its encapsulated nature within the clusters.

A notable observation is the re-fluidization effect in the PC and $LC^3$ samples with low and medium metakaolinite content, see Figure 4.4 and Table 8.2, where fluidity increases over time as a result of the continued release of PCE, leading to oversaturation of the system. Conversely, the slump for the $LC^3$-50 sample with high metakaolinite content remains constant over time.

Figure 4.3. shows two particles with a similar diameter, but different specific surface area and the same number of PCE chains. In case a), the particle surface is saturated with PCE, whereas in case b), it is not saturated due to the larger specific surface area.

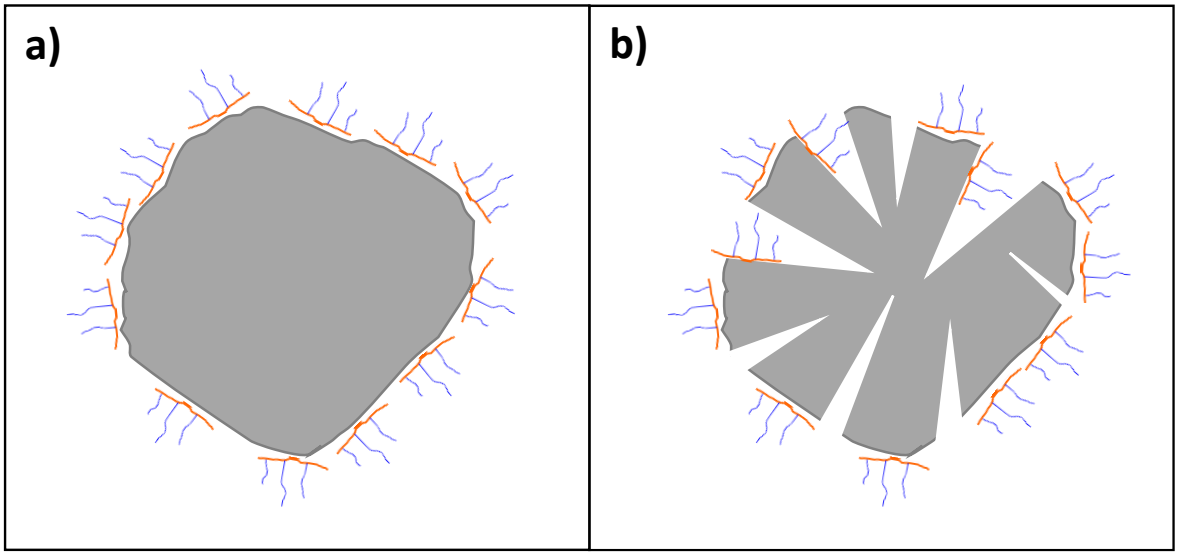


*Figure 4.3. Schematic illustration of a) a particle fully saturated with PCE and b) a partially saturated particle.*

These phenomena can be explained by the release of PCE encapsulated within the clusters, which causes oversaturation in the PC and $LC^3$-50 samples with low kaolinite content but does not have the same effect on the $LC^3$-50 sample with high kaolinite content. Thus, it can be concluded that the use of this superplasticizer with ICS technology is not necessary for plain PC or $LC^3$ systems containing low levels of metakaolinite, as it does not provide additional benefits in terms of workability.

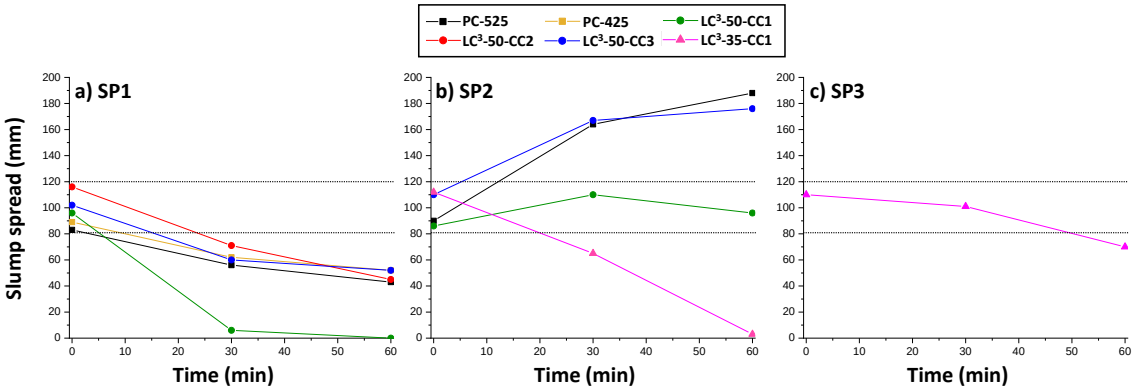


*Figure 4.4. Slump spread (referred to initial 100 mm) vs time for selected mortars prepared with Methodology #5 and w/(c,b) ratio of 0.40 with a) SP1, b) SP2 and c) SP3. Dotted horizontal lines depict the upper and lower target value. Elaborated from data of articles #3, #4 and this thesis.*

However, in the $LC^3$-35 sample which contains high metakaolinite content (71 wt%), a decline in slump is observed over time, even with SP2, Figure 4.4.b., with measurements dropping to nearly 0 mm after one hour.

To resolve the slump issue in the $LC^3$-35 system containing high metakaolinite content and high level of clinker substitution, a different type of superplasticizer (SP3), with a modified ICS technology, was employed (see Figure 4.4.c). As explained in the previous section, a larger quantity of SP is required, with 1.75% of SP3 compared to 1.35% of SP2 needed for the $LC^3$-35 sample. Despite this higher dosage, SP3 exhibits a slower decrease in slump over time, ultimately achieving a diameter of 70 mm after 60 minutes. This improved performance indicates that SP3 is more effective in maintaining the workability of the $LC^3$-35 system, thus providing a viable solution for high clinker replacement and metakaolinite content applications.

In conclusion, the data clearly show that flowability of these systems is heavily influenced by the metakaolinite content and the level of substitution and that the amount and type of superplasticizer used can be optimized. SP1, a conventional polycarboxylate, results in a gradual loss of slump in systems with medium and low metakaolinite content, while systems with high metakaolinite content exhibit a sharp and rapid slump reduction within the first 30 minutes. SP2 and SP3, ICS-based PCEs, with their adaptable release profiles, are particularly well-suited for modern, sustainable cementitious blends like $LC^3$, where high SCM content and extended workability are critical. The ability to tailor the release of polycarboxylates makes these superplasticizers highly versatile, providing enhanced performance and durability even in challenging systems with high SCM content.

### 4.1.3. Factors Influencing SP Consumption

Recent studies have identified the main factors influencing the demand for superplasticizers. The SSA of the calcined clay and the amount of calcined clay in the cement composition are the primary parameters that affect superplasticizer demand, regardless of the type of calcined clay or admixture used. Additionally, other factors may also influence admixture demand, such as the iron content in the mix, although further research is required to confirm this [37].

In this section, we correlate the main factors influencing SP demand, SSA of the blend, see Table 4.2., with the SP required for a target initial slump, see Table 4.3.

In Figure 4.5., the SSAs of the samples are plotted against the amounts of both SP1 and SP2 used to reach the initial target slump 200±20 mm. In Figure 4.5.a., the regression line shows the relationship between two PC and three $LC^3$ samples when a conventional PCE (SP1) is used. As can be observed, there is a strong correlation between the SSA of both PC and $LC^3$ samples and the amount of SP required.

In Figure 4.5.b., the regression line for the studied binders is plotted, this time using SP2 superplasticizer which is specifically designed for $LC^3$ systems, consequently plain PC systems are not plotted in it. Additionally, for a more comprehensive representation, the $LC^3$-20 (CC1) series, Table 8.2., has been included to show a limit case of very high clinker replacement. However, this series has not been further studied due to the low mechanical strengths developed.

In both figures, the amount of SP required to achieve the same initial slump correlates well with the total SSA of the samples.

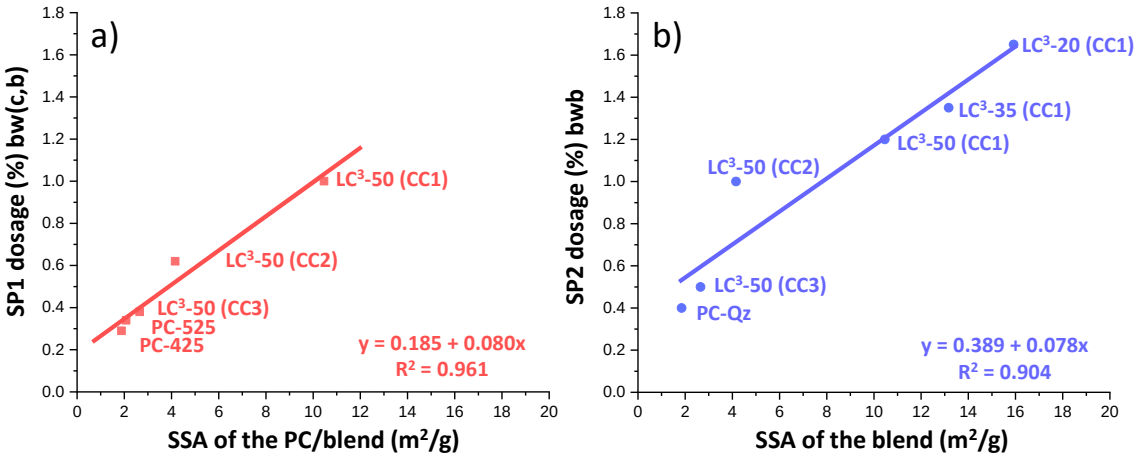


*Figure 4.5. Correlation between SSA and SP demand in $LC^3$ binders to achieve an initial slump spread of 200±20 mm. Elaborated from data of articles A#3, A#4 and this thesis.*

The demand for superplasticizers in cement blends, especially in $LC^3$ systems, is significantly influenced by the specific surface area. Larger surface areas require more SP to adequately disperse the particles and achieve the desired workability (slump). This is evident in $LC^3$ systems where the addition of calcined clays and Mk increases SSA, demanding more SP to maintain flowability.

In the future, research could focus on refining the relationship between secondary factors like iron content, which may further influence SP demand in specialized binders [37].

## 4.2. Strength enhancements admixtures

In this section, the effect of strength enhancing admixtures on mortars performances will be discussed. In this chapter firstly, a brief characterization of the strength enhancing admixtures will be provided, and then their impact on compressive strength, porosity, and hydration kinetics which will be discussed.

The strength enhancing admixtures used in this study are commercially available and are sold as colloidal suspensions. Table 4.4 presents their pH, solid content, and particle size. The pH of these admixtures is a crucial parameter, as it directly influences the cement hydration process and the formation of various hydrates within the cement matrix. A suitable pH level helps optimize the reaction kinetics, facilitating the efficient dissolution of cement particles and promoting the early formation of hydration products like C-S-H, which are essential for early strength development. In this case, all samples exhibit a consistent pH of 12, which is typical for admixtures that speed hydration reaction, called accelerators, used in cementitious systems. This alkaline pH ensures compatibility with the cement matrix, supporting stable interactions between the admixtures and the cement particles.

The solid content reflects the proportion of active material present in the enhancing admixture solution or suspension, determining how much of the enhancing admixture contributes to strength development within the cementitious matrix. XS100 is made of nanometric stabilised calcium silicate hydrate particles, while XS130 and STE53 contain C-S-H seeds along with alkanolamines. For the XS100 sample, the entire solid content consists of the C-S-H admixture stabilized with PCE. In contrast, for XS130 and STE53, the solid content relates to both the C-S-H and the alkanolamines, as well as the stabilizers.

The particle size of the strength enhancing admixtures affects their ability to be dispersed within the material. Smaller particles generally increase the surface area for reactions, potentially leading to improved strength performance and hydration kinetics.

*Table 4.4. pH, solid content, and particle size of the strength enhancing admixtures used in this thesis.*

| Sample | pH | Solid content (wt%) | $D_{v,50}$ (nm) |
|---|---|---|---|
| **XS100** | 12 | 21 | 297 |
| **XS130** | 12 | 25 | 230 |
| **STE53** | 12 | 26 | 234 |

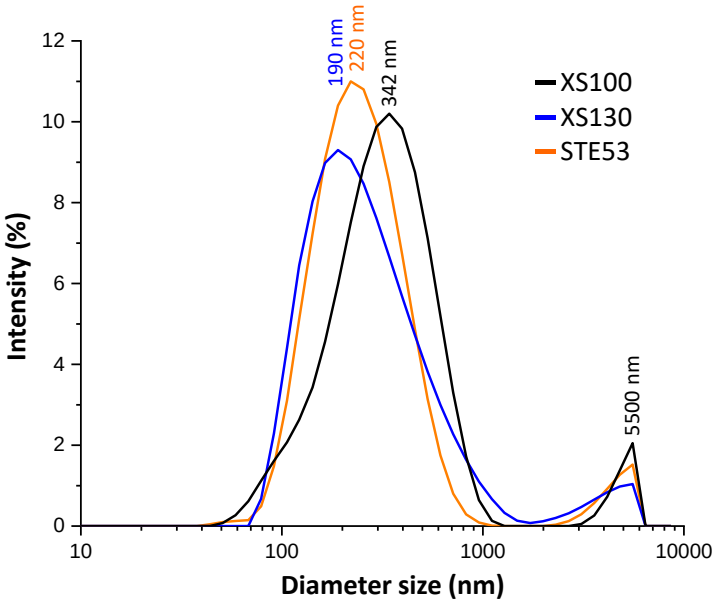


*Figure 4.6. Particle size distribution of the three different strength enhancing admixtures determined by dynamic light scattering in a Zetasizer Nano-ZS (Malvern Panalytical).*

The bimodal distribution in Figure 4.6. illustrates the presence of two distinct particle size populations within the strength-enhancing admixtures. The first peak appears at approximately 340 nm for the XS100 sample, while for the XS130 and STE53 samples the peak shifts to around 200 nm. The second peak, located consistently around 5500 nm for all samples, likely arises from the agglomeration of particles or the presence of larger admixtures.

The TEM images shown in Figure 4.7. provide direct visual evidence that supports the PSD observed in Figure 4.6. In these images, particles with sizes ranging from around 50 nm to larger agglomerates exceeding 500 nm can be observed. This correlates well with the first peak from the PSD curves, where the smaller particles, around 200-340 nm, likely represent aggregates of the primary particles seen in the TEM images. The agglomerations observed in TEM, which exceed 500 nm, may also contribute to the larger particle population in the size distribution.

The correlation between the findings of Figure 4.6. and Figure 4.7., along with previously reported particle sizes from the literature, further strengthens the evidence that these admixtures function by creating finely dispersed, agglomerated C-S-H particles. These structures play a vital role in improving early-age strength and accelerating the hydration process, which ultimately contributes to the enhanced compressive strength of the final product [37,98,107,108].

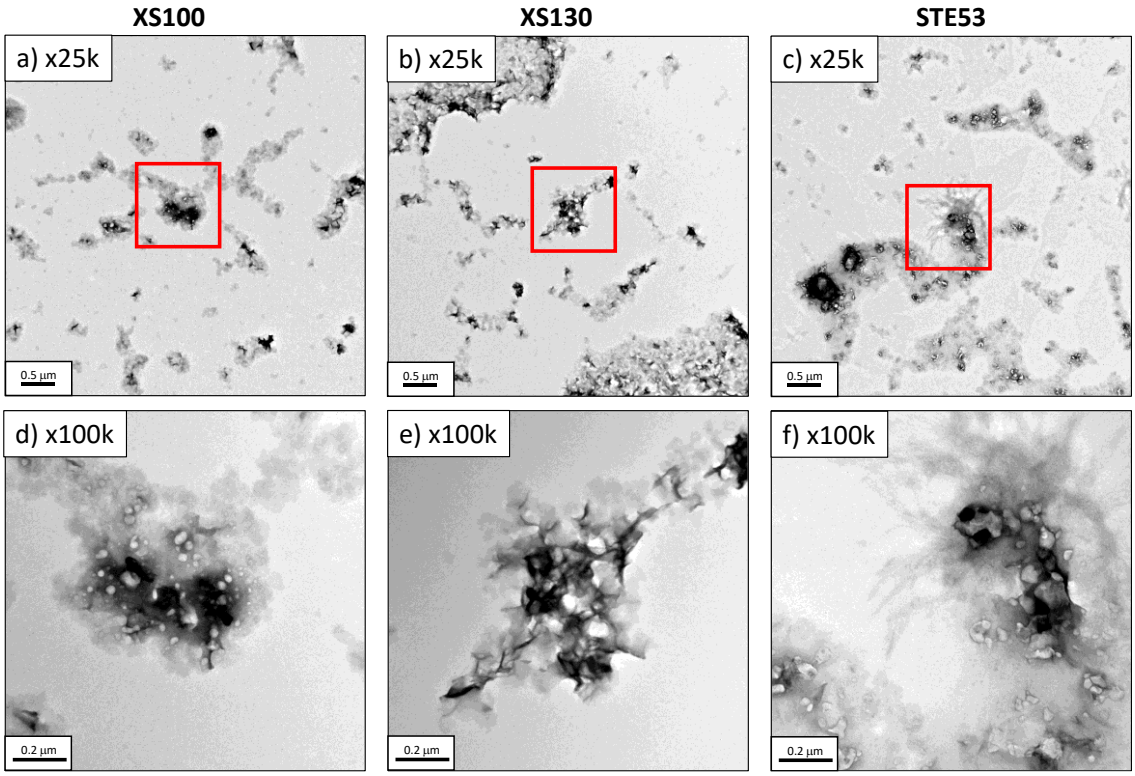


*Figure 4.7. TEM images of three strength enhancing admixtures based on C-S-H seeds. a), b), and c) showing x25k magnification. d), e), and f) showing x100k magnification.*

### 4.2.1. Compressive strengths with strength enhancing admixtures

In this section of the thesis, we will address the improvements in compressive strength achieved through the use of strength enhancing admixtures. The focus will be on the effectiveness of these admixtures in overcoming the common challenge of low early-age strength in low-$CO_2$ cement formulations. We will analyse the performance of both traditional and alternative cement systems, including $LC^3$, by examining the compressive strength improvements at various hydration stages, with a particular emphasis on the benefits observed at early ages.

The primary challenge with low-$CO_2$ cement formulations is their reduced early-age compressive strengths, particularly between 1-3 days. Therefore, it is essential to explore solutions that can mitigate or resolve this issue. One effective approach is the use of strength enhancing admixtures, which significantly improve early-age strengths without negatively impacting, and in some cases even slightly enhancing, long-term strengths. Several studies discuss how strength enhancement admixtures based on C-S-H nucleation seeding improve mechanical strength [80,81,99,108–113].

Figure 4.8. illustrates the compressive strength improvements for a series of samples with the addition of 2.0 wt% of a strength-enhancing admixture (either XS130 or STE53), compared to the same samples without any admixture. In Figure 4.8.a., the 1-day results for three plain cements are presented: one PC-425 and two belite cements. All samples were prepared following Methodology #4, without superplasticizers, and w/c of 0.50. In every case, significant compressive strength gains were observed, ranging from 13% to 72%. Figure 4.8.c. shows the 28-day results, where a more modest improvement, up to 20%, was observed. These findings

highlight the effectiveness of the admixtures in boosting early-age strength, which is critical for practical applications.

In Figure 4.8.b., the compressive strength improvements for $LC^3$-50 and $LC^3$-35 samples are shown with the addition of two commercial C-S-H seeding products (XS130 and STE53), compared to a reference sample without seeding. These samples were prepared according to Methodology #5, using SP2 and a w/(c,b) of 0.40. As shown, seeding significantly enhanced the 1-day compressive strengths. For the $LC^3$-50 samples, the improvement was greater in cases with Mk content in the calcined clay, due to the relatively low initial strength of the reference sample. The strength increase reached up to 110% in $LC^3$ samples with lower Mk content. Figure 4.8.d presents the 28-day results, where the improvement ranged between 20% and 35%. This demonstrates that the strength enhancement not only occurs at 1 day but is sustained through at least 28 days.

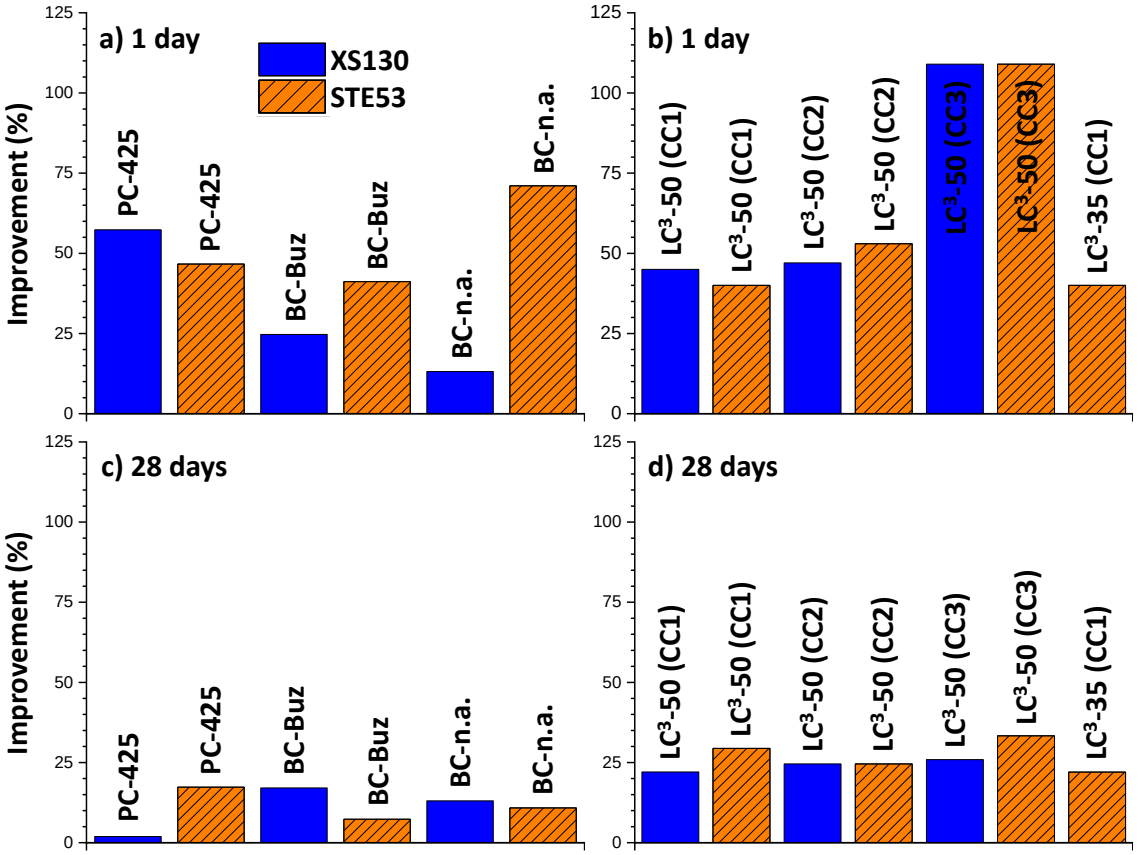


*Figure 4.8. Compressive strength improvements over time with the addition of 2.0 wt% of a strength-enhancing admixture, compared to the same mortar without the admixture. a) Plain cement samples at 1 day, b) $LC^3$ samples at 1 day, c) Plain cement samples at 28 days, and d) $LC^3$ samples at 28 days. Data sourced from articles A#1, A#3, A#4, and A#5. Data of the compressive strength values are summarized in Table 8.3.*

To assess the feasibility of the low $CO_2$ emission samples, an environmental performance indicator was calculated for the studied samples and compared with the reference results. This indicator, as described in [35,101], is determined by the ratio of the binder's $CO_2$ footprint to its compressive strength at the specified hydration time, as shown in Equation 7. The lower the indicator, the more environmentally friendly the sample will be.

$$EP\ (\frac{g_{CO_2}}{MPa}) = \frac{gCO_2\ equivalent\ per\ kilogram}{Compresive\ strength}$$

*Equation 7. Environmental performance*

Table 4.5. outlines the $CO_2$ associated emissions of the materials and the sources of these data. The European Federation of Concrete Admixture Associations provides generic Environmental Product Declarations (EPD) for the different type of admixtures which include the $CO_2$ footprints [114]. According to this federation, the superplasticizers used in this work fall under Group B. As EPD for these specific products are not yet available, the value used is based on a comparable superplasticizer in the same group, as indicated in Table 4.5. For the strength enhancement admixtures no dedicated $CO_2$ footprint analysis has been conducted so far. Thus, the conversion factor applied is derived from the value reported for a related C-S-H nucleation seeding admixture, see Table 4.5.

*Table 4.5.$CO_2$ emissions and data sources for materials and admixtures used*

| Sample | Cement | Calcined clay | Limestone | Gypsum | SP# | Str. Enh. |
|---|---|---|---|---|---|---|
| **kg$CO_2$eq/kg** | 0.85[115] | 0.249[116] | 0.0022[115] | 0.00[115] | 0.689[117] | 0.73[118] |

Figure 4.9 presents the EP values obtained from Equation 7, where for each sample, the starting materials (in the case of binders) and additives used have been considered. For belite cements, the value was approximated by reducing the cement value provided in Table 4.5. by 15%.

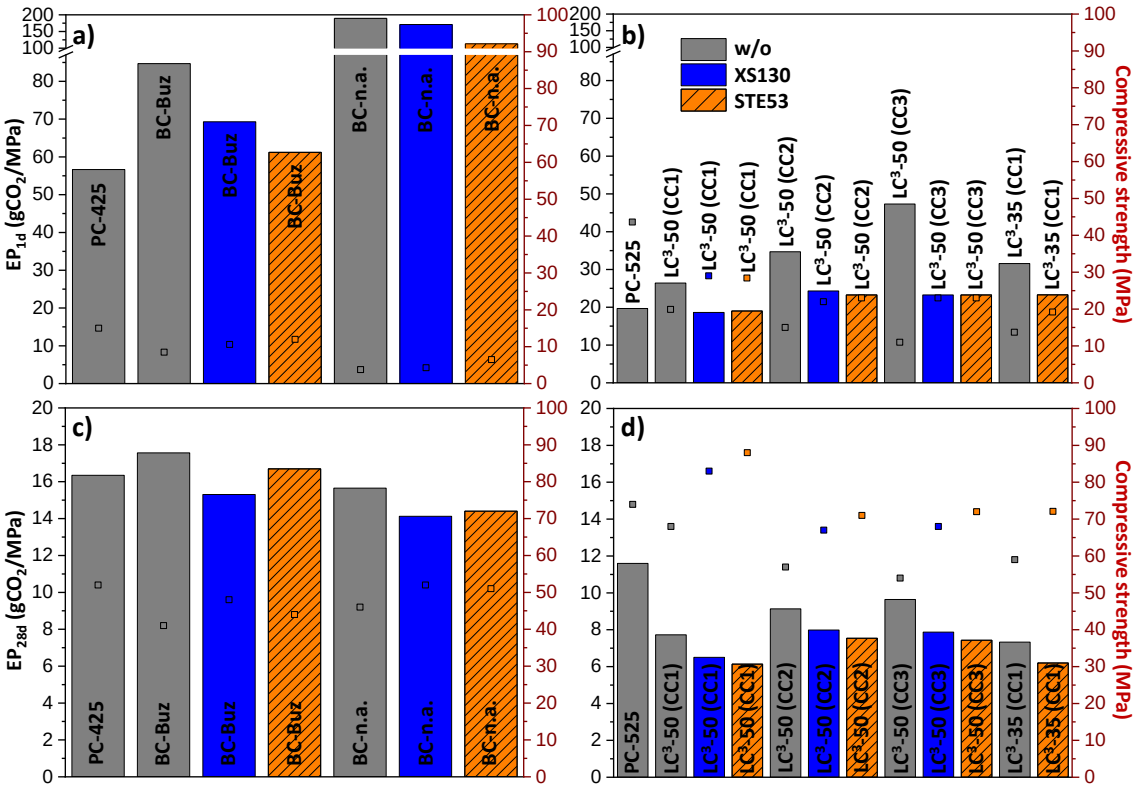


*Figure 4.9. Environmental performance indicator (EP) expressed as bars. a) and c) samples prepared using Methodology #4 at 1 and 28 days, respectively; b) and d) samples prepared following Methodology #5 at 1 and 28 days, respectively. Data sourced from articles A#1, A#3, A#4, and A#5. Mechanical strength are given as squares.*

In Figure 4.9.a., the $EP_{1d}$ results for three plain cements are presented: one PC-425 and two belite cements. All samples were prepared following Methodology #4, without superplasticizers, and with a water/cement ratio of 0.50. The $EP_{1d}$ value for PC-425 is 57 $gCO_2$/MPa, for BC-Buz 85 $gCO_2$/MPa, and for BC-n.a. 190 $gCO_2$/MPa. This higher (worse) value is due to the low initial compressive strength. After seeding, the values slightly decrease, to approximately 65 $gCO_2$/MPa and 140 $gCO_2$/MPa for BC-Buz and BC-n.a., respectively. However, these values remain worse (higher) than those for PC-425.

Figure 4.9.c. shows the $EP_{28d}$ results, with the Y-axis adjusted for better visualization compared to the 1-day results. As expected, all values decrease due to the increased compressive strengths at 28 days. The $EP_{28d}$ values for PC-425, BC-Buz, and BC-n.a. are 16.3, 17.6, and 15.7 $gCO_2$/MPa, respectively. BC-Buz achieves a value close to the reference (PC-425) without requiring seeding, and BC-n.a. shows better performance without seeding. After seeding, these values improve further: BC-Buz-XS130 reaches 15.3 $gCO_2$/MPa and BC-Buz-STE53 16.7 $gCO_2$/MPa. For BC-n.a., the values for XS130 and STE53 are 14.1 and 14.4 $gCO_2$/MPa, respectively. Although these values are slightly better than those for the reference PC-425, these low-$CO_2$ cements require more research to become competitive.

In Figure 4.9.b., the $EP_{1d}$ results for PC-525, $LC^3$-50, and $LC^3$-35 samples are shown with the addition of two commercial C-S-H seeding products (XS130 and STE53). These samples were prepared following Methodology #5, using SP2 and a water/binder ratio of 0.40. As shown, the $EP_{1d}$ for PC-525 is lower (19.7 $gCO_2$/MPa) compared to binders without seeding. Additionally, comparing the different $LC^3$-50 samples, a decrease in metakaolin (MK) content results in an increase in $EP_{1d}$, as expected. The $LC^3$-35 prepared with calcined clay with a high MK content achieves an $EP_{1d}$ of 31.6 $gCO_2$/MPa, which improves to 23.3 $gCO_2$/MPa after seeding. This improvement is due to its low production emissions combined with acceptable 1-day compressive strengths (>10 MPa).

Figure 4.9.d presents the $EP_{28d}$ results for the same series. It shows that PC-525 has a value of 11.6 $gCO_2$/MPa and that all $LC^3$ binders show improvements in $EP_{28d}$, both with and without seeding. The binders that achieve the best values are $LC^3$-50 (CC1) and $LC^3$-35 (CC1) with the STE53 additive, reaching as low as 6.1 $gCO_2$/MPa.

In this thesis, the focus will shift to $LC^3$ materials, as they represent the most promising alternative for reducing $CO_2$ emissions [4,10,16,17,119]. This remarkable reduction in emissions not only contributes to more sustainable construction practices but also aligns with global efforts to mitigate climate change. Furthermore, there is the potential for even greater reductions in $CO_2$ emissions with higher levels of clinker substitution, indicating that $LC^3$ could play a pivotal role in future cement production strategies.

In contrast, BCs, while also beneficial, typically achieve only a 15% reduction in $CO_2$ emissions [120–122]. This highlights the superior environmental performance of $LC^3$ cements. As construction demands grow and environmental regulations become increasingly stringent, the cement industry is under pressure to adopt more eco-friendly practices. The transition to $LC^3$ not only meets these demands but also promotes innovation in materials science, paving the way for further advancements in sustainable construction materials.

Overall, the emphasis on $LC^3$ cements represents a critical step toward achieving significant reductions in greenhouse gas emissions from the cement sector, contributing to a more sustainable future for the construction industry and the planet.

### 4.2.2. Influence of strength enhancing admixtures on microstructure

This section will examine how the porosity of the samples changes after being treated with strength enhancing admixtures, compared to the reference samples, without them. It is well known that the improvements in the compressive strength of mortars are related to the reduction in total porosity, due to a more uniform distribution of the C-S-H gel within the samples [99,123].

#### 4.2.2.1. Porosity of pastes analysis by mercury intrusion porosimetry

The analysis of porosity is a crucial aspect when evaluating the performance of cementitious materials, as it directly influences mechanical properties, durability, and resistance to external factors such as water or chemical ingress. In this study, the addition of strength enhancing admixtures appears to have a significant impact on the microstructure of the material, particularly in terms of porosity [49,50,95,123–127].

When strength enhancing admixtures are introduced into the binder, one of the key effects is a reduction in total porosity. This reduction is closely linked to the more uniform distribution of the C-S-H gel, which is the primary hydration product responsible for binding particles in the cement matrix and contributing to mechanical strength. A more homogeneous C-S-H distribution reduces the amount and size of voids within the matrix, creating a denser and more compact structure. This improved microstructure results in less space for cracks or defects to propagate, which in turn enhances the compressive strength of the material.

Comparing samples treated with strength enhancing admixtures to the reference samples without them, it becomes evident that the untreated samples exhibit a higher level of porosity at the same age. This higher porosity can be attributed to a less efficient hydration process, where the C-S-H gel is not as uniformly distributed, leading to the formation of larger voids and weaker points within the structure. These weaknesses contribute to a lower compressive strength in the reference samples.

Figure 4.10. presents the correlation between total porosity, in percentage, and mechanical strengths of $LC^3$-50 samples (CC1, CC2, and CC3) both without and with a 2.0 wt% of C-S-H seeding (XS130 or STE53). The porosity was measured by MIP in pastes at a maximum pressure of 225 MPa, pastes prepared as detailed in Methodology #3. A clear linear correlation is observed across the different binders ($LC^3$-50), regardless the presence of admixtures.

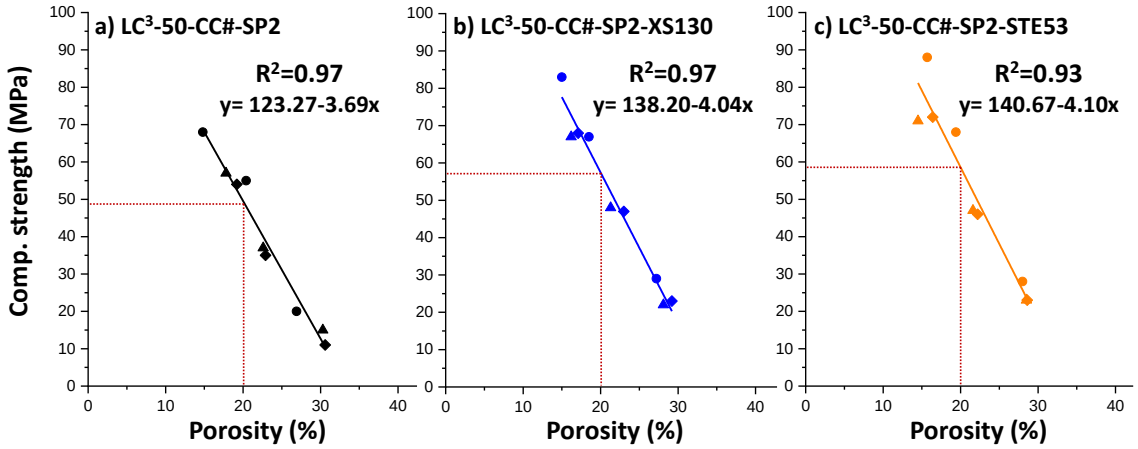


*Figure 4.10. Compressive strength of mortars, prepared with a w/b ratio of 0.40, as a function of total porosity for $LC^3$ pastes, prepared with a w/b ratio of 0.35, a) without strength enhancing admixtures, b) with 2.0 wt% XS130, and c) with 2.0 wt% STE53. The solid lines represent linear regressions of the data points, while the dashed lines highlight the 20% total porosity. Elaborated from data of articles A#3, A#4 and this thesis.*

It is evident that, for the given porosity, samples containing admixtures exhibit higher compressive strength, shown as a higher negative slope in the linear regression in Figure 4.10.b. and Figure 4.10.c. This demonstrates that the admixtures play a key role in improving the material's microstructure, beyond just reducing porosity. As previously discussed, the strength enhancing admixtures promote a more uniform distribution of C-S-H gel within the cement matrix. This not only decreases porosity but also enhances the overall packing density of the hydrated phases, resulting in more efficient load transfer throughout the material.

Moreover, the presence of admixtures like C-S-H seeding agents improves the hydration kinetics, further strengthening the binder matrix. This suggests that the impact of admixtures goes beyond just reducing porosity—they fundamentally alter the nature of the hydrated phases, resulting in a stronger material. In the following sections of this thesis, additional results will be presented that corroborate and reinforce the conclusions outlined in this section. These results will provide further evidence of the positive impact of the additives on the microstructure and mechanical properties of $LC^3$ pastes, thereby validating the claims made in the previous analysis.

Thus, Figure 4.10. highlights that admixtures can enhance the compressive strength even when porosity levels are similar, reinforcing the idea that the strength of the material is influenced not only by the quantity but also by the way in which the hydration products are spatially distributed. The improvements in microstructure, driven by these admixtures, reduce internal weaknesses and result in a material more resistant to both mechanical loading and environmental degradation. This suggests the seeding contributes to the formation of a more refined microstructure [99].

These findings suggest significant potential for further optimizing admixture formulations to enhance both the mechanical properties and long-term durability of cementitious materials. This improvement can be achieved by promoting a more refined microstructure, even when porosity levels remain comparable. Previous studies have already highlighted how C-S-H phases contribute to increased durability, particularly in systems using supplementary cementitious materials [50,83,127–131].

#### 4.2.2.2. Densification of mortars determined by ultrasonic pulse velocity, UPV

Another way to analyse porosity or connectivity is through UPV analysis, where a sound pulse passes through a 40 mm section of the sample. A higher velocity indicates a denser material. Previous studies have explored improvements in cement material densification using this technique through the use of strength enhancing admixtures [108,132].

The UPV in cement systems can sometimes start below the velocity of sound in water (1000 m/s) [133,134], due to several factors. On one hand, when cement is first mixed with water, the solid particles are not yet interconnected, leading to high attenuation of ultrasonic waves [135]. On the other hand, the entrapped air in fresh samples can reduce the velocity in the initials stages [136].

Figure 4.11. presents, the results of an $LC^3$-50 (CC1) mortar, prepared both without and with 2.0 wt% of strength enhancing admixtures (XS130 or STE53). Additionally, a PC-525 mortar is included as reference. In Figure 4.11.a., the velocity of hydration during the first 96 hours is shown, while Figure 4.11.b. represents the acceleration during the first 24 hours.

From Figure 4.11.a., the following observations can be made. As expected, there is a progressive increase in velocity over time due to the hydration process, during which solid material forms and reduces or refines the porosity. Notably, a much more pronounced increase in velocity is observed during the early hours when strength enhancing admixtures based on C-S-H seeds are used. This demonstrates their role in promoting mortar densification and improving the pore structure´s connectivity. When comparing $LC^3$-50 with the reference, a higher initial rate of solid formation is observed in the $LC^3$ sample due to the filler effect [137]. After approximately 36 hours, the PC-525 sample reaches its maximum velocity, while the $LC^3$ samples continue to increase slightly over time. Longer measurement times would be needed to establish their maximum values.

Figure 4.11.b. shows the acceleration. Similar to the heat flow data obtained from calorimetry, the first peak corresponds to the maximum hydration of silicates ($C_3S$), while the second peak is related to sulfate and aluminate hydration. For the samples without strength-enhancing admixtures, the first peak occurs at 5.0 hours for the plain PC-525 and at 4.1 hours for the $LC^3$-50 without admixture, while the accelerated samples reach their maximum at approximately 2.6 hours. Additionally, the second peak occurs at 17.0 hours for PC-525 and 16.1 hours for $LC^3$-50 without admixture, whereas the accelerated samples show greater differentiation in this second peak, with maxima at 9.4 hours for the XS130 sample and 11.4 hours for the STE53 sample. This indicates, first, the filler effect when comparing the plain PC with the $LC^3$-50 binder, and that the alkanolamine present in XS130 primarily accelerates sulfate and aluminate hydration more effectively than STE53.

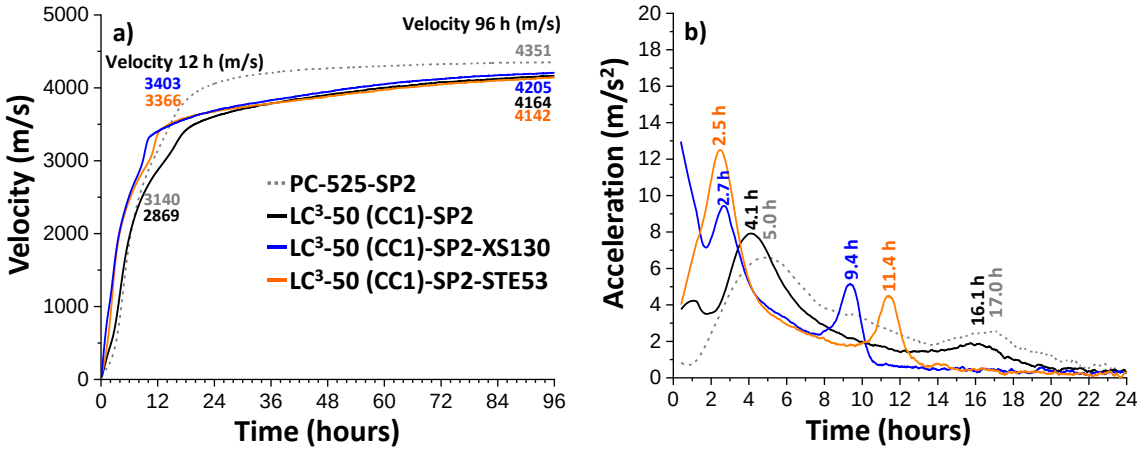


*Figure 4.11. Ultrasonic pulse velocity development with time for PC-525 and LC³-50 (CC1) mortars: a) Velocity during the first 96 hours of hydration. Inset numbers display the velocity values at 12 h. b) Acceleration during the first 24 hours. Inset numbers give the time at the maximums.*

To conclude the comparison between porosity measurements obtained by MIP and UPV, we can observe that both techniques offer complementary insights into the microstructure of the materials and its impact on compressive strength. The MIP results for pastes emphasize that admixtures can significantly improve compressive strength, even when overall porosity levels are comparable. This suggests that the strength is influenced by factors beyond just the total porosity, such as the quality, distribution, and connectivity of the hydration products.

On the other hand, the UPV analysis provides further evidence of this improvement by directly assessing the connectivity of the pore structure for mortars. The increase in UPV velocity, particularly in samples treated with C-S-H seeding strength enhancing admixtures indicates better interconnectivity of the hydration products, leading to a denser and more resilient microstructure. The early acceleration in velocity also demonstrates that these admixtures promote faster hydration, resulting in earlier formation of solid phases that contribute to strength development.

Taken together, these results show that while both MIP and UPV highlight different aspects of porosity and its role in mechanical performance, they align in demonstrating that the admixtures enhance not only the hydration kinetics but also the overall microstructural development. This leads to fewer internal weaknesses and contributes to the material's ability to withstand mechanical loads and resist environmental degradation over time.

### 4.2.3. Effect of strength enhancing admixtures on hydration kinetics

This section the effect of strength enhancing admixtures on the hydration kinetics. The hydration was studied using calorimetry, X-ray diffraction, and thermal analysis. Since much of this data has been published previously, only the most relevant findings are discussed here to avoid redundancy.

#### 4.2.3.1. Heat of hydration

One of the approaches to examining the impact of accelerated hydration caused by strength enhancement admixtures is through calorimetric analysis [108,110,123,132,138].

Figure 4.12. illustrates the calorimetry curves for the LC$^3$-50 (CC1)-SP2 pastes, both without and with a 2.0 wt% of C-S-H seeding (XS130 or STE53), prepared using a w/b of 0.40, following the Methodology #3, articles A#3 and A#4, as a representative example of the LC$^3$-50 heat evolution behaviour.

In Figure 4.12.a., the heat release curves demonstrate that the samples with strength enhancing admixtures reach higher heat values at 1 day compared to those without admixtures. Importantly, this increased heat is maintained even at 7 days (see insets numbers in Figure 4.11), indicating that the strength enhancing admixtures improve the reactivity and hydration rate of the samples over time.

Figure 4.12.b. shows the heat flow curves. The peak associated with $C_3S$ hydration is observed at approximately 5.1 hours in all samples, with no significant acceleration due to the admixtures. However, the peaks related to the hydration of aluminates and sulfates show a marked acceleration. In the sample without admixtures, the peak appears at 13.2 hours, whereas with the addition of the STE53 admixture, the peak shifts to 11.2 hours, and with the XS130 admixture, it accelerates further to 8.1 hours. This suggests that the strength enhancing admixtures significantly accelerate the hydration of the aluminates and sulfates, which contributes to faster strength development.

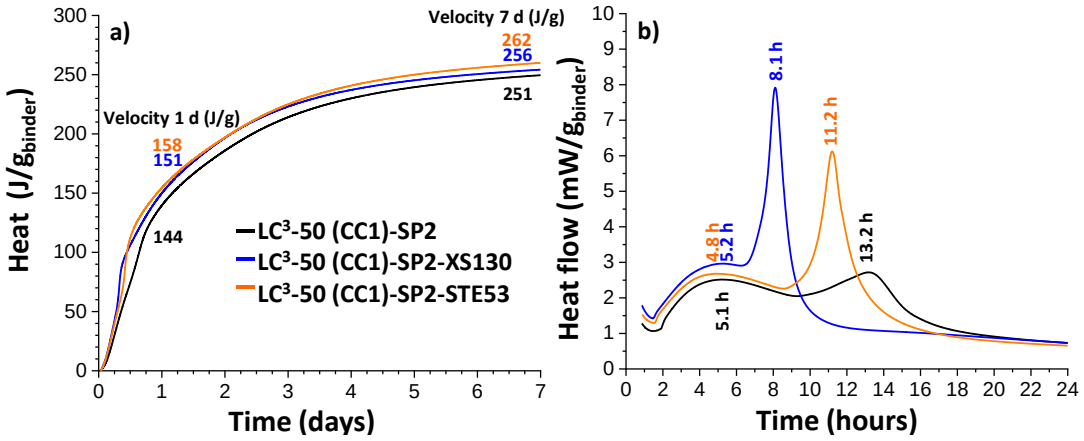


*Figure 4.12. Calorimetry analysis for LC$^3$-50 (CC1) mortars: a) Cumulative heat over the first 7 days of hydration, b) Heat flow curves during the first 24 hours.*

When comparing these calorimetry results with those from the UPV tests—bearing in mind that calorimetry is performed on cement pastes, while UPV is conducted on mortars—several important observations can be made:

Earlier peak appearance in mortars: The hydration peaks appear earlier in mortars than in pastes. This is likely due to the larger surface area provided by the sand particles in the mortars and the increased shear energy applied during the mixing process, which can enhance the hydration kinetics.

Discrepancy in first peak timing: The appearance of the first peak (related to alite hydration) does not show a correlation between the two methods. In the calorimetry results, the timing of this peak remains consistent across all samples, regardless of the presence of admixtures. In contrast, the UPV results show earlier connectivity in the seeded samples, suggesting that while

the overall $C_3S$ reactivity remains unchanged, the admixtures may enhance the uniformity of the phase formation, improving the connectivity between hydrated phases.

Correlation of second peak: The second peak, related to the hydration of aluminates and sulfates, follows the same order of appearance in both calorimetry and UPV results, though the specific times differ. This confirms that the strength enhancing admixtures accelerate the reactions involving aluminates and sulfates, which aligns with the faster connectivity gain observed in the UPV results. The analysis reveals that, after the addition of C-S-H seeding, the paste is nearly lacking in sulfation. This underscores the importance of considering in both the type and quantity of admixture to achieve proper binder sulfation [107,139].

In conclusion, the calorimetry results highlight that strength enhancing admixtures improve hydration by accelerating the reaction of aluminates and sulfates, leading to quicker strength development. Although the $C_3S$ hydration does not appear to be significantly accelerated, the overall improvement in the microstructure, especially in terms of the uniformity and connectivity of hydration products, results in better mechanical performance at earlier stages. These findings, when correlated with the UPV results, reinforce the idea that admixtures contribute not only to faster hydration but also to a more cohesive and efficient cement matrix.

#### 4.2.3.2. Effect of strength enhancing admixtures on degree of hydration of individual phases

In the previous section, the increase in the total heat evolved by the seeded samples indicates a higher overall degree of hydration. Furthermore, the shift of certain signals in the calorimetry curves suggests an acceleration of specific hydration phases. *In-situ* synchrotron X-ray powder diffraction (SXRPD) studies enable the precise determination of the individual degrees of hydration for the various phases, providing deeper insights into the kinetics of phase development during cement hydration [140,141]. Recent studies have explored the use of SXRPD for early-age analysis of the effect of C-S-H on phase hydration [107,108,123].

Figure 4.13. shows the degrees of hydration of the phases in the $LC^3$-50 (CC1) sample with SP2, both without and with 2.0 wt% of C-S-H seeding (XS130 or STE5), based on data obtained from Synchrotron X-ray Powder Diffraction (SXRPD), article A#5, as representative example of $LC^3$.

Figure 4.13.a. presents the reactivity of $C_3S$, where it can be observed that the reactivity is higher in the sample without admixtures. This observation can be correlated with results obtained from other techniques, such as calorimetry and UPV, where no acceleration of the $C_3S$ peaks was noted in the presence of admixtures. The lower degree of alite hydration in the seeded samples may result from the increased reactivity of $C_3A$ and $C_4AF$. It is well known that aluminates in the pore solution retard or inhibit the hydration of alite [51,75,142–145].

Figure 4.13.b. and Figure 4.13.c. show the degrees of hydration of $C_3A$ and $C_4AF$, respectively. In the case of $C_3A$, the degree of hydration increases from 57% in the unseeded sample to 70% after seeding. For $C_4AF$, the hydration increases from 31% to 42% at 20 hours.

These increases can be linked to the earlier acceleration of aluminates and sulfates observed in the calorimetry curves, where the addition of strength enhancing admixtures significantly shifted the peaks to earlier times. Additionally, the higher hydration degrees observed for $C_3A$ and $C_4AF$ align with the improved connectivity seen in UPV measurements, indicating that the

admixtures promote faster and more complete formation of hydrated phases coming from $C_3A$ and $C_4AF$ hydration, contributing to overall better mechanical performance.

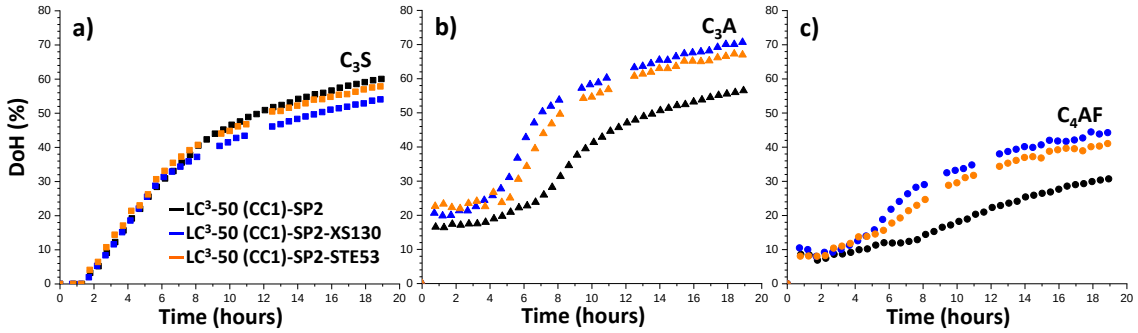


*Figure 4.13. Degree of hydration curves for LC³-50 (CC1) pastes. a) $C_3S$, b) $C_3A$ and c) $C_4AF$.*

#### 4.2.3.3. Thermal analysis, TA

With the objective of obtaining information about the hydration process coming from different and independent methodologies, a comprehensive thermal analysis was conducted for the PC-525 and LC³-50 pastes, focusing on two key parameters: bound water (BW), directly related to degree of hydration, and portlandite (CH) content, directly related to the pozzolanic reaction. The pastes were hydrated following the Methodology #3, and arrested by solvent exchange, ensuring the removal of all free water [146]. However, this method introduces a margin of error, as arresting hydration affects/alter hydrated phases, mainly, AFt content [147,148]. After arresting hydration, the samples underwent TA from ambient temperature to 1000°C. BW values were calculated based on mass loss calculated from the TA data between ambient temperature and 550°C, while the mass loss between 550-900°C, attributed to $CaCO_3$ decomposition, is beyond the scope of this discussion.

##### Bounded water

The study of BW was conducted at hydration intervals of 1, 7, and 28 days. Each series was prepared both without admixtures and with the addition of 2.0 wt% of strength enhancing admixtures XS130 and STE53. Table 4.6. presents the BW values for these series from TA analysis, revealing several important trends. First, as expected, BW content increases with longer hydration periods, indicating the formation of additional hydrated phases. Second, the lower kaolinite content in the pristine clay results in lower BW values, indicating reduced reactivity, especially at 1 day. Lastly, the presence of strength enhancing admixtures leads to higher BW levels, reflecting increased reactivity. These results, which are obtained from an independent method, correlate with the findings from calorimetry, UPV and SXRPD measurements.

*Table 4.6. Bounded water values from TA for a plain PC and three LC³ pastes at 1, 7 and 28 days.*

| Sample | Bounded water (wt%) | | |
|---|---|---|---|
| | 1 d | 7 d | 28 d |
| **PC-525-SP2** | 8.3 | 14.1 | 15.3 |
| **PC-525-SP2-XS130** | 11.4 | 15.3 | 16.9 |
| **PC-525-SP2-STE53** | 11.7 | 15.8 | 17.0 |
| **LC³-50 (CC1)-SP2** | 7.6 | 10.9 | 13.3 |
| **LC³-50 (CC1)-SP2-XS130** | 8.1 | 12.4 | 13.8 |

| | | | |
|---|---|---|---|
| **$LC^3$-50 (CC1)-SP2-STE53** | 8.3 | 12.7 | 14.3 |
| **$LC^3$-50 (CC3)-SP2** | 6.1 | 10.4 | 12.4 |
| **$LC^3$-50 (CC3)-SP2-XS130** | 7.4 | 11.1 | 13.1 |
| **$LC^3$-50 (CC3)-SP2-STE53** | 7.8 | 11.7 | 13.8 |

Figure 4.14. illustrates the relationship between BW and compressive strength in mortars (with a w/b ratio of 0.40, prepared as per section 1.3.3.5. Despite the variation in composition across the nine data points (representing three $LC^3$ types), a strong correlation between BW content and compressive strength is evident.

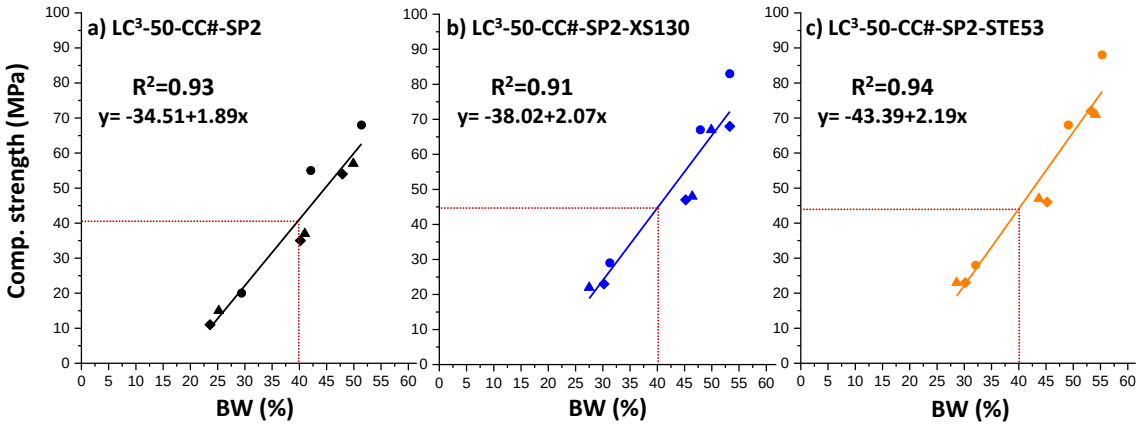


*Figure 4.14. Compressive strength of $LC^3$ mortars as a function of bound water of $LC^3$ pastes for a) samples without strength enhancing admixtures, b) samples with XS130, and c) samples with STE53. Mortars were prepared with a w/b ratio of 0.40, prepared as Methodology #5. Pastes were prepared with w/b of 0.35, Methodology #3. Dashed lines highlight the 40% of BW. Elaborated from data of articles #3, #4 and this thesis.*

The higher slope in the linear regression clearly demonstrates that samples with admixtures consistently achieve higher compressive strength for the same amount of BW. This indicates that, even when the level of chemical reactivity (as reflected by BW content) is similar, the presence of admixtures enhances the material's mechanical performance.

This improvement can be attributed to the fact that admixtures contribute to a more refined and interconnected microstructure. Specifically, admixtures such as C-S-H seeds which, not only promote a more complete and efficient hydration process but also encourage the formation of a denser, more cohesive network of hydration products, particularly the C-S-H gel, which is the main binding phase in cement.

Comparing this information with the previously obtained MIP results, a clear correlation emerges between the findings of both techniques. Both thermal analysis and MIP highlight the critical role of admixtures in enhancing the material's compressive strength, even when key metrics like BW content (a proxy for chemical reactivity) or porosity are similar between samples with and without admixtures. The BW determined by thermal analysis (Figure 4.14.) links the superior strength in samples with admixtures to a more refined microstructure, where C-S-H seeds promote a denser and more cohesive network of hydration products, particularly C-S-H gel. This observation aligns with MIP results (Figure 4.10.), which show that admixtures not only reduce porosity but also improve the distribution and packing density of the hydrated phases. Both analyses converge on the conclusion that admixtures lead to a more interconnected microstructure, facilitating more efficient load transfer and improving mechanical performance.

In both cases, the admixtures influence the internal cohesion and structural integrity of the cement matrix. MIP underscores the importance of how admixtures refine the distribution of C-S-H gel within the pores, reducing weaknesses and improving overall strength. Thermal analysis, on the other hand, emphasizes how admixtures accelerate hydration processes and create a more compact microstructure for the same level of reactivity. Essentially, while one technique focuses on porosity and the other on bounded water, they both highlight that the effectiveness of admixtures extends beyond simple porosity reduction or reactivity enhancement—they fundamentally alter the quality of the microstructure, resulting in a stronger material.

### Portlandite content

The portlandite (CH) content of the samples provides another metric for evaluating their reactivity, specifically, their pozzolanic activity. Table 4.7. summarizes the CH content for PC-525 and two $LC^3$-50 samples—one with high metakaolin content and one with low metakaolin content—measured at 1, 7, and 28 days. These samples were prepared under identical conditions, with and without the strength enhancing admixtures XS130 and STE53. Several observations can be made from this data, offering further insight into the reactivity and hydration behaviour of the different formulations.

At 1 day of hydration, the PC-525 sample has a CH content of 6.0 wt%. For the $LC^3$-50 samples, the expected CH content is at least 3.1 wt% (after applying the dilution factor), since these samples benefit from the filler effect, which enhances reactivity (refer to the calorimeter data). However, in the $LC^3$-50 (CC1) sample, the CH content is lower than expected due to the dilution effect, signalling the starting of the pozzolanic reaction. In contrast, the $LC^3$-50 (CC3) sample shows a slightly higher portlandite content than the diluted plain PC sample, likely due to the filler effect.

At 7 days, the portlandite content increases in the plain PC samples, but this trend is not observed in the $LC^3$ samples. This further confirms the ongoing pozzolanic reaction, which consumes the CH produced by the hydration of $C_3S$, as also shown in the XRD analysis (see the corresponding section).

By 28 days, the portlandite content continues to rise in the plain PC samples. However, in the $LC^3$ samples, there is a significant decrease in CH due to the ongoing pozzolanic reaction.

When comparing the samples with and without C-S-H seeding admixtures, it is clear that the samples with admixtures have lower portlandite content. This reduction could be due to two factors: firstly, the alkanolamine-containing admixtures may slow down the hydration of alite, slightly reducing the amount of CH produced. Secondly, these admixtures may accelerate the pozzolanic reaction [76,149–151], further lowering the CH content.

*Table 4.7. Portlandite content determined by TA for the selected samples.*

| Sample | CH content (wt%) | | |
|---|---|---|---|
| | **1 d** | **7 d** | **28 d** |
| **PC-525-SP2** | 6.0 | 7.7 | 8.3 |
| **PC-525-SP2-XS130** | 3.2 | 5.2 | 5.5 |
| **PC-525-SP2-STE53** | 4.1 | 6.1 | 6.7 |
| **$LC^3$-50 (CC1)-SP2** | 2.3 | 2.3 | 1.3 |
| **$LC^3$-50 (CC1)-SP2-XS130** | 1.3 | 1.4 | 0.6 |

| | | | |
|---|---|---|---|
| **$LC^3$-50 (CC1)-SP2-STE53** | 1.8 | 2.0 | 0.8 |
| **$LC^3$-50 (CC2)-SP2** | 3.3 | 3.4 | 1.6 |
| **$LC^3$-50 (CC2)-SP2-XS130** | 2.2 | 2.4 | 0.9 |
| **$LC^3$-50 (CC2)-SP2-STE53** | 2.7 | 2.9 | 1.0 |
| **$LC^3$-50 (CC3)-SP2** | 3.7 | 3.9 | 1.9 |
| **$LC^3$-50 (CC3)-SP2-XS130** | 2.6 | 2.8 | 1.1 |
| **$LC^3$-50 (CC3)-SP2-STE53** | 3.4 | 3.3 | 1.5 |

The combined analysis of calorimetry, phase analysis, and thermal analysis reveals how admixtures enhance the hydration process and mechanical performance of $LC^3$ samples. Admixtures accelerate the hydration of aluminates and sulfates, promoting early strength development and improving the uniformity and connectivity of hydration products. This leads to better mechanical performance, as supported by UPV and phase analysis data, which show increased hydration of $C_3A$ and $C_4AF$. Although $C_3S$ reactivity is slightly lower, admixtures primarily refine the microstructure. Thermal analysis shows that even with similar chemical reactivity, samples with admixtures achieve higher compressive strength due to a denser microstructure. MIP data supports this, showing reduced porosity and better packing of hydration products. Finally, lower CH levels in admixture-containing samples reflect enhanced pozzolanic reactions, contributing to a more durable and efficient binder.

# 5. Conclusions

The main objective of this thesis is to make a significant contribution to understanding how additives impact the production of sustainable cements, such as $LC^3$ systems. Two key goals are pursued: first, to improve cement flowability and workability through the use of superplasticizers, addressing one of the most critical challenges in the production of low-carbon cements. Second, to optimize mechanical strength and hydration phases by incorporating nucleation additives. These objectives align with the need to reduce $CO_2$ emissions without compromising cement performance.

1. Improving Flowability with Superplasticizers

Enhancing flowability is one of the main challenges in producing low-carbon cements like $LC^3$, as these systems tend to lose workability quickly after mixing. In this context, the use of PCE superplasticizers has proven to be an effective solution for maintaining flowability without affecting other critical properties.

In articles 3 (A#3) and 4 (A#4), the behaviour of the superplasticizer Master$CO_2$re 3240 in $LC^3$ systems was studied. This additive, designed with a gradual release technology of polycarboxylates organized in clusters, successfully solved the problem of fluidity loss that typically affects these cementitious systems. Over time, it was observed that Master$CO_2$re 3240 not only helped maintain the workability of $LC^3$ mixtures but also facilitated an increase in mechanical strength. These superplasticizers contribute significantly to the production of more sustainable cements, allowing greater flexibility in mixing and pouring operations at construction sites.

In article 6 (A#6), another superplasticizer variant, Master$CO_2$re 3400, was evaluated in an $LC^3$-35 system with a high content of calcined clay rich in metakaolin. This additive was particularly effective in retaining fluidity during the first 1-3 hours after mixing. Since loss of workability is one of the main challenges in cements with high clinker substitution, the use of Master$CO_2$re 3400 is positioned as a key solution to maintain fluidity properties during the necessary time on-site, without compromising long-term mechanical performance. This fluidity retention is crucial in low-carbon concrete applications, where reducing clinker content while maintaining or improving mechanical properties is the goal.

Overall, the studies presented in articles A#3, A#4, and A#6 demonstrate that superplasticizers based on gradual release technology are highly effective in maintaining workability in sustainable cementitious systems like $LC^3$. These additives not only solve short-term fluidity loss problems but also contribute to better compaction and cohesion in the material, improving its overall long-term performance.

2. Improving Mechanical Strength and Hydration Phases

Additives based on C-S-H gel nanoparticles, such as Master X-Seed 130 and STE 53, have proven effective in accelerating hydration and improving mechanical strength in various cementitious systems. In particular, these additives have been key in enhancing 1-day strength and the development of late strength in Portland, belitic, and $LC^3$ cements.

In article 1 (A#1), a significant acceleration in the hydration of $C_3A$ and $C_4AF$ phases was reported, resulting in a 40-110% increase in compressive strength at 1 day, which is crucial for projects requiring rapid structural availability.

Article 2 (A#2) complements these findings by showing how combining nucleation additives with alkanolamines can improve hydration in belitic and Portland cement systems. Although no direct acceleration in the reactivity of $C_3S$ and $C_2S$ phases was observed at 1 d or later, there was an improvement in the dissolution of aluminates and calcium sulfate phases, promoting a higher formation rate of hydration products. These findings open the door to additional optimizations to enhance phase reactivity in low-carbon cements.

A key aspect of the research presented in articles 3 (A#3) and 4 (A#4) was the evaluation of hydration acceleration using calorimetry. Additionally, in A#3, X-ray diffraction confirmed the acceleration of $C_4AF$ and $C_3A$ in $LC^3$ systems.

In article 5 (A#5), the use of advanced techniques such as synchrotron X-ray powder diffraction allowed the study of hydration phases in $LC^3$ systems and PC 525R pastes. C-S-H nucleation additives like STE53 and XS130 improved the hydration of calcium aluminate phases in $LC^3$ systems. Additionally, it was noted that pozzolanic activity in $LC^3$ pastes with high metakaolin content began around 7 hours.

Finally, article 6 (A#6) evaluated the performance of an $LC^3$ system with low clinker content using strength-enhancing additives like Master X-Seed STE 53. The use of these additives resulted in a denser and more compact microstructure, contributing to an overall improvement in long-term mechanical performance. An acceleration in the hydration of aluminate and silicate phases was observed, leading to a significant increase in strength at 1 and 7 days.

Together, the results from articles A#1, A#2, A#3, A#4, A#5, and A#6 confirm that C-S-H nucleation additives not only accelerate the hydration of key phases in Portland and belitic cements but also significantly improve early and late strength in low-carbon systems like $LC^3$. By densifying the microstructure and reducing porosity, these additives play a crucial role in enhancing the performance and durability of sustainable cements, allowing for faster strength development without compromising the final product's quality.

Therefore, the findings presented in this thesis highlight the key role of additives, such as superplasticizers and C-S-H nanoparticles, in improving sustainable cements. By addressing the challenges of workability and strength development, these additives not only enable more efficient and low-carbon production but also open new opportunities for future research in the development of more durable and eco-friendly construction materials.

**Future Research**

Based on the findings of this thesis, future research opportunities are vast and aim to optimize both the performance of $LC^3$ and other low-carbon systems.

Durability and Long-Term Performance of $LC^3$

Although $LC^3$ has shown great potential to reduce $CO_2$ emissions while maintaining acceptable mechanical performance, especially after 7 days, more detailed studies are needed on its long-term durability under various environmental conditions. It would be crucial to study its behaviour in aggressive environments, such as exposure to carbon dioxide, sulfates, chlorides, or freeze-thaw cycles, to ensure sustainability goals are met without compromising long-term structural integrity in practical applications.

Development of Superplasticizers with Adaptable Profiles

Another promising research avenue is the exploration of developing PCE superplasticizers with different types of "clusters." Modifying the size and nature of the PCE core could yield additional benefits, such as filler effects or more specific interactions with cementitious phases. This could enable certain superplasticizers to not only act as dispersants but also as strength enhancers, which would be particularly useful in systems with high clinker substitution levels.

Synergies with Other Cement Phases and SCMs

Delving deeper into the synergies between superplasticizers and cement phases, including SCMs, could open new avenues for optimizing low-carbon binders. A more detailed study of these secondary factors could further improve the performance of $LC^3$ and other specialized binders.

# 6. Conclusiones (Conclusions in Spanish)

El objetivo principal de esta tesis es hacer una contribución significativa al entendimiento de cómo los aditivos impactan en la producción de cementos sostenibles como los sistemas $LC^3$. Se persiguen dos metas clave: por un lado, mejorar la fluidez y trabajabilidad del cemento mediante el uso de superplastificantes, abordando uno de los desafíos más críticos en la fabricación de cementos de baja huella de carbono. Por otro lado, se busca optimizar las resistencias mecánicas y las fases de hidratación mediante la incorporación de aditivos de nucleación. Estos objetivos se alinean con la necesidad de reducir las emisiones de $CO_2$ sin comprometer el rendimiento del cemento.

**1. Mejora de la fluidez con superplastificantes**

La mejora de la fluidez es uno de los principales retos en la producción de cementos de baja huella de carbono como el $LC^3$, dado que estos sistemas tienden a perder trabajabilidad rápidamente después de la mezcla. En este contexto, el uso de superplastificantes de PCE ha demostrado ser una solución eficaz para mantener la fluidez sin afectar otras propiedades críticas.

En el artículo 3 (A#3) y artículo 4 (A#4), se estudió el comportamiento del superplastificante Master$CO_2$re 3240 en sistemas $LC^3$. Este aditivo, diseñado con una tecnología de liberación gradual de policarboxilatos organizados en clusters, resolvió con éxito el problema de la pérdida de fluidez que típicamente afecta a estos sistemas cementantes. Se observó que, a lo largo del tiempo, el Master$CO_2$re 3240 no solo ayudaba a mantener la trabajabilidad de las mezclas de $LC^3$, sino que también facilitaba un incremento en la resistencia mecánica. Estos superplastificantes contribuyen significativamente a la producción de cementos más sostenibles, permitiendo una mayor flexibilidad en las operaciones de mezcla y vertido en obras de construcción.

En el artículo 6 (A#6), se evaluó otra variante de superplastificante, el Master$CO_2$re 3400, en un sistema $LC^3$-35 con un alto contenido de arcilla calcinada rica en metacaolín. Este aditivo fue particularmente eficaz en la retención de la fluidez durante las primeras 1-3 horas después de la mezcla. Dado que la pérdida de trabajabilidad es uno de los principales desafíos en cementos con alta sustitución de clínker, el uso de Master$CO_2$re 3400 se posiciona como una solución clave para mantener las propiedades de fluidez durante el tiempo necesario en obra, sin comprometer el rendimiento mecánico a largo plazo. Esta retención de fluidez es crucial en aplicaciones de hormigones de baja huella de carbono, donde se busca reducir la cantidad de clínker mientras se mantienen o mejoran las propiedades mecánicas.

En conjunto, los estudios presentados en los artículos A#3, A#4 y A#6 demuestran que los superplastificantes basados en tecnología de liberación gradual son altamente efectivos para mantener la trabajabilidad en sistemas cementantes sostenibles como el $LC^3$. Estos aditivos no solo resuelven los problemas de pérdida de fluidez a corto plazo, sino que también contribuyen a una mejor compactación y cohesión en el material, lo que mejora su rendimiento general a largo plazo.

## 2. Mejora de resistencias mecánicas y fases de hidratación

Los aditivos basados en nanopartículas de gel C-S-H, como el Master X-Seed 130 y el STE 53, han demostrado su eficacia para acelerar la hidratación y mejorar las resistencias mecánicas en diversos sistemas cementantes. En particular, estos aditivos han sido clave en la mejora de resistencias a 1 día y en el desarrollo de resistencias tardías en cementos Portland, belíticos y $LC^3$.

En el artículo 1 (A#1), se reportó una aceleración significativa en la hidratación de las fases $C_3A$ y $C_4AF$, lo que resultó en un aumento de resistencias a compresión de entre 40-110% a 1 día, lo que es crucial en proyectos que requieren una rápida disponibilidad estructural.

El artículo 2 (A#2) complementa estos hallazgos mostrando cómo la combinación de aditivos de nucleación con alcanolaminas puede mejorar la hidratación en sistemas belíticos y cemento Portland. Aunque no se observó una aceleración directa en la reactividad de las fases $C_3S$ y $C_2S$ a 1 día o posteriormente, sí se evidenció una mejora en la disolución de fases de aluminato y sulfato de calcio, favoreciendo una mayor tasa de formación de productos de hidratación. Estos hallazgos abren la puerta a optimizaciones adicionales para potenciar la reactividad de fases en cementos de baja huella de carbono.

Un aspecto fundamental de la investigación presentado en el artículo 3 (A#3) y artículo 4 (A#4) fue la evaluación de la aceleración de la hidratación mediante calorimetría. Además, en el A#3 se confirmó por difracción de rayos-X de polvo la aceleración de $C_4AF$ y $C_3A$ en sistemas $LC^3$.

En el artículo 5 (A#5), el uso de técnicas avanzadas como la difracción de polvo de rayos X en sincrotrón permitió estudiar las fases de hidratación en sistemas $LC^3$ y pastas de PC 525R. Los aditivos de nucleación de C-S-H, como STE53 y XS130, mostraron la mejora en la hidratación de las fases de aluminato de calcio en sistemas $LC^3$. Además, se destacó que la actividad puzolánica en pastas $LC^3$ con alto contenido de metakaolin empezó sobre las 7 horas.

Finalmente, el artículo 6 (A#6) evaluó el comportamiento de un sistema $LC^3$ con bajo contenido en clínker con aditivos de mejora de fuerza como el Master X-Seed STE 53. El uso de estos aditivos resultó en una microestructura más densa y compacta, contribuyendo a una mejora global en el rendimiento mecánico a largo plazo y se observó una aceleración en la hidratación de las fases de aluminato y silicato, lo que permitió un aumento significativo en las resistencias a 1 y 7 días.

En conjunto, los resultados de los artículos A#1, A#2, A#3, A#4, A#5 y A#6 confirman que los aditivos de nucleación de C-S-H no solo aceleran la hidratación de las fases clave en cementos Portland y belíticos, sino que también mejoran significativamente las resistencias tempranas y tardías en sistemas de baja huella de carbono como el $LC^3$. Estos aditivos, al densificar la microestructura y reducir la porosidad, juegan un papel esencial en la mejora del rendimiento y la durabilidad de cementos sostenibles, permitiendo un desarrollo más rápido de resistencias sin comprometer la calidad del producto final.

Por tanto, los hallazgos presentados en esta tesis destacan el papel clave de los aditivos, como los superplastificantes y las nanopartículas de C-S-H, en la mejora de los cementos sostenibles. Al abordar los desafíos de trabajabilidad y desarrollo de resistencias, estos aditivos no solo

permiten una producción más eficiente y de menor huella de carbono, sino que también abren nuevas oportunidades para la investigación futura en el desarrollo de materiales de construcción más duraderos y ecológicos.

El avance en estas líneas de investigación contribuirá significativamente a la optimización de cementos de baja huella de carbono, permitiendo que tecnologías como el $LC^3$ se implementen a mayor escala con garantías de durabilidad, rendimiento y sostenibilidad a largo plazo.

**Investigaciones futuras**

A partir de los hallazgos de esta tesis, las oportunidades de investigación futura son vastas y apuntan a optimizar tanto el rendimiento del $LC^3$ como de otros sistemas de baja huella de carbono.

Durabilidad y rendimiento a largo plazo en $LC^3$

Aunque el $LC^3$ ha demostrado un gran potencial para reducir las emisiones de $CO_2$ manteniendo un rendimiento mecánico aceptable, especialmente después de 7 días, es necesario realizar investigaciones más detalladas sobre su durabilidad a largo plazo bajo diversas condiciones ambientales. Sería crucial hacer más estudios a su comportamiento en entornos agresivos, como la exposición a dióxido de carbono sulfatos, cloruros o ciclos de congelación y deshielo, para garantizar que los objetivos de sostenibilidad se cumplan sin comprometer la integridad estructural a largo plazo en aplicaciones prácticas.

Desarrollo de superplastificantes con perfiles adaptables

Otra línea de investigación prometedora es la exploración del desarrollo de superplastificantes basados en PCE con diferentes tipos de "clusters". Modificar el tamaño y la naturaleza del núcleo de los PCE podría generar beneficios adicionales, como efectos de relleno o interacciones más específicas con fases cementantes. Esto podría permitir que ciertos superplastificantes no solo actúen como dispersantes, sino también como potenciadores de la resistencia, lo cual sería particularmente útil en sistemas con altos niveles de sustitución de clínker.

Sinergias con otras fases cementantes y SCMs

Profundizar en las sinergias entre los superplastificantes y las fases del cemento, incluyendo los SCM, podría abrir nuevas vías para la optimización de los aglomerantes de baja huella de carbono. Un estudio más detallado de estos factores secundarios podría mejorar aún más el rendimiento del $LC^3$ y de otros aglomerantes especializados.

# 7. Annex: Supporting Information

This annex includes the supplementary information (SI) associated with the scientific papers referenced throughout this thesis. These materials provide additional data, experimental details, and analyses that complement the main findings discussed in the chapters. They are presented here to ensure comprehensive access to the supporting materials used in this research.

## 7.1. Article 1 (A#1): Portland and Belite Cement Hydration Acceleration by C-S-H Seeds with Variable w/c Ratios

## 7.2. Article 2 (A#2): C-S-H seeding activation of Portland and Belite cements: An enlightening *in situ* synchrotron powder diffraction study

## 7.3. Article 5 (A#5): *In situ* synchrotron powder diffraction study of $LC^3$ cement activation at very early ages by C-S-H nucleation seeding

# 8. Annex: Additional Tables

In this section, additional tables are provided that were not included in the main body of the thesis. These tables contain relevant data and analyses that, while important, were not essential for the core discussion but serve to enhance the comprehensiveness of the research. They are presented here for further reference.

*Table 8.1. Summary characterization of the calcined clays used.*

| | $D_{v,10}$ (μm) | $D_{v,50}$ (μm) | $D_{v,90}$ (μm) | SSA ($m^2/g$) | Density ($g/cm^3$) | $R^3$ (J/g) |
|---|---|---|---|---|---|---|
| **CC1** | 1.0 | 9.5 | 45.7 | 29.6 | 2.71 | 763 |
| **CC2** | 2.0 | 10.9 | 46.6 | 8.6 | 2.60 | 508 |
| **CC3** | 2.4 | 11.6 | 44.8 | 3.6 | 2.61 | 445 |

*Table 8.2. Slump spread over time and of samples with different superplasticizer.*

| Samples | Met. | SP (wt%) | Slump spread (mm) | | | SSA ($m^2/g$) | A#x |
|---|---|---|---|---|---|---|---|
| | | | $t_0$ | $t_{30min}$ | $t_{60min}$ | | |
| **PC-425-w/c=0.40-SP1** | #5 | 0.29 | 89 | 62 | 52 | 1.88 | This thesis |
| **PC-425-w/c=0.40-SP2** | #5 | 1.00 | 104 | 170 | 190 | 1.88 | This thesis |
| **PC-525-w/c=0.40-SP1** | #5 | 0.34 | 83 | 56 | 43 | 2.08 | A#3, A#4 |
| **PC-525-w/c=0.40-SP2** | #5 | 1.20 | 90 | 164 | 188 | 2.08 | A#3, A#4 |
| **PC-Qz-w/b=0.40-SP2** | #5 | 0.40 | 111 | 166 | 183 | 1.85 | A#3, A#4 |
| **$LC^3$-50 (CC1)-w/b=0.40-SP1** | #5 | 1.00 | 96 | 6 | 0 | 10.46 | A#3, A#4 |
| **$LC^3$-50 (CC1)-w/b=0.40-SP2** | #5 | 1.20 | 86 | 110 | 96 | 10.46 | A#3, A#4 |
| **$LC^3$-50 (CC2)-w/b=0.40-SP1** | #5 | 0.62 | 116 | 71 | 45 | 4.16 | This thesis |
| **$LC^3$-50 (CC2)-w/b=0.40-SP2** | #5 | 1.00 | 114 | 171 | 184 | 4.16 | A#3, A#4 |
| **$LC^3$-50 (CC3)-w/b=0.40-SP1** | #5 | 0.38 | 102 | 60 | 52 | 2.65 | This thesis |
| **$LC^3$-50 (CC3)-w/b=0.40-SP2** | #5 | 0.50 | 110 | 167 | 176 | 2.65 | A#3, A#4 |
| **$LC^3$-35 (CC1)-w/b=0.40-SP2** | #5 | 1.35 | 112 | 65 | 3 | 13.17 | A#6 |
| **$LC^3$-35 (CC1)-w/b=0.40-SP3** | #5 | 1.75 | 110 | 101 | 70 | 13.17 | A#6 |
| **LC3-20 (CC1)-w/b=0.40-SP2** | #5 | 1.65 | 118 | 24 | 0 | 15.92 | This thesis |

*Table 8.3. Compressive strength and improvement value of various samples.*

| Samples | Met. | Compressive strength (MPa) | | | Improvement (%) | | | A#x |
|---|---|---|---|---|---|---|---|---|
| | | 1 d | 7 d | 28 d | 1 d | 7 d | 28 d | |
| **PC-425-w/c=0.50** | #4 | 15 | 34 | 52 | - | - | - | A#1 |
| **PC-425-w/c=0.50-XS130** | #4 | 23.6 | 43.2 | 53 | 57 | 27 | 2 | A#1 |
| **PC-425-w/c=0.50-STE53** | #4 | 22 | 49 | 61 | 47 | 44 | 17 | A#1 |
| **BC-Buz-w/c=0.50** | #4 | 8.5 | 27.4 | 41 | - | - | - | A#1 |
| **BC-Buz-w/c=0.50-XS130** | #4 | 10.6 | 31.6 | 48 | 25 | 15 | 17 | A#1 |
| **BC-Buz-w/c=0.50-STE53** | #4 | 12 | 34 | 44 | 41 | 24 | 7 | A#1 |
| **BC-n.a.-w/c=0.50** | #4 | 3.8 | 14.3 | 46 | - | - | - | A#1 |
| **BC-n.a.-w/c=0.50-XS130** | #4 | 4.3 | 17.1 | 52 | 13 | 20 | 13 | A#1 |
| **BC-n.a.-w/c=0.50-STE53** | #4 | 6.5 | 15 | 51 | 71 | 5 | 11 | A#1 |
| **$LC^3$-50 (CC1)-w/b=0.40-SP2** | #5 | 20 | 55 | 68 | - | - | - | A#3, A#4 |
| **$LC^3$-50 (CC1)-w/b=0.40-XS130-SP2** | #5 | 29 | 67 | 83 | 45 | 22 | 22 | A#4 |
| **$LC^3$-50 (CC1)-w/b=0.40-STE53-SP2** | #5 | 28 | 68 | 88 | 40 | 24 | 29 | A#3 |
| **$LC^3$-50 (CC2)-w/b=0.40-SP2** | #5 | 15 | 37 | 57 | - | - | - | A#3, A#4 |
| **$LC^3$-50 (CC2)-w/b=0.40-XS130-SP2** | #5 | 22 | 48 | 67 | 47 | 30 | 18 | A#4 |
| **$LC^3$-50 (CC2)-w/b=0.40-STE53-SP2** | #5 | 23 | 47 | 71 | 53 | 27 | 25 | A#3 |
| **$LC^3$-50 (CC3)-w/b=0.40-SP2** | #5 | 11 | 35 | 54 | - | - | - | A#3, A#4 |
| **$LC^3$-50 (CC3)-w/b=0.40-XS130-SP2** | #5 | 23 | 47 | 68 | 109 | 34 | 26 | A#4 |
| **$LC^3$-50 (CC3)-w/b=0.40-STE53-SP2** | #5 | 23 | 46 | 72 | 109 | 31 | 33 | A#3 |
| **$LC^3$-35 (CC1)-w/b=0.40-SP2** | #5 | 13.7 | 40 | 59 | - | - | - | A#6 |
| **$LC^3$-35 (CC1)-w/b=0.40-STE53-SP2** | #5 | 19.2 | 56 | 72 | 40 | 40 | 22 | A#6 |

# 9. Annex: Other Publications

This annex includes a selection of the author's publications that were not included in the thesis for various reasons. Some of these works are not directly related to the subject matter of the dissertation, while others, although relevant, do not meet the necessary criteria for inclusion, such as the requirement for the author to be the primary author. These publications are provided to showcase the author's broader research contributions.

Article I.

**Morales-Cantero, A.**; De la Torre, A.G.; Cuesta, A.; Fraga-Lopez, E.; Shirani, S.; Aranda, M.A.G. Belite hydration at high temperature and pressure by in situ synchrotron powder diffraction. Construction and Building Materials , 2020, 262, 120825. 10.1016/j.conbuildmat.2020.120825

Article II.

Shirani, S.; Cuesta, A.; **Morales-Cantero, A.**; De la Torre, A.G.; Olbinado, M.P.; Aranda, M.A.G. Influence of curing temperature on belite cement hydration: A comparative study with Portland cement. Cement and Concrete Research, 147 (2021) 106499. 10.1016/j.cemconres.2021.106499

Article III.

Perez-Bravo, R.; **Morales-Cantero, A.**; Bruscolini, M.; Aranda, M.A.G.; Santacruz, I.; De la Torre, A.G. Effect of boron and water-to-cement ratio on the performances of laboratory prepared Belite-Ye'elimite-Ferrite (BYF) cements. Materials, 2021, 14, 4862. 10.3390/ma14174862

Article IV.

**Morales-Cantero, A.**; Cuesta, A.; Santacruz, I.; Aranda, M.A.G.; De la Torre, A.G. Phase-selective degree of hydration at setting: An in situ synchrotron diffraction study. Construction and Building Materials, 2022, 328, 127117. 10.1016/j.conbuildmat.2022.127117

Article V.

Redondo-Soto, C.; **Morales-Cantero A.**; Cuesta A.; Santacruz I.; Gastaldi, D.; Canonico, F.; Aranda, M. A. G. Limestone calcined clay binders based on a Belite-rich cement. Cement and Concrete Research, 2023, 163, 107018. 10.1016/j.cemconres.2022.107018

Article VI.

Cuesta A.; **Morales-Cantero A.**; De la Torre, A.; Aranda, M. A. G. Recent Advances in C-S-H Nucleation Seeding for Improving Cement Performances. Materials, 2023, 16, 1462. 10.3390/ma16041462

Article VII.

Perez-Bravo, R.; **Morales-Cantero, A.**; Cuesta, A.; Aranda, M.A.G.; Santacruz, I.; De la Torre. Early hydration of belite-ye'elimite-ferrite cements: Role of admixtures. Construction and Building Materials 2023, 371, 130765. 10.1016/j.conbuildmat.2023.130765

Article VIII.

Shirani, S.; Cuesta, A.; **Morales-Cantero, A.**; Santacruz, I.; Diaz, A.; Trtik, P.; Holler, M.; Rack, A.; Lukic, B.; Brun, E.; Salcedo, I.R.; Aranda, M.A.G. 4D nanoimaging of early age cement hydration. Nature Communications 2023, 14, 2652. 10.1038/s41467-023-38380-1

Article IX.

Shirani, S.; Cuesta, A.; De la Torre, A.G.; Santacruz, I.; **Morales-Cantero, A.**; Koufany, I.; Redondo-Soto, C.; Salcedo, I.R.; León-Reina, L.; Aranda, M.A.G. Mix and measure - Combining in situ X-ray powder diffraction and microtomography for accurate hydrating cement studies. Cement and Concrete Research, 2024, 175, 107370. https://doi.org/10.1016/j.cemconres.2023.107370

Article X.

Romero-Espinosa, A.; Sanfélix, S.G.; **Morales-Cantero, A.**; Cuesta, A.; Kjøniksen, A.; Aranda, M.A.G.; De la Torre, A.G.; Santacruz, I. Processing of calcium sulfoaluminate eco-cement coatings containing microencapsulated phase change materials. Advance in Cement Research 2024. 10.1680/jadcr.23.00077

# References


[1] IEA, Tracking Industry 2020 – Analysis, (2020). https://www.iea.org/reports/tracking-industry-2020 (accessed April 7, 2022).

[2] S.J. Davis, N.S. Lewis, M. Shaner, S. Aggarwal, D. Arent, I.L. Azevedo, S.M. Benson, T. Bradley, J. Brouwer, Y.M. Chiang, C.T.M. Clack, A. Cohen, S. Doig, J. Edmonds, P. Fennell, C.B. Field, B. Hannegan, B.M. Hodge, M.I. Hoffert, E. Ingersoll, P. Jaramillo, K.S. Lackner, K.J. Mach, M. Mastrandrea, J. Ogden, P.F. Peterson, D.L. Sanchez, D. Sperling, J. Stagner, J.E. Trancik, C.J. Yang, K. Caldeira, Net-zero emissions energy systems, Science. 360 (2018) eaas9793. https://doi.org/10.1126/science.aas9793.

[3] P. Fennell, J. Driver, C. Bataille, S.J. Davis, Cement and steel — nine steps to net zero, Nature. 603 (2022) 574–577. https://doi.org/10.1038/d41586-022-00758-4.

[4] G. Habert, S.A. Miller, V.M. John, J.L. Provis, A. Favier, A. Horvath, K.L. Scrivener, Environmental impacts and decarbonization strategies in the cement and concrete industries, Nat. Rev. Earth Environ. 1 (2020) 559–573. https://doi.org/10.1038/s43017-020-0093-3.

[5] S.A. Miller, R.J. Myers, Environmental Impacts of Alternative Cement Binders, Environ. Sci. Technol. 54 (2020) 677–686. https://doi.org/10.1021/acs.est.9b05550.

[6] S.A. Miller, F.C. Moore, Climate and health damages from global concrete production, Nat. Clim. Chang. 10 (2020) 439–443. https://doi.org/10.1038/s41558-020-0733-0.

[7] C. Shi, B. Qu, J.L. Provis, Recent progress in low-carbon binders, Cem. Concr. Res. 122 (2019) 227–250. https://doi.org/10.1016/j.cemconres.2019.05.009.

[8] L. Barcelo, J. Kline, G. Walenta, E. Gartner, Cement and carbon emissions, Mater. Struct. 47 (2014) 1055–1065. https://doi.org/10.1617/s11527-013-0114-5.

[9] Paris Agreement, (2015) 27. https://unfccc.int/sites/default/files/english_paris_agreement.pdf.

[10] UN Environment, K.L. Scrivener, V.M. John, E. Gartner, Eco-efficient cements: Potential, economically viable solutions for a low-CO2, cement-based materials industry, Cem. Concr. Res. 114 (2018) 2–26. https://doi.org/10.1016/j.cemconres.2018.03.015.

[11] International Energy Agency, IEA; Cement Sustainability Initiative, CSI; World Business Council for Sustainable Development, WBCSD, Technology Roadmap Low-Carbon Transition in the Cement Industry, 2018. https://www.iea.org/reports/technology-roadmap-low-carbon-transition-in-the-cement-industry.

[12] J.G.J. Olivier, G. Janssens-Maenhout, M. Muntean, J.A.H.W. Peters, Trends in global CO2 emissions:2016 report, PBL Publishers, The Hague, 2016. https://www.pbl.nl/sites/default/files/cms/publicaties/pbl-2016-trends-in-global-co2-emisions-2016-report-2315.pdf (accessed September 11, 2019).

[13] H.F.W. Taylor, Cement chemistry, 2nd ed., Thomas Telford Pub, London, UK, 1997.

[14] W. Kurdowski, S. Duszak, B. Trybalska, Belite produced by means of low-temperature synthesis, Cem. Concr. Res. 27 (1997) 51–62. https://doi.org/10.1016/S0008-8846(96)00198-6.

[15] A. Cuesta, A. Ayuela, M.A.G. Aranda, Belite cements and their activation, Cem. Concr. Res. 140 (2021) 106319. https://doi.org/10.1016/j.cemconres.2020.106319.

[16] M.C.G. Juenger, R. Snellings, S.A. Bernal, Supplementary cementitious materials: New sources, characterization, and performance insights, Cem. Concr. Res. 122 (2019) 257–273. https://doi.org/10.1016/j.cemconres.2019.05.008.

[17] M.C.G. Juenger, R. Siddique, Recent advances in understanding the role of supplementary cementitious materials in concrete, Cem. Concr. Res. 78 (2015) 71–80. https://doi.org/10.1016/j.cemconres.2015.03.018.

[18] R. Snellings, Assessing, Understanding and Unlocking Supplementary Cementitious Materials, RILEM Tech. Lett. 1 (2016) 50–55. https://doi.org/10.21809/RILEMTECHLETT.2016.12.

[19] B. Sabir, S. Wild, J. Bai, Metakaolin and calcined clays as pozzolans for concrete: A review, Cem. Concr. Compos. 23 (2001) 441–454. https://doi.org/10.1016/S0958-9465(00)00092-5.

[20] A. Alujas, R. Fernández, R. Quintana, K.L. Scrivener, F. Martirena, Pozzolanic reactivity of low grade kaolinitic clays: Influence of calcination temperature and impact of calcination products on OPC hydration, Appl. Clay Sci. 108 (2015) 94–101. https://doi.org/10.1016/j.clay.2015.01.028.

[21] R. Fernandez, F. Martirena, K.L. Scrivener, The origin of the pozzolanic activity of calcined clay minerals: A comparison between kaolinite, illite and montmorillonite, Cem. Concr. Res. 41 (2011) 113–122. https://doi.org/10.1016/j.cemconres.2010.09.013.

[22] K. Weise, N. Ukrainczyk, E. Koenders, Pozzolanic Reactions of Metakaolin with Calcium Hydroxide: Review on Hydrate Phase Formations and Effect of Alkali Hydroxides, Carbonates and Sulfates, Mater. Des. 231 (2023) 112062. https://doi.org/10.1016/J.MATDES.2023.112062.

[23] J. Skibsted, R. Snellings, Reactivity of supplementary cementitious materials (SCMs) in cement blends, Cem. Concr. Res. 124 (2019) 105799. https://doi.org/10.1016/J.CEMCONRES.2019.105799.

[24] M. Murat, Hydration reaction and hardening of calcined clays and related minerals. I. Preliminary investigation on metakaolinite, Cem. Concr. Res. 13 (1983) 259–266. https://doi.org/10.1016/0008-8846(83)90109-6.

[25] F. Zunino, Y. Dhandapani, M. Ben Haha, J. Skibsted, S. Joseph, S. Krishnan, A. Parashar, M.C.G. Juenger, T. Hanein, S.A. Bernal, K.L. Scrivener, F. Avet, Hydration and mixture design of calcined clay blended cements: review by the RILEM TC 282-CCL, Mater. Struct. Constr. 55 (2022) 234. https://doi.org/10.1617/s11527-022-02060-1.

[26] P.S. de Silva, F.P. Glasser, Hydration of cements based on metakaolin: thermochemistry,

Adv. Cem. Res. 3 (1990) 167–177. https://doi.org/10.1680/adcr.1990.3.12.167.

[27] F. Zunino, K.L. Scrivener, The reaction between metakaolin and limestone and its effect in porosity refinement and mechanical properties, Cem. Concr. Res. 140 (2021) 106307. https://doi.org/10.1016/j.cemconres.2020.106307.

[28] K. Scrivener, F. Martirena, S. Bishnoi, S. Maity, Calcined clay limestone cements (LC3), Cem. Concr. Res. 114 (2018) 49–56. https://doi.org/10.1016/j.cemconres.2017.08.017.

[29] F. Avet, R. Snellings, A. Alujas Diaz, M. Ben Haha, K.L. Scrivener, Development of a new rapid, relevant and reliable (R3) test method to evaluate the pozzolanic reactivity of calcined kaolinitic clays, Cem. Concr. Res. 85 (2016) 1–11. https://doi.org/10.1016/j.cemconres.2016.02.015.

[30] F. Avet, K.L. Scrivener, Investigation of the calcined kaolinite content on the hydration of Limestone Calcined Clay Cement (LC3), Cem. Concr. Res. 107 (2018) 124–135. https://doi.org/10.1016/j.cemconres.2018.02.016.

[31] H. Maraghechi, F. Avet, H. Wong, H. Kamyab, K.L. Scrivener, Performance of Limestone Calcined Clay Cement (LC3) with various kaolinite contents with respect to chloride transport, Mater. Struct. 51 (2018) 125. https://doi.org/10.1617/s11527-018-1255-3.

[32] A. Favier, K. Scrivener, Alkali Silica Reaction and Sulfate Attack: Expansion of Limestone Calcined Clay Cement BT - Calcined Clays for Sustainable Concrete, in: F. Martirena, A. Favier, K. Scrivener (Eds.), Springer Netherlands, Dordrecht, 2018: pp. 165–169.

[33] K.L. Scrivener, F. Avet, H. Maraghechi, F. Zunino, J. Ston, W. Hanpongpun, A. Favier, Impacting factors and properties of limestone calcined clay cements (LC3), Green Mater. 7 (2019) 3–14. https://doi.org/10.1680/jgrma.18.00029.

[34] M. Ben Haha, P. Termkhajornkit, A. Ouzia, S. Uppalapati, B. Huet, Low clinker systems - Towards a rational use of SCMs for optimal performance, Cem. Concr. Res. 174 (2023) 107312. https://doi.org/10.1016/j.cemconres.2023.107312.

[35] J. Sun, F. Zunino, K. Scrivener, Hydration and phase assemblage of limestone calcined clay cements (LC3) with clinker content below 50 %, Cem. Concr. Res. 177 (2024) 107417. https://doi.org/10.1016/J.CEMCONRES.2023.107417.

[36] J. Yu, H.L. Wu, D.K. Mishra, G. Li, C.K. Leung, Compressive strength and environmental impact of sustainable blended cement with high-dosage Limestone and Calcined Clay (LC2), J. Clean. Prod. 278 (2021) 123616. https://doi.org/10.1016/J.JCLEPRO.2020.123616.

[37] S. Dhers, A. Müller, R. Guggenberger, D. Freimut, K. Weldert, B. Sachsenhauser, V. Yermakou, N. Mikanovic, P. Schwesig, On the relationship between superplasticizer demand and specific surface area of calcined clays in LC3 systems, Constr. Build. Mater. 411 (2024) 134467. https://doi.org/10.1016/J.CONBUILDMAT.2023.134467.

[38] UNE-EN 197-5. Parte 5: Cemento Portland compuesto CEM II/C-M y cemento compuesto CEM VI, (2021).

[39] P.C. Aiticin, Accelerators, in: P.C. Aiticin, R.J. Flatt (Eds.), Sci. Technol. Concr. Admixtures, Elsevier, Amsterdam, 2016: pp. 405–413. https://doi.org/10.1016/B978-0-08-100693-1.00019-9.

[40] J. Cheung, A. Jeknavorian, L. Roberts, D. Silva, Impact of admixtures on the hydration kinetics of Portland cement, Cem. Concr. Res. 41 (2011) 1289–1309. https://doi.org/10.1016/J.CEMCONRES.2011.03.005.

[41] Y. Wang, C. Shi, Y. Ma, Y. Xiao, Y. Liu, Accelerators for shotcrete – Chemical composition and their effects on hydration, microstructure and properties of cement-based materials, Constr. Build. Mater. 281 (2021) 122557. https://doi.org/10.1016/j.conbuildmat.2021.122557.

[42] Q. Yuan, D. Zhou, H. Huang, J. Peng, H. Yao, Structural build-up, hydration and strength development of cement-based materials with accelerators, Constr. Build. Mater. 259 (2020) 119775. https://doi.org/10.1016/J.CONBUILDMAT.2020.119775.

[43] Y. Wang, L. Lei, J. Liu, Y. Ma, Y. Liu, Z. Xiao, C. Shi, Accelerators for normal concrete: A critical review on hydration, microstructure and properties of cement-based materials, Cem. Concr. Compos. 134 (2022) 104762. https://doi.org/10.1016/J.CEMCONCOMP.2022.104762.

[44] L. Lei, M. Palacios, J. Plank, A.A. Jeknavorian, Interaction between polycarboxylate superplasticizers and non-calcined clays and calcined clays: A review, Cem. Concr. Res. 154 (2022) 106717. https://doi.org/10.1016/j.cemconres.2022.106717.

[45] Y. He, S. Liu, X. Zhang, W. Liu, G. Liao, M. Xu, Influence of triethanolamine on mechanical strength and hydration performance of blended cement containing fly ash, limestone and slag, J. Build. Eng. 44 (2021) 102879. https://doi.org/10.1016/j.jobe.2021.102879.

[46] Y. Wang, L. Lei, X. Hu, Y. Liu, C. Shi, Effect of diethanolisopropanolamine and ethyldiisopropylamine on hydration and strength development of Portland cement, Cem. Concr. Res. 162 (2022) 106999. https://doi.org/10.1016/j.cemconres.2022.106999.

[47] J.J. Thomas, H.M. Jennings, J.J. Chen, Influence of Nucleation Seeding on the Hydration Mechanisms of Tricalcium Silicate and Cement, J. Phys. Chem. C. 113 (2009) 4327–4334. https://doi.org/10.1021/jp809811w.

[48] R. Alizadeh, L. Raki, J.M. Makar, J.J. Beaudoin, I. Moudrakovski, Hydration of tricalcium silicate in the presence of synthetic calcium-silicate-hydrate, J. Mater. Chem. 19 (2009) 7937–7946. https://doi.org/10.1039/b910216g.

[49] E. John, T. Matschei, D. Stephan, Nucleation seeding with calcium silicate hydrate – A review, Cem. Concr. Res. 113 (2018) 74–85. https://doi.org/10.1016/j.cemconres.2018.07.003.

[50] G. Artioli, G. Ferrari, M.C. Dalconi, L. Valentini, Nanoseeds as modifiers of the cement hydration kinetics, in: M. Shahir Liew, P. Nguyen-Tri, T.A. Nguyen, S. Kakooei (Eds.), Smart Nanoconcretes Cem. Mater. Prop. Model. Appl., Elsevier, 2020: pp. 257–269. https://doi.org/10.1016/B978-0-12-817854-6.00010-6.

[51] T. Hirsch, Z. Lu, D. Stephan, Effect of different sulphate carriers on Portland cement hydration in the presence of triethanolamine, Constr. Build. Mater. 294 (2021) 123528. https://doi.org/10.1016/j.conbuildmat.2021.123528.

[52] M. Katsioti, P.E. Tsakiridis, P. Giannatos, Z. Tsibouki, J. Marinos, Characterization of various cement grinding aids and their impact on grindability and cement performance, Constr. Build. Mater. 23 (2009) 1954–1959. https://doi.org/10.1016/J.CONBUILDMAT.2008.09.003.

[53] S. Ma, W. Li, S. Zhang, Y. Hu, X. Shen, Study on the hydration and microstructure of Portland cement containing diethanol-isopropanolamine, Cem. Concr. Res. 67 (2015) 122–130. https://doi.org/10.1016/J.CEMCONRES.2014.09.002.

[54] L. Chang, J. Wang, S. Cui, H. Liu, Y. Wang, Hydration, microstructure and properties of cement-based materials in the presence of tertiary alkanolamines: A review, Constr. Build. Mater. 424 (2024) 135954. https://doi.org/10.1016/j.conbuildmat.2024.135954.

[55] J. Chen, J. Jia, M. Zhu, L. Zhang, Advances of alkanolamine in hydration of Portland cement, Mater. Today Commun. 37 (2023) 107129. https://doi.org/10.1016/J.MTCOMM.2023.107129.

[56] F. Zunino, K.L. Scrivener, Assessing the effect of alkanolamine grinding aids in limestone calcined clay cements hydration, Constr. Build. Mater. 266 (2021) 121293. https://doi.org/10.1016/j.conbuildmat.2020.121293.

[57] E. Gartner, D. Myers, Influence of Tertiary Alkanolamines on Portland Cement Hydration, J. Am. Ceram. Soc. 76 (1993) 1521–1530. https://doi.org/10.1111/j.1151-2916.1993.tb03934.x.

[58] Z. Xu, W. Li, J. Sun, Y. Hu, K. Xu, S. Ma, X. Shen, Research on cement hydration and hardening with different alkanolamines, Constr. Build. Mater. 141 (2017) 296–306. https://doi.org/10.1016/j.conbuildmat.2017.03.010.

[59] X. ling Liao, H. Huang, F. qiang He, C. hui Yang, Microstructural characterization of cement in the presence of alkanolamines, Mater. Today Commun. 27 (2021) 102386. https://doi.org/10.1016/J.MTCOMM.2021.102386.

[60] R. Pérez-Bravo, A. Morales-Cantero, A. Cuesta, M.A.G. Aranda, I. Santacruz, A.G. De La Torre, Early hydration of belite-ye'elimite-ferrite cements: Role of admixtures, Constr. Build. Mater. 371 (2023) 130765. https://doi.org/10.1016/j.conbuildmat.2023.130765.

[61] Q. Zhai, K. Kurumisawa, J. Moon, I.H. Hwang, Advances in understanding the effect of alkanolamine in cement-based materials, J. Clean. Prod. 452 (2024) 142167. https://doi.org/10.1016/J.JCLEPRO.2024.142167.

[62] H. Huang, X. Li, F. Avet, W. Hanpongpun, K. Scrivener, Strength-promoting mechanism of alkanolamines on limestone-calcined clay cement and the role of sulfate, Cem. Concr. Res. 147 (2021) 106527. https://doi.org/10.1016/j.cemconres.2021.106527.

[63] Y.R. Zhang, X.M. Kong, Z.C. Lu, Z.B. Lu, Z. Qing, B.Q. Dong, X. Feng, Influence of triethanolamine on the hydration product of portlandite in cement paste and the

mechanism, Cem. Concr. Res. 87 (2016) 64–76. https://doi.org/10.1016/J.CEMCONRES.2016.05.009.

[64] L. Nicoleau, A. Nonat, D. Perrey, The di- and tricalcium silicate dissolutions, Cem. Concr. Res. 47 (2013) 14–30. https://doi.org/10.1016/j.cemconres.2013.01.017.

[65] L. Nicoleau, New calcium silicate hydrate network, Transp. Res. Rec. (2010) 42–51. https://doi.org/10.3141/2142-07.

[66] P. Juilland, E. Gallucci, R. Flatt, K.L. Scrivener, Dissolution theory applied to the induction period in alite hydration, Cem. Concr. Res. 40 (2010) 831–844. https://doi.org/10.1016/j.cemconres.2010.01.012.

[67] Z. Xu, W. Li, J. Sun, Y. Hu, K. Xu, S. Ma, X. Shen, Hydration of Portland cement with alkanolamines by thermal analysis, J. Therm. Anal. Calorim. 131 (2018) 37–47. https://doi.org/10.1007/S10973-017-6271-Y/METRICS.

[68] Z. Lu, X. Kong, D. Jansen, C. Zhang, J. Wang, X. Pang, J. Yin, Towards a further understanding of cement hydration in the presence of triethanolamine, Cem. Concr. Res. 132 (2020) 106041. https://doi.org/10.1016/J.CEMCONRES.2020.106041.

[69] Y.L. Yaphary, Z. Yu, R.H.W. Lam, D. Lau, Effect of triethanolamine on cement hydration toward initial setting time, Constr. Build. Mater. 141 (2017) 94–103. https://doi.org/10.1016/J.CONBUILDMAT.2017.02.072.

[70] J. Wang, B. Ma, H. Tan, C. Du, Z. Chu, Z. Luo, P. Wang, Hydration and mechanical properties of cement-marble powder system incorporating triisopropanolamine, Constr. Build. Mater. 266 (2021) 121068. https://doi.org/10.1016/J.CONBUILDMAT.2020.121068.

[71] Y. Zhang, X. Zhang, X. Cai, L. Gao, Q. Li, X. Kong, A further understanding on the strength development of cement pastes in the presence of triisopropanolamine used in CRTS III slab track, Constr. Build. Mater. 315 (2022) 125743. https://doi.org/10.1016/J.CONBUILDMAT.2021.125743.

[72] X. Lu, Z. Ye, L. Zhang, P. Hou, X. Cheng, The influence of ethanol-diisopropanolamine on the hydration and mechanical properties of Portland cement, Constr. Build. Mater. 135 (2017) 484–489. https://doi.org/10.1016/J.CONBUILDMAT.2016.12.191.

[73] L. Nicoleau, Accelerated growth of calcium silicate hydrates: Experiments and simulations, Cem. Concr. Res. 41 (2011) 1339–1348. https://doi.org/10.1016/j.cemconres.2011.04.012.

[74] E. Pustovgar, R.P. Sangodkar, A.S. Andreev, M. Palacios, B.F. Chmelka, R.J. Flatt, J.B. D'Espinose De Lacaillerie, Understanding silicate hydration from quantitative analyses of hydrating tricalcium silicates, Nat. Commun. 7 (2016) 10952. https://doi.org/10.1038/ncomms10952.

[75] L. Nicoleau, E. Schreiner, A. Nonat, Ion-specific effects influencing the dissolution of tricalcium silicate, Cem. Concr. Res. 59 (2014) 118–138. https://doi.org/10.1016/j.cemconres.2014.02.006.

[76] V. Kanchanason, J. Plank, Effect of calcium silicate hydrate – polycarboxylate ether (C-S-H–PCE) nanocomposite as accelerating admixture on early strength enhancement of slag and calcined clay blended cements, Cem. Concr. Res. 119 (2019) 44–50. https://doi.org/10.1016/J.CEMCONRES.2019.01.007.

[77] C. Ouellet-Plamondon, S. Scherb, M. Köberl, K.C. Thienel, Acceleration of cement blended with calcined clays, Constr. Build. Mater. 245 (2020) 118439. https://doi.org/10.1016/J.CONBUILDMAT.2020.118439.

[78] G. Ferrari, A. Brocchi, F. Castiglioni, A. Bravo, E. Moretti, D. Salvioni, M. Squinzi, G. Artioli, M.C. Dalconi, L. Valentini, G. Dal Sasso, A new multifunctional additive for blended cements, Constr. Build. Mater. 354 (2022) 129086. https://doi.org/10.1016/j.conbuildmat.2022.129086.

[79] Y. Wang, L. Lü, Y. He, F. Wang, S. Hu, Effect of Calcium Silicate Hydrate Seeds on Hydration and Mechanical Properties of Cement, J. Wuhan Univ. Technol. Mater. Sci. Ed. 36 (2021) 103–110. https://doi.org/10.1007/s11595-021-2382-1.

[80] G. Liang, D. Ni, H. Li, B. Dong, Z. Yang, Synergistic effect of EVA, TEA and C-S-Hs-PCE on the hydration process and mechanical properties of Portland cement paste at early age, Constr. Build. Mater. 272 (2021) 121891. https://doi.org/10.1016/j.conbuildmat.2020.121891.

[81] H. Li, Y. Xiang, C. Xu, Effect of C–S–H seed/PCE nanocomposites and triisopropanolamine on portland cement properties: Hydration kinetic and strength, J. Build. Eng. 57 (2022) 104946. https://doi.org/10.1016/j.jobe.2022.104946.

[82] X. Chen, X. Yang, K. Wu, Q. Chen, Z. Yang, L. Xu, H. Li, Understanding the role of C – S – H seed / PCE nanocomposites , triethanolamine , sodium nitrate and PCE on hydration and performance at early age, Cem. Concr. Compos. 139 (2023) 105002. https://doi.org/10.1016/j.cemconcomp.2023.105002.

[83] L. Tian, S. Dai, X. Yao, H. Zhu, Q. Wu, Z. Liu, S. Cheng, Effect of nucleation seeding and triisopropanolamine on the compressive strength, chloride binding capacity and microstructure of cement paste, J. Build. Eng. 52 (2022) 104382. https://doi.org/10.1016/j.jobe.2022.104382.

[84] F. Zou, K. Shen, C. Hu, F. Wang, L. Yang, S. Hu, Effect of Sodium Sulfate and C–S–H Seeds on the Reaction of Fly Ash with Different Amorphous Alumina Contents, ACS Sustain. Chem. Eng. 8 (2020) 1659–1670. https://doi.org/10.1021/ACSSUSCHEMENG.9B06779.

[85] S. Shirani, A. Cuesta, A.G. De la Torre, I. Santacruz, A. Morales-Cantero, I. Koufany, C. Redondo-Soto, I.R. Salcedo, L. León-Reina, M.A.G. Aranda, Mix and measure - Combining in situ X-ray powder diffraction and microtomography for accurate hydrating cement studies, Cem. Concr. Res. 175 (2024) 107370. https://doi.org/10.1016/J.CEMCONRES.2023.107370.

[86] J. Fernandez-Sanchez, A. Cuesta, S. Shirani, C. Redondo-Soto, A.G. De la Torre, I. Santacruz, I.R. Salcedo, L. Leon-Reina, M.A.G. Aranda, Mix and measure II: joint high-energy laboratory powder diffraction and microtomography for cement hydration studies, J. Appl. Crystallogr. 57 (2024) 1067–1084.

https://doi.org/10.1107/s1600576724004527.

[87] B. Lothenbach, P. Durdzinski, K. De Weerdt, Thermogravimetric analysis, in: B.L. K. Scrivener, R. Snellings (Ed.), A Pract. Guid. to Microstruct. Anal. Cem. Mater., CRC Press, U.S.A, 2017: pp. 177–211. https://doi.org/10.1201/b19074.

[88] M. Palacios, H. Kazemi-Kamyad, S. Mantellato, P. Bowen, Laser diffraction and gas adsorption techniques, in: K. Scrivener, R. Snellings (Eds.), A Pract. Guid. to Microstruct. Anal. Cem. Mater., CRC Press, Boca Raton, 2017: pp. 445–484. https://doi.org/10.1201/b19074.

[89] M. Merlini, G. Artioli, C. Meneghini, T. Cerulli, A. Bravo, F. Cella, The early hydration and the set of Portland cements: In situ X-ray powder diffraction studies, Powder Diffr. 22 (2007) 201–208. https://doi.org/DOI: 10.1154/1.2754713.

[90] G. Alvarez-Pinazo, A. Cuesta, M. García-Maté, I. Santacruz, E.R. Losilla, S.G. Sanfélix, F. Fauth, M.A.G. Aranda, A.G. De La Torre, In-situ early-age hydration study of sulfobelite cements by synchrotron powder diffraction, Cem. Concr. Res. 56 (2014) 12–19. https://doi.org/10.1016/j.cemconres.2013.10.009.

[91] F. Fauth, I. Peral, C. Popescu, M. Knapp, The new Material Science Powder Diffraction beamline at ALBA Synchrotron, Cambridge University Press, 2013. https://doi.org/10.1017/S0885715613000900.

[92] B.H. Toby, R.B. Von Dreele, IUCr, GSAS-II: the genesis of a modern open-source all purpose crystallography software package, Urn:Issn:0021-8898. 46 (2013) 544–549. https://doi.org/10.1107/S0021889813003531.

[93] A.G. De la Torre, S. Bruque, M.A.G. Aranda, Rietveld quantitative amorphous content analysis, J. Appl. Crystallogr. 34 (2001) 196–202. https://doi.org/10.1107/S0021889801002485.

[94] L. Wadsö, Operational issues in isothermal calorimetry, Cem. Concr. Res. 40 (2010) 1129–1137. https://doi.org/10.1016/j.cemconres.2010.03.017.

[95] K.L. Scrivener, R. Snellings, B. Lothenbach, A Practical Guide to Microstructural Analysis of Cementitious Materials, CRC Press, Boca Raton, FL, 2017. https://doi.org/10.1201/b19074.

[96] L. Nicoleau, E. Jetzlsperger, D. Fridrich, M. Vierle, K. Lorenz, G. Albrecht, D. Schmitt, T. Wohlhaupter, R. Dorfner, H. Leitner, M. Bräu, C. Hesse, P.S. Montero, S. Zürn, M. Kutschera., Plasticizer-containing hardening accelerator composition, WO2010026155A1, WO2010026155A1, 2010. https://patents.google.com/patent/WO2010026155A1/en.

[97] L. Nicoleau, G. Albrecht, K. Lorenz, E. Jetzlsperger, D. Fridrich, T. Wohlhaupter, R. Dorfner, H. Leitner, M. Vierle, D. Schmitt, M. Braeu, C. Hesse, S. Montero-Pancera, S. Zuern, M. Kutschera, Hardening accelerator composition containing phosphated polycondensates, WO2011026720A1, WO2011026720A1, 2011. https://patents.google.com/patent/WO2011026720A1/en.

[98] O. Akhlaghi, T. Aytas, B. Tatli, D. Sezer, A. Hodaei, A. Favier, K.L. Scrivener, Y.Z. Menceloglu, O. Akbulut, Modified poly(carboxylate ether)-based superplasticizer for enhanced flowability of calcined clay-limestone-gypsum blended Portland cement, Cem. Concr. Res. 101 (2017) 114–122. https://doi.org/10.1016/j.cemconres.2017.08.028.

[99] X. Li, J. Dengler, C. Hesse, Reducing clinker factor in limestone calcined clay-slag cement using C-S-H seeding – A way towards sustainable binder, Cem. Concr. Res. 168 (2023) 107151. https://doi.org/10.1016/J.CEMCONRES.2023.107151.

[100] J. Ren, J. Guo, Y. Jin, F. Liu, B. Liu, S. Yan, W. Yan, C. Lu, S. Shi, Enhancing workability of high-volume calcined clay blend cement pastes through optimized addition sequences of PCE superplasticizer, Case Stud. Constr. Mater. 21 (2024) e03541. https://doi.org/10.1016/J.CSCM.2024.E03541.

[101] A. Morales-Cantero, D. Vallina, A.G. De la Torre, A. Cuesta, I. Santacruz, A. Dalla-Libera, P. Borralleras, S. Dhers, P. Schwesig, O. Mazanec, M.A.G. Aranda, Enhancing fluidity and mechanical properties in Limestone Calcined Clay cements with one-third Portland clinker content, J. Build. Eng. 95 (2024) 110334. https://doi.org/10.1016/j.jobe.2024.110334.

[102] N. Nair, K. Mohammed Haneefa, M. Santhanam, R. Gettu, A study on fresh properties of limestone calcined clay blended cementitious systems, Constr. Build. Mater. 254 (2020) 119326. https://doi.org/10.1016/j.conbuildmat.2020.119326.

[103] L. Lei, J. Plank, Synthesis and Properties of a Vinyl Ether-Based Polycarboxylate Superplasticizer for Concrete Possessing Clay Tolerance, Ind. Eng. Chem. Res. 53 (2014) 1048–1055. https://doi.org/10.1021/ie4035913.

[104] P. Borralleras, I. Segura, M.A.G. Aranda, A. Aguado, Absorption conformations in the intercalation process of polycarboxylate ether based superplasticizers into montmorillonite clay, Constr. Build. Mater. 236 (2020) 116657. https://doi.org/10.1016/j.conbuildmat.2019.08.038.

[105] P. Borralleras, I. Segura, M.A.G. Aranda, A. Aguado, Influence of the polymer structure of polycarboxylate-based superplasticizers on the intercalation behaviour in montmorillonite clays, Constr. Build. Mater. 220 (2019) 285–296. https://doi.org/10.1016/j.conbuildmat.2019.06.014.

[106] Intelligent cluster system, (2024). https://info.master-builders-solutions.com/en/masterco2re.

[107] A. Morales-Cantero, A.G. De la Torre, A. Cuesta, I. Santacruz, O. Mazanec, A. Dalla-Libera, P. Borralleras, M.A.G. Aranda, In situ synchrotron powder diffraction study of LC3 cement activation at very early ages by C-S-H nucleation seeding, Cem. Concr. Res. 178 (2024) 107463. https://doi.org/10.1016/j.cemconres.2024.107463.

[108] A. Morales-Cantero, A. Cuesta, A.G. De la Torre, I. Santacruz, O. Mazanec, P. Borralleras, K.S. Weldert, D. Gastaldi, F. Canonico, M.A.G. Aranda, C-S-H seeding activation of Portland and Belite Cements: an enlightening in situ synchrotron powder diffraction study, Cem. Concr. Res. 161 (2022) 106946. https://doi.org/10.1016/j.cemconres.2022.106946.

[109] C. Redondo-Soto, A. Morales-Cantero, A. Cuesta, I. Santacruz, D. Gastaldi, F. Canonico, M.A.G. Aranda, Limestone calcined clay binders based on a Belite-rich cement, Cem. Concr. Res. 163 (2023) 107018. https://doi.org/10.1016/j.cemconres.2022.107018.

[110] A. Morales-Cantero, A. Cuesta, A.G. De la Torre, O. Mazanec, P. Borralleras, K.S. Weldert, D. Gastaldi, F. Canonico, M.A.G. Aranda, Portland and Belite Cement Hydration Acceleration by C-S-H Seeds with Variable w/c Ratios, Materials (Basel). 15 (2022) 3553. https://doi.org/10.3390/MA15103553.

[111] J. He, G. Long, K. Ma, Y. Xie, Z. Cheng, Improvement of the Hydration of a Fly Ash-Cement System by the Synergic Action of Triethanolamine and C-S-H Seeding, ACS Sustain. Chem. Eng. 9 (2021) 2804–2815. https://doi.org/10.1021/acssuschemeng.0c08618.

[112] A. Cuesta, A. Morales-Cantero, A.G. De la Torre, I. Santacruz, O. Mazanec, A. Dalla-Libera, S. Dhers, P. Schwesig, P. Borralleras, M.A.G. Aranda, Activation of LC3 binders by C-S-H nucleation seeding with a new tailored admixture for low-carbon cements, Ce/Papers - Proc. Civ. Eng. 6 (2023) 446–453. https://doi.org/10.1002/cepa.2786.

[113] A. Morales-Cantero, A.G. De la Torre, A. Cuesta, I. Santacruz, O. Mazanec, A. Dalla-Libera, S. Dhers, P. Borralleras, M.A.G. Aranda, Activation of LC3 low-carbon cements by C-S-H seeding, in: Proc. 16th Int. Congr. Chem. Cem. - Vol I, Bangkok, 2023: pp. 247–250. https://doi.org/10.13140/RG.2.2.26594.09920.

[114] EFCA, European Federation of Concrete Admixtures Associations, (2023). https://www.efca.info/efca-publications/environmental/.

[115] R.G. Pillai, R. Gettu, M. Santhanam, S. Rengaraju, Y. Dhandapani, S. Rathnarajan, A.S. Basavaraj, Service life and life cycle assessment of reinforced concrete systems with limestone calcined clay cement (LC3), Cem. Concr. Res. 118 (2019) 111–119. https://doi.org/10.1016/J.CEMCONRES.2018.11.019.

[116] Y. Cancio Díaz, S. Sánchez Berriel, U. Heierli, A.R. Favier, I.R. Sánchez Machado, K.L. Scrivener, J.F. Martirena Hernández, G. Habert, Limestone calcined clay cement as a low-carbon solution to meet expanding cement demand in emerging economies, Dev. Eng. 2 (2017) 82–91. https://doi.org/10.1016/J.DEVENG.2017.06.001.

[117] MasterCO2re 3240, (2024). https://assets.ctfassets.net/ctspkgm1yw3s/3X1W84AEOGKtMyzHFEHh7J/73fbee217e51b59040fd791defd35c63/MasterCO2re_3240_EFCA-mEPD_Group_B.pdf.

[118] Master X-Seed STE 54, (2024). https://assets.ctfassets.net/ctspkgm1yw3s/2fNa9BdTRv4wzpLBoKXOUd/3bf8c957c5441f5362e5b79e98e6cdc5/Master_X-Seed_STE_54_EPD_2027-07-21.pdf.

[119] M. Sharma, S. Bishnoi, F. Martirena, K. Scrivener, Limestone calcined clay cement and concrete: A state-of-the-art review, Cem. Concr. Res. 149 (2021) 106564. https://doi.org/10.1016/j.cemconres.2021.106564.

[120] R.J. Flatt, N. Roussel, C.R. Cheeseman, Concrete: An eco material that needs to be improved, J. Eur. Ceram. Soc. 32 (2012) 2787–2798. https://doi.org/10.1016/J.JEURCERAMSOC.2011.11.012.

[121] F. Boscaro, M. Palacios, R.J. Flatt, Formulation of low clinker blended cements and concrete with enhanced fresh and hardened properties, Cem. Concr. Res. 150 (2021) 106605. https://doi.org/10.1016/J.CEMCONRES.2021.106605.

[122] A. Cuesta, A. Ayuela, M.A.G. Aranda, Belite cements and their activation, Cem. Concr. Res. 140 (2021) 106319. https://doi.org/10.1016/j.cemconres.2020.106319.

[123] X. Li, J. Bizzozero, C. Hesse, Impact of C-S-H seeding on hydration and strength of slag blended cement, Cem. Concr. Res. 161 (2022) 106935. https://doi.org/10.1016/j.cemconres.2022.106935.

[124] A. Cuesta, A. Morales-Cantero, A.G. De la Torre, M.A.G. Aranda, Recent advances in C-S-H nucleation seeding for improving cement performances, Materials (Basel). 16 (2023) 1462. https://doi.org/https://doi.org/10.3390/ma16041462.

[125] G. Artioli, L. Valentini, M.C. Dalconi, M. Parisatto, M. Voltolini, V. Russo, G. Ferrari, Imaging of nano-seeded nucleation in cement pastes by X-ray diffraction tomography, Int. J. Mater. Res. 105 (2014) 628–631. https://doi.org/10.3139/146.111049.

[126] D. Zhao, R. Khoshnazar, Hydration and microstructural development of calcined clay cement paste in the presence of calcium-silicate-hydrate (C–S–H) seed, Cem. Concr. Compos. 122 (2021) 104162. https://doi.org/10.1016/j.cemconcomp.2021.104162.

[127] L. Valentini, G. Ferrari, V. Russo, M. Štefančič, V.Z. Serjun, G. Artioli, Use of nanocomposites as permeability reducing admixtures, J. Am. Ceram. Soc. 101 (2018) 4275–4284. https://doi.org/10.1111/JACE.15548.

[128] A. Alzaza, K. Ohenoja, M. Illikainen, Improved strength development and frost resistance of Portland cement ground-granulated blast furnace slag binary binder cured at 0 °C with the addition of calcium silicate hydrate seeds, J. Build. Eng. 48 (2022) 103904. https://doi.org/10.1016/j.jobe.2021.103904.

[129] F. Zhou, G. Pan, R. Mi, M. Zhan, Improving the properties of concrete using in situ-grown C-S-H, Constr. Build. Mater. 276 (2021) 122214. https://doi.org/10.1016/j.conbuildmat.2020.122214.

[130] J. Sobczak-Piąstka, U. Marushchak, O. Mazurak, A. Mazurak, Nanomodified rapid hardening concretes, IOP Conf. Ser. Mater. Sci. Eng. 960 (2020) 032058. https://doi.org/10.1088/1757-899X/960/3/032058.

[131] A. Alzaza, K. Ohenoja, I. Langås, B. Arntsen, M. Poikelispää, M. Illikainen, Low-temperature (−10 $^{o}$C) curing of Portland cement paste – Synergetic effects of chloride-free antifreeze admixture, C–S–H seeds, and room-temperature pre-curing, Cem. Concr. Compos. 125 (2022) 104319. https://doi.org/10.1016/j.cemconcomp.2021.104319.

[132] H.C. Pedrosa, O.M. Reales, V.D. Reis, M. das D. Paiva, E.M.R. Fairbairn, Hydration of Portland cement accelerated by C-S-H seeds at different temperatures, Cem. Concr. Res. 129 (2020) 105978. https://doi.org/10.1016/j.cemconres.2020.105978.

[133] N. De Belie, C.U. Grosse, J. Kurz, H.W. Reinhardt, Ultrasound monitoring of the influence of different accelerating admixtures and cement types for shotcrete on setting and

hardening behaviour, Cem. Concr. Res. 35 (2005) 2087–2094. https://doi.org/10.1016/J.CEMCONRES.2005.03.011.

[134] G. Ye, K. Breugel, A.L.A. Fraaij, Experimental study on ultrasonic pulse velocity evaluation of the microstructure of cementitious material at early age, HERON, Vol. 46 (3), 2001. 46 (2001).

[135] ÖZLEM KASAP KESKİN, MONITORING THE DEVELOPMENT OF PROPERTIES IN FRESH CEMENT PASTE AND MORTAR BY ULTRASONIC WAVES, MIDDLE EAST TECHNICAL UNIVERSITY, 2009.

[136] M.J.W. POVEY, Ultrasonic Techniques for Fluids Characterization, 1997.

[137] V.M. John, B.L. Damineli, M. Quattrone, R.G. Pileggi, Fillers in cementitious materials — Experience, recent advances and future potential, Cem. Concr. Res. 114 (2018) 65–78. https://doi.org/10.1016/j.cemconres.2017.09.013.

[138] B. Szostak, G.L. Golewski, Rheology of cement pastes with siliceous fly ash and the csh nano-admixture, Materials (Basel). 14 (2021) 3640. https://doi.org/10.3390/ma14133640.

[139] H. Zhu, C. Liao, Z. Chen, C. Hu, F. Wang, Role of C-F-S-H/PCE nanocomposites on the hydration of Portland cement with varying gypsum levels, Constr. Build. Mater. 426 (2024) 136155. https://doi.org/10.1016/J.CONBUILDMAT.2024.136155.

[140] M.A.G. Aranda, Recent studies of cements and concretes by synchrotron radiation crystallographic and cognate methods, Crystallogr. Rev. 22 (2016) 150–196. https://doi.org/10.1080/0889311X.2015.1070260.

[141] M.A.G. Aranda, A. Cuesta, A.G. De la Torre, I. Santacruz, L. León-Reina, Diffraction and crystallography applied to hydrating cements, in: H. Pöllmann (Ed.), Cem. Mater. Compos. Prop. Appl., De Gruyter, Berlin, Boston, Germany, 2017: pp. 31–60. https://doi.org/10.1515/9783110473728-003.

[142] E.M.J. Bérodier, A.C.A. Muller, K.L. Scrivener, Effect of sulfate on C-S-H at early age, Cem. Concr. Res. 138 (2020) 106248. https://doi.org/10.1016/j.cemconres.2020.106248.

[143] W. Li, M. Fall, Sulphate effect on the early age strength and self-desiccation of cemented paste backfill, Constr. Build. Mater. 106 (2016) 296–304. https://doi.org/10.1016/J.CONBUILDMAT.2015.12.124.

[144] E. Pustovgar, R.K. Mishra, M. Palacios, J.-B. d'Espinose de Lacaillerie, T. Matschei, A.S. Andreev, H. Heinz, R. Verel, R.J. Flatt, Influence of aluminates on the hydration kinetics of tricalcium silicate, Cem. Concr. Res. 100 (2017) 245–262. https://doi.org/10.1016/j.cemconres.2017.06.006.

[145] D. Wagner, F. Bellmann, J. Neubauer, Influence of aluminium on the hydration of triclinic C3S with addition of KOH solution, Cem. Concr. Res. 137 (2020) 106198. https://doi.org/10.1016/j.cemconres.2020.106198.

[146] A. Mezhov, D. Kulisch, A. Goncharov, S. Zhutovsky, A Comparative Study of Factors

Influencing Hydration Stoppage of Hardened Cement Paste, Sustain. 15 (2023) 1080. https://doi.org/10.3390/su15021080.

[147] J. Zhang, G.W. Scherer, Comparison of methods for arresting hydration of cement, Cem. Concr. Res. 41 (2011) 1024–1036. https://doi.org/10.1016/j.cemconres.2011.06.003.

[148] R. Snellings, J. Chwast, Ö. Cizer, N. De Belie, Y. Dhandapani, P. Durdzinski, J. Elsen, J. Haufe, D. Hooton, C. Patapy, M. Santhanam, K. Scrivener, D. Snoeck, L. Steger, S. Tongbo, A. Vollpracht, F. Winnefeld, B. Lothenbach, Report of TC 238-SCM: hydration stoppage methods for phase assemblage studies of blended cements—results of a round robin test, Mater. Struct. Constr. 51 (2018). https://doi.org/10.1617/s11527-018-1237-5.

[149] V. Kanchanason, J. Plank, Effectiveness of a calcium silicate hydrate – Polycarboxylate ether (C-S-H–PCE) nanocomposite on early strength development of fly ash cement, Constr. Build. Mater. 169 (2018) 20–27. https://doi.org/10.1016/J.CONBUILDMAT.2018.01.053.

[150] J. Sun, H. Dong, J. Wu, J. Jiang, W. Li, X. Shen, G. Hou, Properties evolution of cement-metakaolin system with C-S-H/PCE nanocomposites, Constr. Build. Mater. 282 (2021) 122707. https://doi.org/10.1016/j.conbuildmat.2021.122707.

[151] C. Xu, H. Li, X. Yang, Effect and characterization of the nucleation C-S-H seed on the reactivity of granulated blast furnace slag powder, Constr. Build. Mater. 238 (2020) 117726. https://doi.org/10.1016/J.CONBUILDMAT.2019.117726.